A Thesis report on

KINEMATIC STUDY OF A SPATIAL HYBRID MANIPULATOR FOR ROBOT-ASSISTED SURGERY

Submitted in the partial fulfillment of requirement for the award of degree of

MASTER OF ENGINEERING

IN

CAD/CAM Engineering

Submitted by

Amanpreet Singh

Roll No. 801281004

Under the joint guidance of

Dr. Ashish Singla
Assistant Professor,
Mechanical Engineering Department,
Thapar University, Patiala.

Mr. Sanjeev Soni
Senior Scientist, Biomedical
Instrumentation Division, CSIR-CSIO,
Chandigarh.

MECHANICAL ENGINEERING DEPARTMENT

Thapar University, Patiala

July, 2014

DECLARATION

I hereby declare that the seminar report entitled **"KINEMATIC STUDY OF A SPATIAL HYBRID MANIPULATOR FOR ROBOT ASSISTED SURGERY"** is an authentic record of my study carried out as requirement for the award of degree of **Master of Engineering in CAD/CAM Engineering** during 4th semester (Jan 2014 – July 2014) at CSIR-CSIO Chandigarh and Thapar University, Patiala, under the joint supervision of **Dr. Ashish Singla** (Assistant Professor, Mechanical Engineering Department) and **Mr. Sanjeev Soni** (Senior Scientist, Biomedical Instrumentation Division, CSIR-CSIO, Chandigarh).

Date: July 18, 2014

Amanpreet Singh
Roll No. 801281004

It is certified that the above statement made by the student is correct to the best of our knowledge and belief.

Dr. Ashish Singla
Assistant Professor,
Mechanical Engineering Department,
Thapar University, Patiala.

Mr. Sanjeev Soni
Senior Scientist, Biomedical
Instrumentation Division,
CSIR-CSIO, Chandigarh.

संजीव सोनी / Sanjeev Soni
वरिष्ठ वैज्ञानिक/Senior Scientist
बायोमेडिकल इंस्ट्रूमेंटेशन यूनिट
Biomedical Instrumentation Unit
केन्द्रीय वैज्ञानिक उपकरण संगठन
Central Scientific Instruments Organisation,
सैक्टर 30-सी, चंडीगढ़-160030
Sector 30-C, Chandigarh-160030

Countersigned by:

Dr. S. K. Mohapatra
Senior Professor and
Dean of Academic Affairs,
Thapar University, Patiala.

Dr. Ajay Batish
Professor and Head,
Mechanical Engineering Dept.,
Thapar University, Patiala.

ii

ACKNOWLEDGEMENT

Through this, I would like to acknowledge those great people who have a significant influence on my professional life. It was seven-eight years back, when I was studying in Bachelors, I got an inspiration to pursue higher studies in the field of robotics from **Mr. Deepak Bhandari**. I am mainly influenced by his level of knowledge, way to present it, how to make the things easier. At that time, I thought of myself like him and decided to do research in the field of Robotics.

Unfortunately, up-to June- 2012, I didn't get any chance to fulfil my desire. However, in July 2012, I got admission in the same discipline in the most prestigious university (Thapar University, Patiala). Thereafter, one year of M.E has gone. I was seeking to work on robots analytically as well as experimentally. However, still i didn't get any chance.

Fortunately, in September 2013, I got that opportunity which I was looking for since long i.e to work in the field of robotics under the guidance of my mentor, who is a person with excellent knowledge, has the best way to present it, with excellent creativity and a great personality, which inspires lot of others in day-to-day life. Thereafter, I went to **CSIR-CSIO** Chandigarh and found myself fortune enough to meet another great personality, who let me to work on *medical/surgical* robots (also referred as future robots).

Now, it's my pleasure to acknowledge, **Dr. Ashish Singla** (Assistant Professor, Mechanical Engineering Department, Thapar University, Patiala) and **Mr. Sanjeev Soni** (Senior Scientist, Biomedical Instrumentation Division, CSIR-CSIO, Chandigarh), who fulfilled my all desires. I am greatly thankful for their valuable suggestions, motivation, guidance, encouragement, efforts, timely help and the attitude with which they resolved all of my queries.

I would like to say thanks to **Dr. Ekta Singla** (Assistant Professor, SMMEE, IIT Ropar) for her support during my thesis. I would like to say thanks to **Mr. Vipin Sharma** for his kindness and support during my thesis. Also, I am deeply indebted to my family for their love, encouragement and ample support.

Amanpreet Singh

ABSTRACT

The recent developments in the field of robotics lead to the replacement of conventional machines as well as human beings employed to a specific work. In the last three decades, a lot of research has been carried out in all the major domains of robotics like kinematics, dynamics and controls. The scope of this thesis is limited to kinematic study only. It has been found in the literature that the pioneer work done by Denavit and Hartenberg to develop the kinematic model of a serial manipulator, is limited to open-loop manipulators only. A couple of other ambiguities are also reported by different researchers in the past. The main focus of this work is to develop the kinematic model of a hybrid manipulator, which is a combination of open- and closed-loop chains containing planar and spatial links. The positional and orientational inconsistencies are observed, when such hybrid manipulators are modeled with the D-H parameter method. To overcome these inconsistencies, the concept of dummy frames is proposed in the present thesis and successfully implemented on the prototype of a hybrid manipulator, which is a 7-DOF manipulator being developed for medical/surgical applications at CSIR-CSIO lab, Chandigarh. Moreover, the analytical formulation of the spring design for gravity balancing of the hybrid manipulator is also presented in the current thesis.

CONTENTS

LIST OF FIGURES

LIST OF SYMBOLS

a_i = link length parameter

α_i = link twist parameter

d_i = joint offset parameter

θ_i = joint angle parameter

$\boldsymbol{x_i}$ = unit vector along x- axis

$\boldsymbol{y_i}$ = unit vector along y- axis

$\boldsymbol{z_i}$ = unit vector along joint axis (z- axis)

i = joint axis

O_i = origin of i^{th} link-frame

$\boldsymbol{u, v, w}$ = unit vectors of frame , at proximal end of a link

$\boldsymbol{x, y, z}$ = unit vectors of frame , at distal end of a link

m = number of end-effectors

n = number of joints

t_{jk} = common normal from w_j to z_k

a_{jk} = distance measured from w_j to z_k along t_{jk}.

α_{jk} = angle measured from w_j to z_k about t_{jk}.

b_{jk} = distance measured from t_{jk} to x_k along z_k.

β_{jk} = angle measured from t_{jk} to x_k about z_k.

c_{jk} = distance measured from u_j to t_{jk} along w_j.

γ_{jk} = angle measured from u_j to t_{jk} about w_j.

θ_j = angle measured from u_j to x_j about common joint axis z_j, w_j.

α_i = angle measured from z_{i-1} to z_i about x_{i-1}.

d_i	=	distance measured from O_{i-1} to z_i along x_{i-1}.
r_i	=	distance measured from O_{i-1} to x_{i-1} along z_i.
θ_i	=	angle measured from x_{i-1} to x_i about z_i.
$\emptyset$	=	base link
γ_j	=	angle measured from x_i to x_i' about z_i.
ϵ_j	=	distance measured from O_i to O_i' along z_i.
α_j	=	angle measured from z_i to z_j about x_i'.
d_j	=	distance measured from O_i' to z_j.
r_j	=	distance measured from O_j to x_i'.
θ_j	=	angle measured from x_i' to x_i about z_j.
${}^{i}_{j}\boldsymbol{T}$	=	transformation matrix mapping j^{th} frame into i^{th}
dof	=	degree-of-freedom
$\alpha_i, \beta_i, \theta_i$	=	joint variables
${}^{i}_{i-1}T$	=	mapping of $(i-1)^{th}$ frame to i^{th} frame
R_x	=	rotation about x- axis
R_y	=	rotation about y- axis
R_z	=	rotation about z- axis
q_i	=	joint variable
$\theta_t, \alpha_{t,t+1}, L_{t-1}$ and d_t	=	kinematic parameters of quaternion theory based method
s_t	=	unit line vector which defines the axis of joint 't'
$a_{t,t+1}$	=	define the common perpendicular to the axes of joints t and $(t+1)$,
$\boldsymbol{s}, \boldsymbol{a}$	=	unit vectors along x- and z- axis.

$\mathbb{R}^3$	=	cartesian space
$\mathbb{R}^n$	=	joint space
$\boldsymbol{p}$	=	position vector
$\boldsymbol{a}$, $\boldsymbol{R}$	=	fundamental rotation matrix
$\boldsymbol{A_1}$	=	homogeneous coordinate transformation matrix
$\boldsymbol{x_1}$, $\boldsymbol{y_1}$	=	point vectors in $\mathbb{R}^3$
a, b	=	real numbers
$\overline{\theta_k}$, $\overline{\alpha_k}$	=	dual angles
$\bar{\boldsymbol{M}}_0^n$	=	transformation matrix mapping n^{th} frame to base frame
$[\boldsymbol{p}]^A$	=	position vector with respect to frame a.
p_1, p_2 and p_3	=	components of position vector $\boldsymbol{p}$
$\boldsymbol{\eta}^T$	=	perspective vector
σ	=	non-zero scale factor
{a}, {b}	=	orthonormal coordinate frames in $\mathbb{R}^3$
${}_B^A[\mathbf{T}]$	=	homogeneous transformation matrix mapping frame {b} into frame {a}
t_i	=	amount of translation along i^{th} unit vector of frame {a}
t_j	=	amount of translation along j^{th} unit vector of frame {a}
t_k	=	amount of translation along k^{th} unit vector of frame {a}
${}^B\boldsymbol{p}$	=	position vector of point p w.r.t frame {b}
L_i	=	i^{th} link of a kinematic chain
N	=	total number of links

J	=	total number of joints
L	=	total number of closed-loop (s)
c_i	=	$\cos\theta_i$; $i = 1$ to n.
s_{i}	=	$\sin\theta_i$; $i = 1$ to n.
c_{ij}	=	$\cos\ (\theta_i + \theta_j)$
c_{ijk}	=	$\cos\ (\theta_i + \theta_j + \theta_k)$
s_{ij}	=	$\sin\ (\theta_i + \theta_j)$
s_{ijk}	=	$\sin\ (\theta_i + \theta_j + \theta_k)$
$\tilde{a}_{ij}, \tilde{b}_{ij}, \tilde{c}_{ij}, \tilde{e}_{ij}, \tilde{f}_{ij}, \tilde{g}_{ij}$	=	elements of homogeneous transformation matrices
$\boldsymbol{T}$	=	effective spring force
k	=	stiffness of spring
G	=	centre of mass
$\boldsymbol{\tau}_{Pose_1}$	=	joint torque in first pose.
$\boldsymbol{\tau}_{Pose_1}$	=	joint torque in second pose.
$\boldsymbol{\tau}_{sp_1}$	=	resisting torque offered by spring in first pose.
$\boldsymbol{\tau}_{sp_2}$	=	resisting torque offered by spring in second pose.
$\boldsymbol{F}_{sp_1}$	=	spring force in first pose
$L_F = a$	=	free length of spring
a'	=	compressed length of spring
b, c	=	distance from pivot point to point of attachment of spring.
g	=	acceleration due to gravity
mg	=	weight to be balanced

LIST OF TABLES

Chapter 1

Introduction

1.1 Robots

Since last three decades, the field of robotics has widens its range of applications. This is because of the fast growing trends of manufacturing, medical surgeries, defense weapons, space vehicles, under water-manipulators etc. Out of these applications, except first, all manipulators being used in medical, defense, space and under-water are advanced applications of robotics. This is because of relatively complex mechanical structure of robotic manipulators. Depending upon the configuration robots can be classified to different classes. The detailed classification of robots are given in the next section (Section 1.2).

1.2 Robot Classification

Based on the kinematic configuration of the robot structure, robots can be broadly classified as

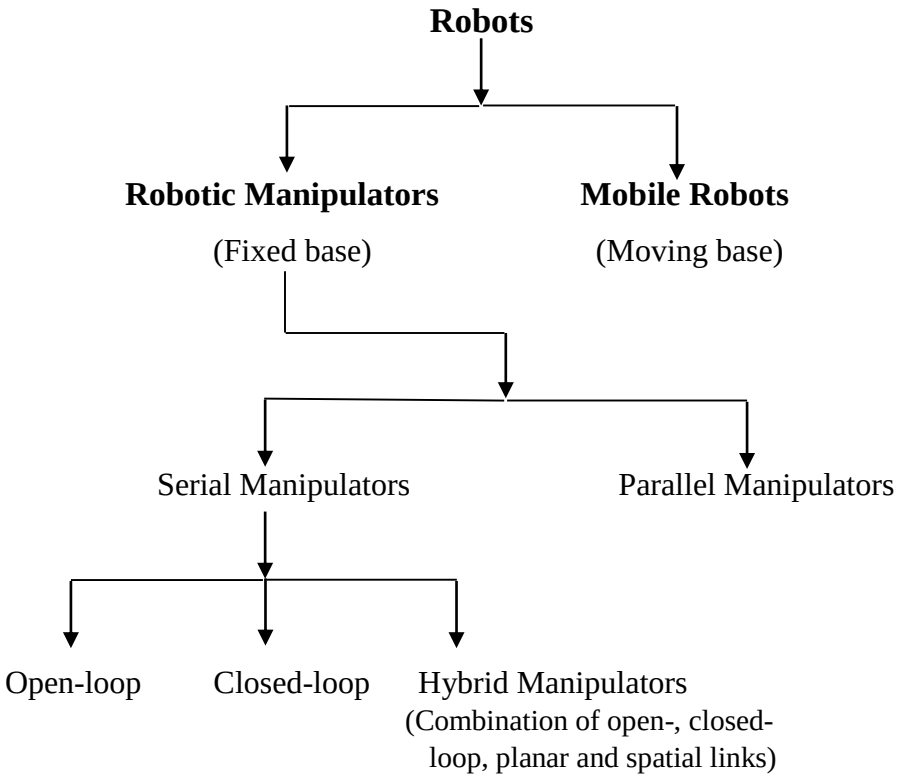

With reference to the flow chart, robots can be broadly classified as *robotic manipulators* and *mobile robots* respectively. Now, the main difference between these classifications lies in the fact that one of the links, comprising a robotic manipulator, is fixed whereas all links of a mobile robot are free to move in Cartesian space. The fixed link is known as base of manipulator. In other words, to differentiate them a simple way is to identify that is there is any change in position of robot during an operation? If so, it will be characterized as a mobile robot. However, if it does not happen in that case it will be termed as a robotic manipulator. Figures 1.1-(a) and 1.1-(b), presents the examples of a serial and a mobile robot. The brief introduction of further classifications is presented in Section 1.1.1.

Fig. 1.1-(a): General mechanical structure of a robotic manipulator [G1].

Fig. 1.1-(b): General mechanical structure of a mobile robot [G2].

1.2.1 Serial Manipulators

A robotic manipulator is referred to as a serial manipulator, when the links comprising the same are connected in a progressive sequence, forming an open- or closed-loop kinematic

chain. Now, if there is only one feasible/possible path to track from one end of chain to other, it is known as an open-loop serial manipulator, whereas if there are more than one feasible paths to reach from one end to other end of chain in that case, it is referred as a closed-loop serial manipulator. Also, a closed-loop manipulator contains a closed kinematic chain.

Generally, these manipulators are consist of planar links which leads to their simple mechanical structure. Due to this simplicity, their kinematic modeling is easy. The examples of the open-loop serial manipulators may include a 4-axis SCARA robot, 5-axis articulated arm (Microbot Alpha 2, Rhino XR-3), 6-axis Puma 560 etc. Figure 1.2-(a), shows the mechanical structure of an open-loop serial manipulator. While the mechanical structure of a closed-loop robot manipulator is shown in Fig. 1.2-(b).

Fig. 1.2-(a): An open-loop Serial manipulator [G3]. Fig. 1.2-(b): A closed-loop serial manipulator [G4].

From first figure, it can be observed that the in the first figure links are connected in a sequential order. The base of manipulator is fixed and there is only one possible way to track from base to end point (known as tool-tip) of manipulator, whereas in second figure,

links are also connected in sequence. However, there are two possible ways to track the tool-tip with respect to base.

1.2.2 Hybrid Manipulators

The word *hybrid* denotes the combination of open- and closed-loop chains containing planar and spatial links. Further, depending upon this combination the resultant manipulator can be described accordingly. For example, the manipulator studied in this thesis is a combination of planer links, spatial links and parallelogram linkage (closed-loop), referred as *spatial hybrid manipulator*. Also, the open serial chains can be combined to form a parallel-serial hybrid manipulator. Now, as a hybrid manipulator is a combination of reported open- and closed-loop robots, so it can be expected that their mechanical structure will be complex as compared to them. Likewise, these manipulators are difficult to model kinematically.

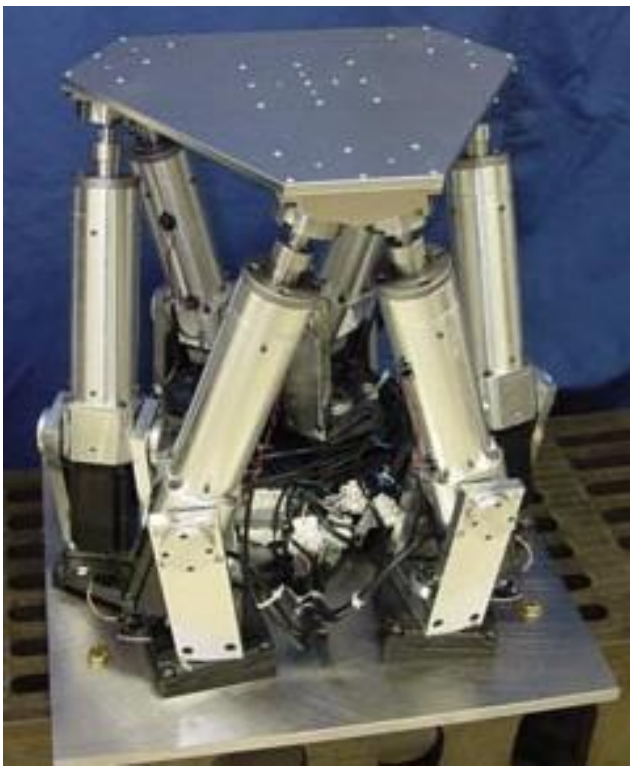

Fig. 1.3: A parallel-serial hybrid manipulator [G5].

In the present thesis, the real-time experience of working on the hybrid manipulator is shared, which is being developed in the context of medical/surgical applications.

1.3 Motivation

The main focus of this thesis is to study the hybrid manipulators, which is being used in robotic assisted medical surgery. Now, there are some reasons which demands the research in the field of hybrid manipulators. These reasons are, first, since a spatial hybrid manipulator is a combination of planar and spatial links, an open-loop (s) and a closed-loop chain (s). Thus, undoubtedly, their mechanical structure will be more complex as compared to open- or closed-loop serial manipulators. Likewise their kinematic formulations will be relatively more difficult. Second, limited robot kinematics methodologies are available to describe these manipulators. Moreover, design strategies are very limited, if range of application of hybrid manipulators need to be extended. This is mainly due to the complexity of their kinematic configuration. Also, this is because of author's interest in the domain of robotics. So, all these reasons provides the motivation to do research in the area of hybrid manipulators.

1.4 Application of Work

The work reported in this thesis is an in-house project, coined as **Robotic Assisted Minimal Invasive Surgery (RAMIS)**, of **Central Scientific Instruments Organization Chandigarh, Ministry of Science & Technology, Govt. of India**. The project is in the field of *medical/surgical* robots. The general layout of this project is similar to as presented in Fig. 1.1. In RAMIS, generally two types robotic manipulators are employed. One manipulator is on surgeon side (Surgeon handle) while the other is on patient side (Robotic arm). The manipulator studied in this thesis, referred as Manipulator for Medical Applications (MMA), is a surgeon side manipulator. The detailed description of MMA is given in Chapter 4.

Now, in a surgical task, while sitting on surgeon console, as surgeon make some hand movements, the same are recorded by the sensors equipped to surgeon handle, which is MMA for the present case. Thereafter, recorded motion is transferred to robotic arm through master controller, which is a computer. Master controller sends the signals to slave controller, which controls the motion of robotic arm. Finally, recorded motion is executed by robotic arm, which actually perform the surgical task. A continuous sensory feedback is

received by the surgeon about the contact of end-effector to patient's body, by means of force sensors.

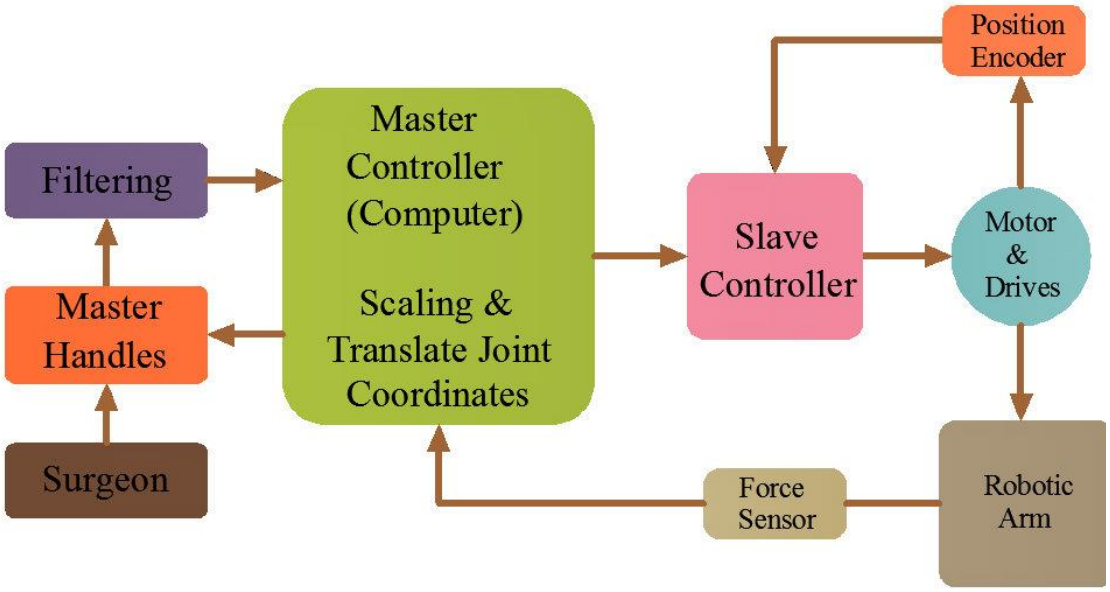

Fig. 1.4-(a): Description of application of the MMA.

Fig. 1.4-(b): Real-time application of MMA by surgeon [G6].

Figure 1.5 describes the real-time application of the master handle. The platform on which surgeon sit is known as surgeon console. Here, surgeon sits comfortably while performing the surgical task.

1.5 Scope of the Thesis

In this thesis, the kinematic study of variety of robotic manipulators has been discussed. The description of these manipulators is carried, first, starting with kinematically simple structures (open-loop serial manipulators), thereafter moving towards the complicated mechanisms which includes, closed-loop, tree-like structures and hybrid manipulators. Since, it has been reported in literature that dealing with kinematics of a closed-loop manipulators may or may not be feasible. So, from this reported work it can be concluded that dealing with kinematics of hybrid manipulators is undoubtedly a challenging task and this is the main focus of this thesis. Also, presented work, is an application of robotics to the medical field. Now, it has been observed from literature that limited design strategies are there for medical robots. This is because of the complexity of motions as required by the surgeon. So, from both these points, it can be said that research on hybrid manipulators should be carried, in order to develop the new design strategies for the same.

Fig. 1.5: Real-time demonstration of “da Vinci surgical system” [G7].

Figure 1.6, demonstrates the real-time application of a robotic assisted surgical system which is “da Vinci surgical system”. By using this system, most of the surgeries performed in conventional manner, can be performed in minimal invasive manner.

1.6 Organization of the Thesis

The organization of the thesis is as given below:

In **Chapter 2**, literature on different methodologies, dealing with kinematic study of different classes of robotic manipulators, has been reviewed. In this review, the general procedures of each method, describing the structure of a manipulator, is presented. Also, an attempt has been made to present these methods, in the sense of their development.

In **Chapter 3**, the kinematic study of general *serial* manipulators is presented. The pioneer work, referred as Denavit and Hartenberg (D-H) parameter method, is used to describe the structure of an open−as well as closed-loop manipulators. Thereafter, suitable examples for two variants of D-H parameter method has been presented. Also, Sheth and Uicker method presented in Chapter 2, is applied to different classes of industrial manipulators. Finally, observations in terms of relative simplicity, with which these methods can be used to deal with kinematic problems, are made.

In **Chapter 4**, the kinematic study of *hybrid* manipulators is presented. The method described in Chapter 3, that how to deal with kinematics of a closed-loop manipulator is referred, to deal with kinematics of a hybrid manipulator. In the present work, a *recognizable* deficiency in D-H parameter method has been observed, for the case of a manipulator for medical applications (MMA), which is a hybrid manipulator. However, the observed deficiency is eliminated successfully, by introducing the concept of *dummy* frames. Finally, introduction of dummy frame concept can be stated as an extension of D-H parameter method, is extended to hybrid manipulators.

In **Chapter 5**, gravity balancing of robotic manipulators has been discussed. The chapter starts with an introduction to gravity balancing and grows with literature review on different techniques of gravity balancing. The chapter closes with the analytical development of the spring design for the MMA.

In **Chapter 6**, the major finding of this thesis are reported. It also highlights of future directions of present work.

Chapter 2

Literature Review

2.1 Introduction

In this chapter, literature on kinematics of robotic manipulators has been reviewed. A lot of researchers in the past have worked in the domain of kinematics, dynamics and control of robotic manipulators, since these devices are extensively used in various applications like industrial (welding, painting, pick and place etc.), medical/surgical operations, space vehicles, unmanned army vehicles used in battle fields etc. The main focus of this review is the robot kinematics, its different variations and methodologies used in past. Since, the pioneer work by Denavit and Hartenberg in 1955, a lot of robot kinematics methods have been evolved. In this chapter, those methods are discussed in detail.

2.2 Different Methods for Describing Robot Kinematics

Based on the literature review, the robot kinematics can be broadly classified into two main categories as given below in the flow chart

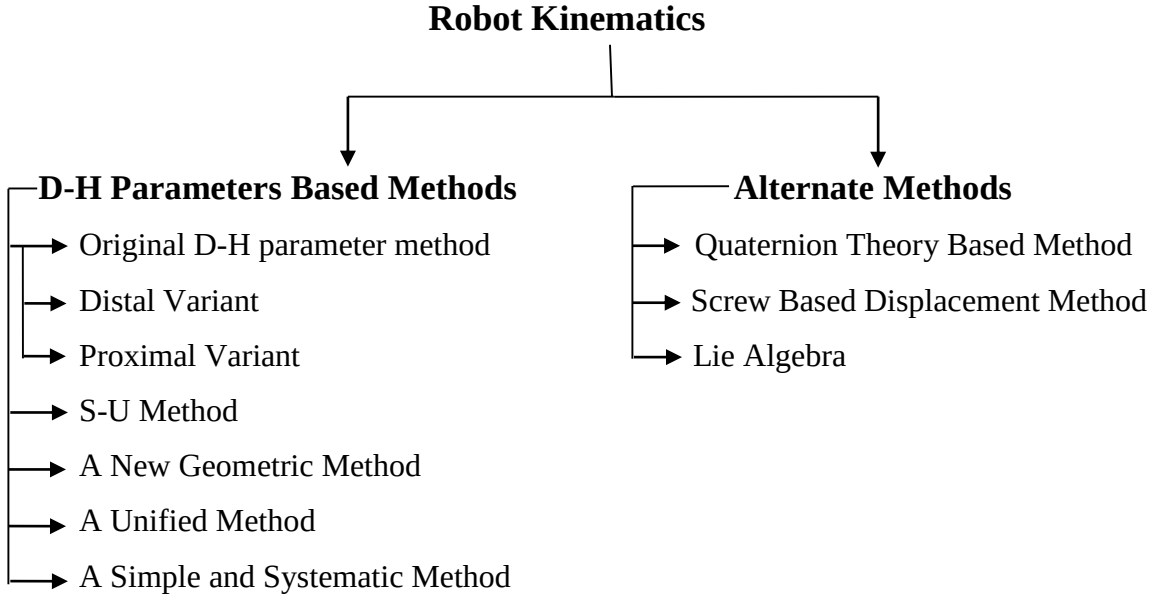

2.2.1 Denavit and Hartenberg Method (D-H):

In 1955, Jacques Denavit and Richard S. Hartenberg [1] introduced a consistent and concise method to assign reference coordinate frames to serial mechanisms. In this method four parameters, popularly known as *D-H parameters*, are defined to provide the geometric description to serial mechanisms. Out of the four, two are known as *link parameters*−describes the relative location of two attached axes in space, these are: 1) link length (a_i) which is measured from z_i to z_{i+1} along x_{i+1}; 2) link twist (α_i) which is measured from z_i to z_{i+1} about x_{i+1}; while remaining two are described as *joint parameters*− describe the connection of any link to its neighboring link [2] these are: 3) joint offset (d_i) which is measured from x_i to x_{i+1} along z_i; 4) joint angle (θ_i) which is measured from x_i to x_{i+1} about z_i. Figure 2.1, describes the schematic representation of original D-H parameters method with the help of two spatial links forming a lower pair (surface to surface contact) where link parameters a_1, α_1 are measured along x_2, however joint parameters d_1 and $\theta_1$were measured along z_1.

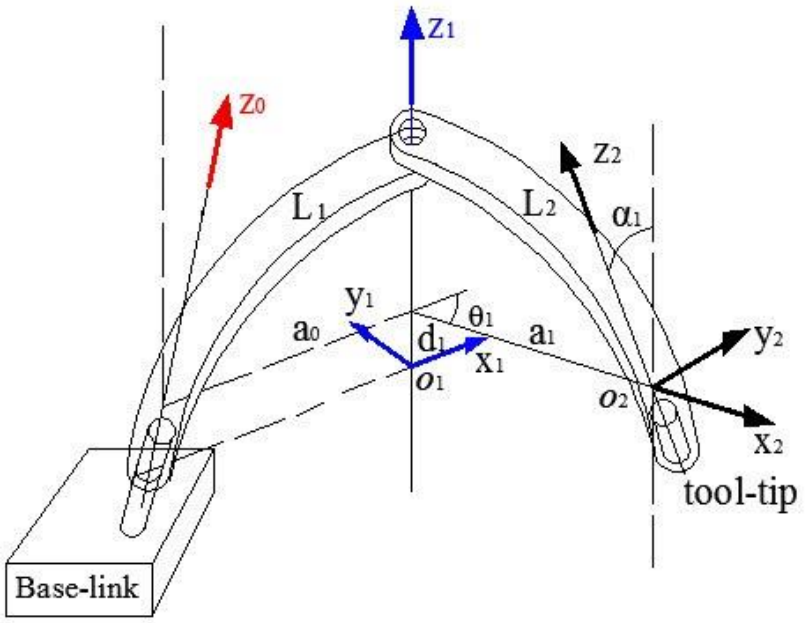

Fig. 2.1: Schematic representation of original D-H parameter method [3].

Four D-H parameters can be expressed using vector forms which takes account the sign of displacements,

$$\cos \alpha_1 = z_1 . z_2, \quad (2.1)$$

$$\sin \alpha_1 = z_1 \times z_2 . x_2, \quad (2.2)$$

$$\cos \theta_1 = x_1 . x_2, \quad (2.3)$$

$$\sin \theta_1 = x_1 \times x_2 . z_1, \quad (2.4)$$

$$a_1 = Vec\,(O_1O_2) . x_2, \quad (2.5)$$

$$d_1 = Vec\,(O_1O_2) . z_1, \quad (2.6)$$

where *Vec* (O_1O_2) represents a vector from O_1 to O_2.

Frame 1 can be mapped to frame 2 by considering two screw transformations [3]. First, about the axis z_1 by distance d_1 and angle θ_1 followed by second, about axis x_2 by distance $a_1$and an angle of α_1.

$$T_{12} = screw\,(\theta_1, d_1, z_1) \cdot screw\,(\alpha_1, a_1, x_2), \quad (2.7)$$

$$T_{12} \triangleq \begin{bmatrix} 1 & 0 & 0 & 0 \\ a_1 \cos\theta_1 & \cos\theta_1 & -\sin\theta_1 \cos\alpha_1 & \sin\theta_1 \sin\alpha_1 \\ a_1 \sin\theta_1 & \sin\theta_1 & \cos\theta_1 \cos\alpha_1 & -\cos\theta_1 \sin\alpha_1 \\ d_1 & 0 & 0 & \cos\alpha_1 \end{bmatrix}, \quad (2.8)$$

where T_{12} is 4×1 homogeneous transformation matrix which gives position of frame 2 relative to frame 1.

a. Variants of D-H Method:

Two modifications of this method have been reported in literature – first by Kahn and Roth [4] and second by Featherstone [5]. These are as follow:

i. Distal Variant

First modified method is known as *distal* variant of D-H parameters method. Objective of this modification was to make the parameter identification simpler [6] and is used world widely for kinematic description of serial robotic manipulators, as reported by Lipkin [3]. The term distal refers to the location of the link-frame relative to manipulator base and

according to this variant, a frame is attached to farther end point of link, when travelling from manipulator base towards end effector.

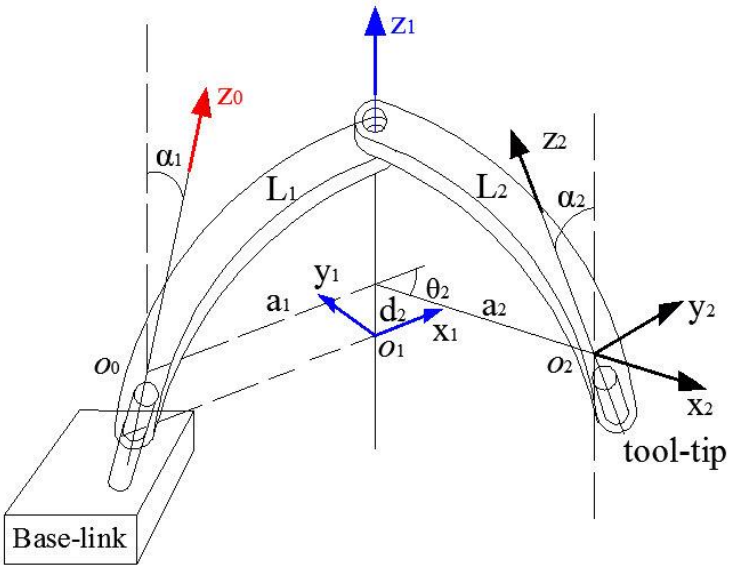

Fig. 2.2: Distal variant of original D-H parameter method.

Figure 2.2, describes the schematic representation of distal variant. The coordinate frame having components x_1, y_1 and z_1 is attached at father end point of first moving link L_1. Later on, this variant was popularized by Paul [7] and Shilling [8] and has been applied to different kinds of kinematic problems [6, 9−12]. It differs from original D-H parameter method in the sense of parameters measurement. In original D-H method, link parameters, a_i and α_i, are measured from z_i to z_{i+1} about x_{i+1}, whereas in this variant, link parameters are measured from z_{i-1} to z_i about x_i. Also, joint parameters θ_i and d_i are measured from x_{i-1} to x_i about z_{i-1} rather than measuring from x_i to x_{i+1} about z_i as in original D-H parameters method. From Figure 2, it can be seen that a_2 and α_2 were measured about x_2, whereas d_2 and θ_2 were measured about z_1.

Procedure to assign link-frame according to this variant [8]:

a) First of all, draw the schematic diagram of a given kinematic chain showing the links and joints axes. Mark the joint number from 1 to n, starting with base and proceeding towards end-effector. Thereafter, assign $z_i - axis$ to $(i+1)^{th}$ joint axis about which

motion is taking place, for $i = 1$ to $(n - 1)$. However, base frame z-axis, z_0-axis is always aligned with 1st joint axis. There is no fixed rule to assign $z_n - axis$ [15]. For convenience, z_n can be taken along the approach vector.

b) Locate a point at the intersection of axes z_{i-1} and z_i. Mark it as origin (O_i) of i^{th} frame. From this point, draw a common normal to z_{i-1} and z_i. Assign x-axis from O_i along common normal. However, if z_{i-1} and z_i don't intersect, as in case when two consecutive joint axes are parallel to each other, consider the point of intersection between z_i and common normal as origin (O_i). The x-axis, is assigned in the same way as before however, away from z_{i-1}.

c) Assign y-axis according to right hand thumb rule.

d) Finally, calculate the corresponding D-H parameters.

ii. Proximal Variant

Second modified method is known as *proximal* variant of D-H parameter method. Again, reason behind this modification was same as in case of distal variant i.e to make the parameters identification simpler. In this method, the term proximal refers location of frame, being rigidly attached to link, relative to manipulator base. According to this variant, coordinate frame is placed at that end of the link which is closer to manipulator base or which comes first, when travelling from base towards end effector. Later on, this variant, is popularized by Craig [2] and followed by [13, 14] in their respective work. It differs from original D-H parameter method in the sense that link parameters a_i and α_i are measured from z_i to z_{i+1} about x_i rather than measuring from z_i to z_{i+1} about x_{i+1} as in case of original method. Also, joint parameters θ_i and d_i are measured from x_{i-1} to x_i about z_i rather than measuring from x_i to x_{i+1} about z_i. With reference to Figure 2.3, it can be seen that link coordinate frame having components x_1, y_1 and z_1 is attached at closer end point of first moving link L_1 and link parameters a_2 and α_2 were measured about x_2 whereas d_2 and θ_2 were measured about z_2.

Procedure to assign link-frame to a kinematic chain, according to this variant [2]:

a) First of all, draw the schematic line diagram of given kinematic chain. Mark the joint axes as $z_i - axis$, for $i = 1$ to n. The *z-axes*, z_0 and z_{n+1}, of base and end-effector frames can be chosen arbitrarily. However, it can be aligned with 1st joint axis for base frame and along the approach vector for end-effector frame.

b) Find the common normal between i^{th} and $(i+1)^{th}$ joint axes or point of intersection of same axes. Mark this point as origin of i^{th} frame. However, if these joint axes does not intersect origin can be chosen arbitrarily at the intersection of common normal and i^{th} joint axis, so that joint distance become zero. Assign *x-axis* along common normal from marked origin.

c) Assign y-axis, following right hand thumb rule, to complete the link frame definition.

d) Finally, calculate corresponding the D-H parameters.

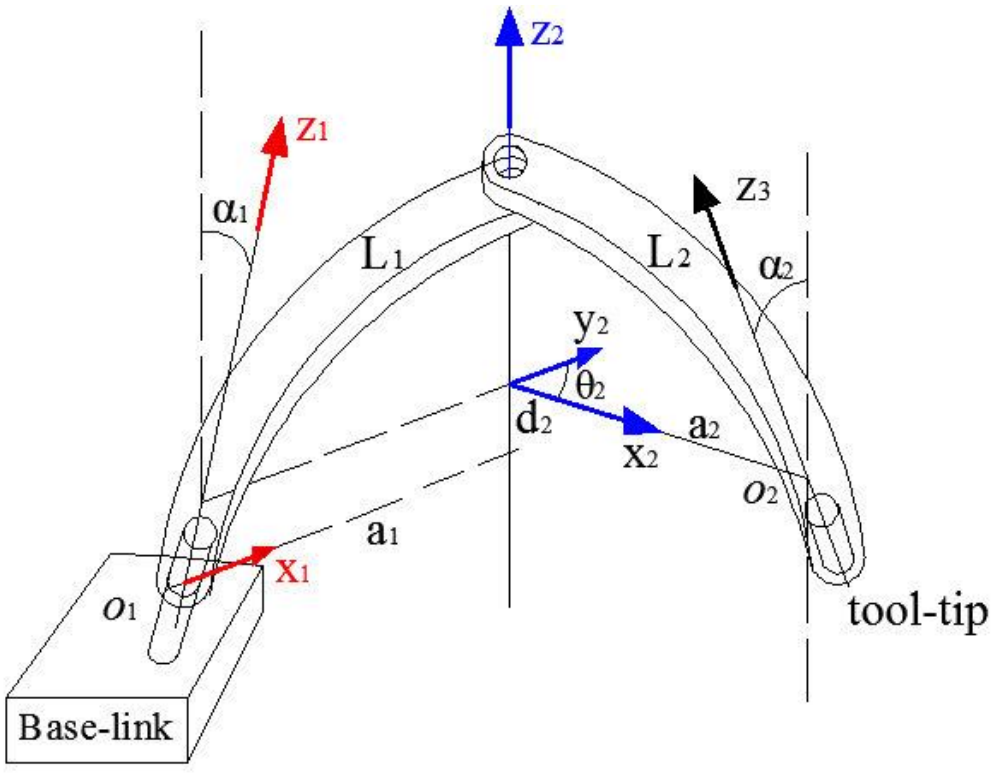

Fig. 2.3: schematic representation of proximal variant of D-H parameters method [3].

b. Comparison between Original D-H parameter method and its variants:

With reference to above discussion of Original D-H parameters method and its variants, it can be observed that parameter identification is easiest in proximal variant than distal and original D-H method. This is because the subscript index of axes (x_i and z_i), about which link and joint parameters are being measured, are same whereas this is not true in the case of original and its distal variant. Which creates a confusion in remembering the definition of these parameter measurement. However, distal variant is more widely used as compared to original and proximal D-H method. This comparison is summarized in Table 1.1.

Table 2.1: Comparison of original D-H parameter method and its variants in terms of parameter representation.

Parameter (s)	Original D-H method	Distal variant	Proximal variant
$\cos\alpha_1$	$z_1.z_2$	$z_0.z_1$	$z_1.z_2$
$\sin\alpha_1$	$z_1 \times z_2.x_2$	$z_0 \times z_1.x_1$	$z_1 \times z_2.x_1$
$\cos\theta_1$	$x_1.x_2$	$x_0.x_1$	$x_0.x_1$
$\sin\theta_1$	$x_1 \times x_2.z_1$	$x_0 \times x_1.z_0$	$x_0 \times x_1.z_1$
a_1	$vec(O_1O_2).x_2$	$vec(O_0O_1).x_1$	$vec(O_1O_2).x_1$
d_1	$vec(O_1O_2).z_1$	$vec(O_0O_1).z_0$	$vec(O_1O_2).z_1$

c. Limitations of D-H parameter method:

1. Two limitations of D-H parameter method has been reported by Sheth and Uicker [18], these are:
   i. In case of mechanisms containing links with more than one joint there is a problem, known as *multi-parameters* sets. Now, if there is a binary joint between two links, one binary and other ternary, then according to D-H parameters method there will be two parameters set for describing this joint with respect to ternary link (previous link). This problem arises because D-H parameters for link under consideration not

only depends on its shape, rather they are also depend upon the shape of previous link in a serial kinematic chain under consideration.

ii. Evaluating D-H parameters for some spatial linkages become quite cumbersome. This is due to the strong requirement of the common perpendicular between two skew lines in space.

2. D-H parameters method is applicable to serial mechanisms only, as pointed by Thomas et al. [16] and Khalil and Kleinfinger [29].
3. D-H parameters method defines only *z-axis* for base coordinate frame. However, it does not give unique representation of direction of *x*-axis. Also, for tool-tip frame, n^{th} in case of distal variant and $(n+1)^{th}$ in case of proximal variant, directions of *x* and *z*-axes are not defined uniquely rather these are chosen arbitrarily as reported by Siciliano et al. [15].
4. Parallel and hybrid manipulators contains joints, like spherical or cardan joints, with more than one degree of freedom, describing these joints by using D-H parameter method results non-uniqueness representation as reported by Thomas et al. [16]. Also, problem of multiple parameters set arises.
5. Homogeneous link coordinate transformation matrix (4×4), on which this method is based, is highly redundant as it uses twelve parameters to represent six degree of freedom as pointed out by Sahu et al. [17].

2.2.2 Sheth and Uicker Method

A new method, describing the manipulator kinematics, has been proposed by Sheth and Uicker [18]. The proposed method is quite general and has a very wide range of applicability to all types of rigid link mechanisms. These mechanisms include open-loop, closed-loop, hybrid or tree-like structured robots. Also, the problem of multi-parameters sets, as reported in limitations of D-H method, has been successfully solved by this method. Later, based on this method, many researchers [19-27] have reported significant contributions. The general purpose mechanism analysis computer program has been modified by Vandervaart and Cipra [19], kinematic equations of motion of wheeled mobile robots has been developed by Muir and Neuman [20], two methods, first, of kinematic modeling and second, of forward kinematics computation has been described. Thereafter, the same has been implemented to

a new kinematic modeling software, named as CAD-2-SIM by Bongardt [21], an efficient approach to the inverse kinematic analysis of redundant moving base robot has been presented by Dutta and Wong [22], a simple radial distance linear transducer has been used by Goswami et al. [23] for identification of robot kinematic parameters, method of structural synthesis, direct and inverse kinematic modeling has been presented by Baigunchekov et al. [24], Megahed− modeled [25] human hand as a tree structure and proposed a new notation [26], [27].

In this method, each link of a serial chain has assigned with two coordinate frames. The frame which is at proximal end has components *u*, *v* and *w*, whereas the frame at the distal end has components as *x, y* and *z.* With reference to Figure 2.4, following procedure has been given by the authors to apply this method to a spatial mechanism:

i. First of all, draw the joint axes of infinite length at the points where links form the connection.

ii. Assign w_i axis to proximal end and z_j to the distal end of a link.

iii. For next link, at proximal end assign w_j- axis which should be along the z_j-axis of previous link and z_k-axis at distal end along the joint axis.

iv. Rest of the two coordinate's *u, v* for proximal frame and *x, y* for distal frame can be chosen arbitrarily.

v. Draw the common normal t_{jk} from w_j to z_k where z_k is the axis assigned (refer Fig. 5) to later link w.r.t pair being considered.

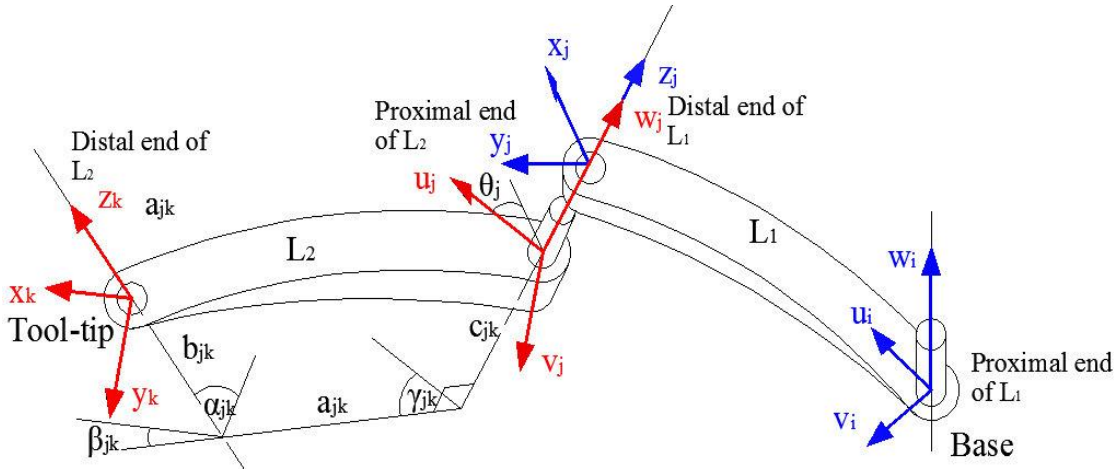

Fig. 2.4: Schematic representation of the S-U method.

For better understanding of S-U parameters, it is important to first know that for any two links, being considered. First link frame has components as u_i, v_i, w_i, at proximal end and second frame has x_j, y_j, z_j components at its distal end. Next, second link has two frames u_j, v_j, w_j and x_k, y_k, z_k at respective ends.

The S-U parameters are defined as follows:

a_{jk} = distance measured from w_j to z_k along t_{jk}.

α_{jk} = angle measured from w_j to z_k about t_{jk}.

b_{jk} = distance measured from t_{jk} to x_k along z_k.

β_{jk} = angle measured from t_{jk} to x_k about z_k.

c_{jk} = distance measured from u_j to t_{jk} along w_j.

γ_{jk} = angle measured from u_j to t_{jk} about w_j.

θ_j = angle measured from u_j to x_j about common joint axis z_j, w_j.

Next, in order to perform the coordinate mapping (transformation), the proposed method can be used directly with existing matrix method of coordinate transformation. However, to reduce the task of data collection, a numerical scheme has been presented by the authors.

In proposed method, each transformation matrix consists of two parts, which are as follows:

i) **Shape matrix:** a constant part specifying the shape of a link by using six parameters. The shape of link is specified by relative orientation of a coordinate frame at the beginning of link and one which is at following end of link. To determine the constant shape parameters for a link, the common perpendicular is found between two axes. This common perpendicular is assigned with arbitrarily positive direction.

ii) **Joint matrix:** a homogeneous link coordinate transformation matrix which is a function of joint variable (revolute or prismatic). Moreover, it is a distinct variable part representing the joint motion.

a. **Advantages of S-U method:**

S-U method has following advantages over the D-H parameter method:

i. Applicable to all rigid link mechanisms which include open, closed, hybrid and tree like structures.

ii. It solves the problem of multi-parameters sets for the definition of single joint, which is encountered in case of a mechanism containing ternary or higher order links in addition to binary links, when D-H parameters method is used.

iii. Two frames one for each link, at the point where two links connect to form a joint, can be chosen independently, which provides more flexibility. The same is not true in case of D-H parameter method and its counter parts, where a frame is defined with respect to common perpendicular between two consecutive joint axes.

b. **Limitations of S-U method:**

Though S-U method is quite powerful and generalized method, still have some limitations, which are:

i. It uses non-minimal parameter representation (seven parameters) to kinematically describe a link shape and joint motion with respect to previous link, as compared to four parameters by D-H.

ii. Due to the complexity of D-H method, it is more suitable to closed-loop chains only [27, 28].

iii. It involves high degree of complicacy because of more number of coordinate frames, as reported by Reichenbach and Kovacic [29].

2.2.3 A New Geometric Method

The problem of multiple parameter set, encountered when D-H parameter method applied to a multi-chain mechanism containing ternary or higher order links in addition to binary links, can also be solved by using a new method, which is an *extension* of well-known D-H parameters method, proposed by Khalil and Kleinfinger [30]. The proposed method is applicable to an open-loop, closed-loop or tree-like robot structures and uses four parameters, in case of links with 2 joints, to describe a link shape and joint motion with respect to previous joint. However, these parameters become six, in case if the links contain

more than two joints. The objective of the new method was to easily describe a close-loop robot kinematically without any ambiguity.

Later, this method has been followed by many researchers [31-53]. A virtual reality based system for rapid design, prototyping and simulation, known as CINEGEN, has been developed by Fluckinger et al. [32, 33], An efficient algorithm [34] for inverse− kinematics as well as dynamics control of robots in Cartesian space, a direct method [35] to determine the minimum number of inertial parameters of a robot, the closed-form solutions for the inverse and direct dynamic model [36] of Gough-Stewart platform, a general method [37] to compute the direct and inverse dynamic models of parallel robots, a novel solution [38] for kinematic and dynamic modeling of 3-PRS parallel robot, the experimental identification of dynamic parameters of Orthoglide [39], two universal (applicable to open-loop as well as graph structured robots) numerical methods [40], a comparison study [41] on the geometric parameter calibration methods of robots (examples are Puma and Stanford manipulators), to determine the set of base parameters, a symbolic method [42] to find the minimum set of inertial parameters of robots containing parallelogram closed-loop, a new method [43] for calibration of geometric parameters of links and tool of serial robots, two methods [44] to calculate the direct dynamic model of walking robots and a comparison for each method, two methods [45] for calibration of geometric parameters of serial robots, direct and inverse dynamic modeling, using recursive Newton-Euler formulism, of tree, parallel and closed-loop robot structures [46], a new method [47] for calculation of filtered dynamic model of robots, human-body is modeled kinematically as a series of revolute joints [48], an algorithm based on generalized Newton-Euler models of flexible manipulators [49], the general and unified presentation of dynamic modelling and identification issues of car [50], an efficient method [51] for the calculation of inverse dynamic models of tree structure robots, four methods for identification of inertial parameters of the load of a manipulator [52], dynamic modelling of multi-body systems [53], the modeling, simulation and control of high speed machine tools using robotics formulism [54], [55], has been presented/carried by Khalil et al.

The proposed method is based on following assumptions:

i. The axis of joint (i) will be z_i.

ii. The coordinate frame attached to link *'i'* is fixed with respect to it.

The parameters which define the frame *'i'* have subscript as *'i'*.

a. Demonstration of the Proposed method

Thereafter, proposed method has been demonstrated for three different cases, two cases has been presented here:

Case-I: Open-loop Robot

An open-loop mechanism can be considered as consists of $(n+1)$ links. Base link and terminal link are abbreviated as link (0) and link (n) respectively. Further, joint (i) connects link $(i-1)$ to link (i). The x_i is defined along common perpendicular to z_i and z_{i+1}.

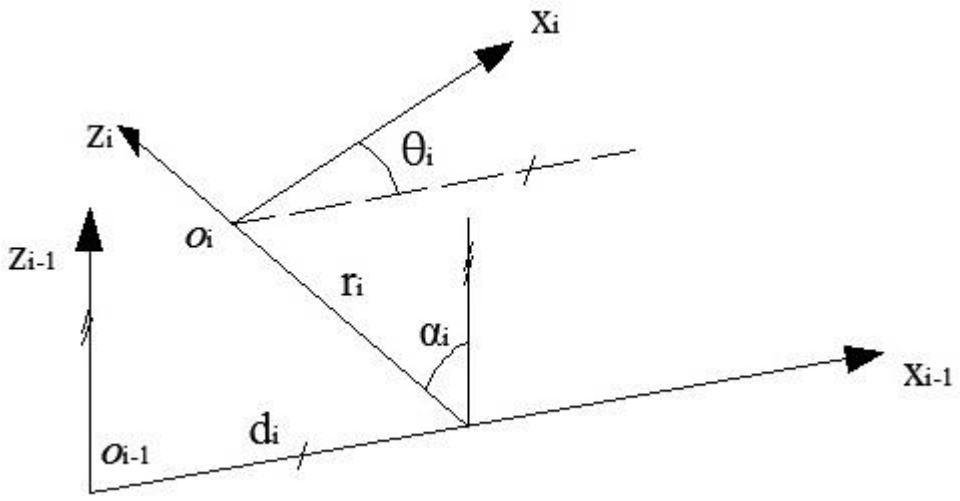

Fig. 2.5: Khalil and Kleinfinger method for binary Links.

Parameters required to define frame *'i'* w.r.t *'i-1'* are as follow:

α_i = angle measured from z_{i-1} to z_i about x_{i-1}.

d_i = distance measured from O_{i-1} to z_i along x_{i-1}.

r_i = distance measured from O_{i-1} to x_{i-1} along z_i.

θ_i = angle measured from x_{i-1} to x_i about z_i.

The proposed method is similar to D-H method. It can be observed from authors reported work that parameters of new method $\theta_i, r_i,\ d_{i+1}$ and α_{i+1} are similar to $\theta_i,\ r_i, d_i,$ α_i respectively of D-H parameter method.

Case-II: Tree-Structure Robot

A Tree-like structured robot can be considered as consists of $(n+1)$ links, (n) joints and (m) end effectors as shown in Fig. 2.6. The link and joints are numbered as follows:

i. Base is considered as link ϕ.
ii. As we goes from base towards end effector the number of links and joints are increasing at each branch.
iii. Link *'i'* is articulated to joint (*i*) that is joint (*i*) connects link (*a* (*i*)), where *'a* (*i*)*'* is the number of link antecedent to the link (*i*) when traversing from base.
iv. Frame 'i' is defined fixed w.r.t the link (*i*) and z_i is the axis of joint (*i*).

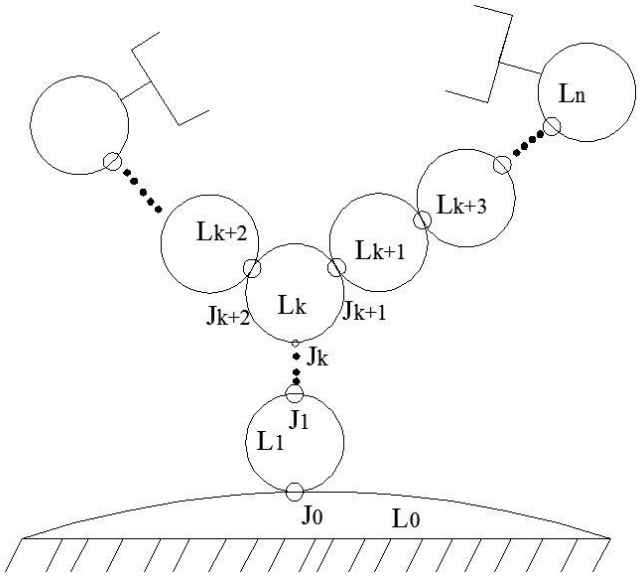

Fig. 2.6: Khalil and Kleinfinger method for tree-like structured robots.

With reference to the Figure 2.7, it can be observed that links have more than two joints. For these cases, frames are defined as follows:

Draw the common perpendicular to joint axes z_i and z_j on the same link, where *i = a* (*j*), (*j = k, l, m…*).

a) Consider one of the common perpendicular as x_i. It is preferred to consider x_i as that corresponding to the common perpendicular of joint on which is articulated longest branch.
b) All other common perpendiculars are denoted by x_i', x_i'' ..... . Hence, some other auxiliary frames R_i' will be defined w.r.t fixed link (i).

Thereafter, transformation matrix defined by using four parameters (θ_i, r_i, d_i, α_i). Rest of the succeeding frames are defined in general as given below:

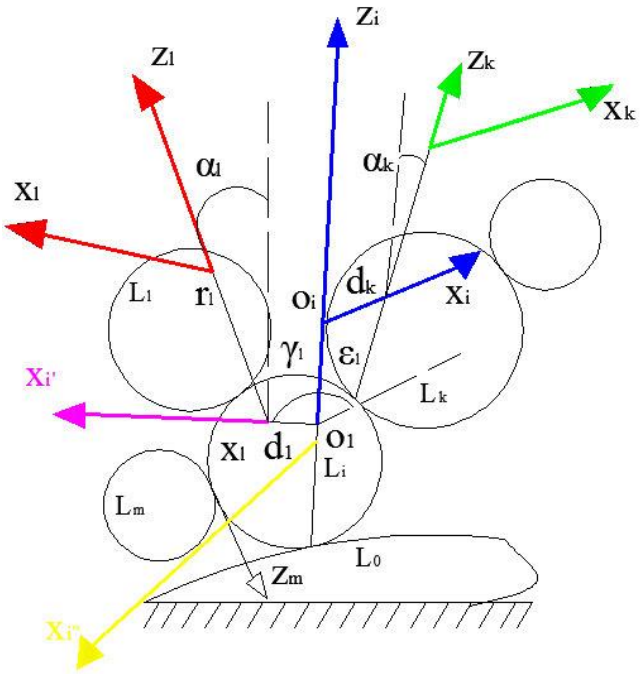

Fig. 2.7: Khalil and Kleinfinger Method for links with more than two joints.

Parameter for links with more than two joints:

γ_j = angle measured from x_i to x_i' about z_i.

ϵ_j = distance measured from O_i to O_i' along z_i.

α_j = angle measured from z_i to z_j about x_i'.

d_j = distance measured from O_i' to z_j.

r_j = distance measured from O_j to x_i'.

θ_j = angle measured from x_i' to x_i about z_j.

For this case, the transformation matrix ${}^{i}_{j}T$ is defined by:

$$ {}^{i}_{j}T = {}^{i}_{i'}T \, {}^{i'}_{j}T \tag{2.9} $$

where ${}^{i}_{i'}T$ = Rot (Z, γ_j) Trans (Z, ϵ_j).

b. Advantages of Khalil and Kleinfinger Method over S-U Method:

As reported by Fluckinger et al. [31, 32].

i. Degree of simplicity is similar to D-H parameter method in case of serial robotic manipulators.
ii. Though the mechanism under consideration is complex, this method uses lesser number of parameters to define shape of link and joint motion.

2.2.4 A Unified Method

This method, developed by Thomas et al. [16], provides a unique representation of spherical or cardan joints involving in a parallel or hybrid manipulator. However, this is not true for the case, when D-H parameter method is applied to same joints, as reported earlier in limitations of D-H method. This method is based on previous work of Belfirore and Benedetto [56]. Belfirore and Benedetto have used graph to represent serial, parallel and hybrid redundant kinematic structures where each joint has one degree of freedom. It has been reported Thomas et al. that there was a boost in industrial applications of parallel manipulators. However, available hardware/software tools related to parallel manipulators are limited or in growing stage. To describe such various manipulators, researchers used their individual methods according to the type of structure. So, it has been observed by Thomas et al. that there was need to propose a method which describe a parallel robotic manipulator, with an unique parameter set, as D-H does in case of serial manipulators. The proposed method is unified in the sense that it can be applied to kinematic description of serial, parallel, hybrid robotic manipulators or articulated machine tools and it is an extension of, most widely used, D-H method.

This method is based on following conventions, for *uniqueness* of extended D-H method:

i. Link *'i'* has origin of coordinate system located at joint $(i+1)$.
ii. Axis of joint $(i+1)$ will be *z-axis*. For spherical joint *z-axis* is assigned to direction given by cross product of joint normal vectors of succeeding and preceding joints.
iii. $x-axis$ of link *'i'* will be collinear to normal of joint and points toward higher indexed joint.
iv. Right hand thumb rule is applied to obtain *y-axis* direction.
v. For one DOF θ_i will be joint variable, if joint has two DOFs θ_i, and β_i are variables, whereas if DOF is three in that case θ_i, β_i and α_i are variables.

Thereafter, proposed method has been applied to spherical and cardan joints having degree of freedom more than one. With this method a spherical joint can be represented by five parameters only instead of twelve as in case of conventional D-H method. Following link coordinate transformation has been used to map frame *'i'* to $(i+1)$:

$$ {}^{i}_{i-1}T = \text{Rot}(z_{i-1}, \theta_i)\ \text{Trans}(z_{i-1}, d_i)\ \text{Rot}(y_{i-1}, \beta_i)\ \text{Trans}(x_i, a_i)\ \text{Rot}(x_i, \alpha_i) \quad (2.10) $$

a. Advantages of Unified Method

i. Proposed method has wide range of applicability.
ii. It provides unique representation of higher degree-of-freedom joints like spherical or cardan joints.
iii. This method uses only five parameters to represent a spherical joint whereas D-H parameter method uses twelve parameters for same.

b. Limitations of Unified Method:

i. Very limited applications to kinematic problems as compared to other methods.

2.2.5 A Simple and Systematic Method

Another method has been proposed by Coke [57] and consists of following two steps:

1. Moving an imagined right handed coordinate base frame, which can be chosen arbitrarily, from manipulator base to end effector executing series of fundamental

translations and rotations. This step is also known as *walk through.* Also, end effector coordinate frame can be chosen arbitrarily.

2. Applying set of algebraic rules to transform these fundamental transformations into form that can be factorized as link transform and which can be represented into standard or modified D-H form. Transformation rules are as follows:

   i. Push the constant terms as far, towards right, as possible using commutative rule which is:

$$T_1(r_1)\, T_2(r_2) \;=\; T_2(r_2)\, T_1(r_1) \tag{2.11}$$

   ii. To transform series of fundamental transformations into standard D-H form, rotations about x or $y-axis$ are transformed to be about $z-axis$ and translations about $y-axis$ are transformed to be about $x\ or\ z\ axes$ as per requirement. To do it transformation rules are as follow:

$$R_x(\, q_i) \;=\; R_y\, R_z(q_i)\, R'_y \tag{2.12}$$

$$R_y(\, q_i) \;=\; R'_x\, R_z(q_i)\, R_x \tag{2.13}$$

$$T_x(q_i) \;=\; R_y\;\; T_z(q_i)\, R'_y \tag{2.14}$$

$$T_y(\, q_i) \;=\; R'_x\;\; T_z(q_i)\, R_x \tag{2.15}$$

   iii. To eliminate undesirable transformations about $y-axis$ use following:

$$R_y(q_i) \equiv R_z\, R_x(q_i)\, R'_z \equiv R'_x\, R_z(q_i)\, R_x. \tag{2.16}$$

$$T_y(q_i) \equiv R_z\, T_z(q_i)\, R'_z \equiv R'_x\;\; T_z(q_i)\, R_x. \tag{2.17}$$

   iv. Joint angle offset, if required, is introduced automatically to have by the chosen zero-angle configuration.

Thereafter, an algorithm has been presented by the Corke for automatic symbolic manipulation. Also, proposed method has been applied to PUMA robot. The proposed method is applicable to serial manipulators only. This method has been used by Minas et al. [58] to propose a systematic notation to quantify anthropomorphism of robot hands.

2.2.6 Quaternion Algebra based Method

A Quaternion algebra based method, for kinematic representation of link shape and joint motion, has been proposed by Sahu et al. [59]. This method is faster because it requires less number of parameters, as compared to method based on homogeneous transformation matrix, to define six degree of freedom. Also, less complications are there in understanding the representations derived with this method. It has been reported by the Sahu et al. that quaternion algebra has been used to represent rigid body translations and rotations. However, it has not been used yet for practical applications of robotic manipulators. So, objective of authors was to develop a novel method, based on quaternion algebra, to represent robot kinematics and an algorithm proposed by the authors is given below:

1. First of all, assign coordinate frame to base and every link.
2. Find the kinematic parameters for links 1 to '*n'*.
3. Calculate the unit vector line which is coincident with common normal between t^{th} and $(t+1)^{th}$ axis and s_t as unit vector line along z-axis of t^{th} joint.
4. The position vector of end effector is given by:

$$P_n = \sum_{t-1}^{n} (d_t s_t + L_t a_{t,t+1}) \tag{2.18}$$

5. The orientation matrix of end effector is given by three vectors given below:

$$n_n = a_{n,n+1} \tag{2.19}$$

$$o_n = s_{n+1} \times a_{n,\ n+1} \tag{2.20}$$

$$a_n = s_{n+1}. \tag{2.21}$$

where

$\theta_t, \alpha_{t,t+1}, L_{t-1}$ and d_t = kinematic parameters of method,

s_t = unit line vector which defines the axis of joint 't',

$a_{t,t+1}$ = define the common perpendicular to the axes of joints t and $(t+1)$,

's' and 'a' = unit vectors along x- and $z-axis$.

The direction of $y - axis$ is given by cross product of 's' and *'a'*.

Applying these steps to any manipulator can be represented kinematically. To illustrate the proposed method, an example of 3R manipulator has been presented by Sahu et al. Thereafter, a comparison of quaternion and homogeneous matrix method, on the basis of calculations required, has been made and it has been reported that quaternion method involves quite less multiplications, additions and subtractions as compared to homogeneous matrix method.

2.2.7 Screw Theory Based Displacement Method

The fundamental transformations (rotation and translation) of a rigid-body can be described by a geometric entity, which is a *screw*. It consists of an axis, about which these transformations are defined, and a scalar *pitch*, which establishes the relationship between rotation and translation. According to this method [6], the motion of a link with respect to its previous link can be represented by a screw ($\$_i$). The position and orientation of a given link can be obtained by using homogeneous transformation matrix $\boldsymbol{A}$.

$$\boldsymbol{A} = \begin{bmatrix} \boldsymbol{R}(\theta) & \vdots & \boldsymbol{p}(t) \\ - & \vdots & - \\ 0 & \vdots & 1 \end{bmatrix} \qquad ()$$

where

$$\boldsymbol{R}(\theta) = \begin{bmatrix} c_\theta + s_x^2(1-c_\theta) & s_y s_x(1-c_\theta) - s_z s_\theta & s_z s_x(1-c_\theta) - s_y s_\theta \\ s_y s_x(1-c_\theta) - s_z s_\theta & c_\theta + s_y^2(1-c_\theta) & s_y s_z(1-c_\theta) - s_x s_\theta \\ s_z s_x(1-c_\theta) - s_y s_\theta & s_y s_z(1-c_\theta) - s_x s_\theta & c_\theta + s_z^2(1-c_\theta) \end{bmatrix} \qquad ()$$

$$\boldsymbol{p}(t) = t\boldsymbol{s} + [\mathbf{I} - \mathbf{R}(\theta)]\boldsymbol{s_0}$$

$\boldsymbol{s}, \boldsymbol{s_0}, \boldsymbol{\theta}$ and $\boldsymbol{t}$ are the Rodrigues parameters.

$\boldsymbol{s}$ is the screw axis and $\boldsymbol{s_0}$ is the position vector of a point in screw axis.

The position and orientation of last link of a kinematic chain consisting of n links can be obtained by pre-multiplication of transformation matrices, given the joints displacements:

$$^0_n\boldsymbol{A} = {}^0_1\boldsymbol{A}\,{}^1_2\boldsymbol{A}\,{}^2_3\boldsymbol{A} \dots\dots\dots\dots\dots\dots {}^{n-1}_n\boldsymbol{A}.$$

Procedure to apply the method:

1. Consider fixed coordinate system with respect to which a screw is to be defined.

2. Define the reference configuration of the chain, relative to which screw parameters $\boldsymbol{s}$ and $\boldsymbol{s_0}$ for each joint to be determined.
3. For each joint, identify Rodrigues parameters $\boldsymbol{s}, \boldsymbol{s_0}, \boldsymbol{\theta}$ and $\boldsymbol{t}$ as well as joint variable.
4. Obtain the homogeneous transformation matrix for each joint.
5. Finally, obtain the position and orientation of last link of kinematic chain by pre-multiplication of matrices obtained in step 4.

Advantages:

1. For kinematic description of robotic manipulators screw based methods uses only two frames for entire chain. However, this is not true in the case of methods like D-H parameter method, Sheth and Uicker method, Khalil and Kleinfinger method etc.

2.2.8 Lie Algebra

The Lie algebra of Lie group of Euclidean motions in E_3 has been explained as the vector space by Dekret and Baska [78]. All sub-algebras and 3-dimensional sub-spaces of A_6 has been described by them. These reported algebras and spaces are orthogonal as these follows the Klein form. Thereafter, kinematic descriptions of these algebras has been presented. The Dekret and Baska have prefer the algebra of vector couples to dual number and dual quaternion technique, because of cleaner geometrical and mechanical interpretation.

2.3 Summary

With reference to above discussion, methods like D-H parameter method and its variants, S-U method, Khalil and Kleinfinger method, A unified method, Quaternion theory based method, screw based displacement methods etc has been found in literature. From this review, it has been observed that for the kinematic description of serial manipulators, the distal variant of D-H parameter method is used most widely, as compared to original D-H parameter method and its proximal variant. However, it leads to ambiguities when applied to parallel, closed-loop or tree like structured robots. Later on, these ambiguities has been removed by method proposed by Sheth and Uicker (S-U), which is the most generalized method, because of its wide range of applicability, for dealing with kinematic problem of any rigid link mechanism. Still, because of its complexity (two number of frames per link for serial chains and non-minimal parameter representation), it is applied to closed-loop

robots only. Thereafter, a new geometric method has been proposed by Khalil and Kleinfinger which is also applicable to open, closed-loop or tree like structured robots and simple to use as compared to S-U method. In literature review performed in this thesis, it has been observed that this method has a wide range of applications. Another method, coined as a Unified method for serial, parallel, hybrid manipulators, has been proposed by Thomas et al. However, its application to kinematic problems is very limited as compared to other methods. The Quaternion theory based method is faster as compared to methods based on homogeneous transformations as it requires lesser number of parameters to define link shape and joint motion. None of the method discussed above has used the two frames for entire chain except screw based method.

Chapter 3

Kinematics of General Serial Manipulators

3.1 Introduction

Robotic manipulators are essentially motion devices [6]. Almost, every robotic application involves the relative motion of links, constituting a robotic manipulator, through the three dimensional Cartesian space ($\mathbb{R}^3$). For example, during a simple manipulation task, end-effector of manipulator has to follow a prescribed path in $\mathbb{R}^3$. However, a robotic manipulator is served in '*n*' dimensional space (*joint space*, $\mathbb{R}^n$), where *'n'* is DOF of manipulator. So, there should be a mathematical model, which transforms Cartesian space into '*n'* dimensional space or vice versa. This process of formulating such kind of models is referred as *kinematic modeling* of robotic manipulators. A kinematic model describes relation between links and joints of a manipulator [6]. Further, with reference to the kinematic analysis of robotic manipulators these models are of two types– i) *forward or direct kinematics:* transformation from joint space to Cartesian space i.e given the joint variables ($\boldsymbol{q}$), find the position ($\boldsymbol{p}$) and orientation ($\boldsymbol{R}$) of tool-tip of end-effector; ii) *inverse or indirect kinematics:* transformation from Cartesian space to joint space i.e given the position ($\boldsymbol{p}$) and orientation ($\boldsymbol{R}$) of tool-tip, find the set of joint variables ($\boldsymbol{q}$), as shown in Fig. 3.1.

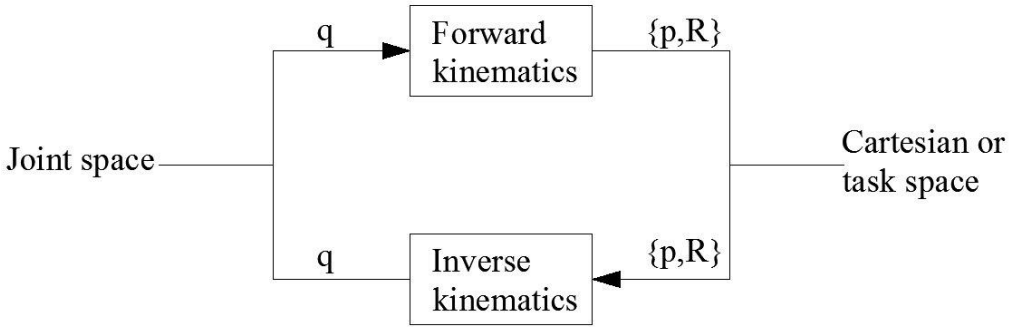

Fig. 3.1: General description of kinematics of robotic manipulators.

In previous chapter, methods describing manipulator kinematics of different classes of manipulators, have been reviewed. Whereas, this chapter deals first, with coordinate mapping and general description of some of key methods describing manipulator kinematics, generally used for forward kinematic modeling. Thereafter, application of described methods to different classes of manipulators and finally, compare how they differ in terms of relative easiness to apply, number of parameters required to define shape of link and joint motion, number of frames required per link and range of applicability.

3.2 Link Coordinate Transformations

To know about the relative position and orientation of different links of a manipulator in $\mathbb{R}^3$, it is required to map the frame attached to an arbitrary point on rigid-link, into base coordinate frame. In literature, two such types of transformations are available and are given as:

3.2.1 Point Transformations

A very usual method of coordinate transformation is the *point* transformations. These are those transformations in which a point in $\mathbb{R}^3$ is transformed (translated or rotated or both) by a homogeneous transformation matrix (4×4). In general, expression of homogeneous coordinate transformation can be written as [60].

$$\boldsymbol{y} = \boldsymbol{A}\,\boldsymbol{x} + \boldsymbol{b} \tag{3.1}$$

$$\boldsymbol{y_1} = \boldsymbol{A_1}\,\boldsymbol{x_1} \tag{3.2}$$

Both Eqns. (3.1) and (3.2) represent the transformation of a point in $\mathbb{R}^3$. In Eqn. (3.1), $\boldsymbol{A}$ is a fundamental rotation matrix, rotating point '$\boldsymbol{x}$' about a given axis and $\boldsymbol{b}$ represents a column matrix translating the same point along specified axes. Whereas in Eqn. (3.2), $\boldsymbol{A_1}$ is a 4×4 homogeneous coordinate transformation matrix, ether rotating, translating or both point $\boldsymbol{x_1}$ in $\mathbb{R}^3$. Homogeneous transformations are discussed in detail in Section 3.3.

3.2.2 Line Transformations

Translation, rotation or both of a line about an axis is known as a line transformation. A line transformation [61] can be represented by any of three representations:

i. dual number, $a + \epsilon\, b$.

ii. complex number, $a + ib$.

iii. double dual number, $a + j\,b$.

Where a and b are ordered real numbers and $i^2 = -1, \epsilon^2 = 0,$ and $j^2 = 1$.

Out of three numbers, dual number has been used by Gu and Luh [60] to describe the coordinate transformations in $\mathbb{R}^3$. In order to transform end-effector coordinate frame to base frame D-H parameters of a given manipulator are needed to be modified, which are as follows.

$$\overline{\theta_k} = \theta_k + \epsilon\, d_k. \tag{3.3}$$

$$\overline{\alpha_k} = \alpha_k + \epsilon\, a_k. \tag{3.4}$$

where

$\overline{\theta_k}$ and $\overline{\alpha_k}$ are known as dual angles.

θ_k, d_k, α_k and a_k are D-H parameters of a given manipulator.

General procedure for dual transformation consists of mainly two steps:

a) First, multiplication of all 3×3 rotation matrices, which transforms orientation of end-effector's frame into base frame:

$$\boldsymbol{R}(\theta, k) \triangleq \begin{bmatrix} 1 & 0 & 0 \\ 0 & c_{\theta_k} & -s_{\theta_k} \\ 0 & s_{\theta_k} & c_{\theta_k} \end{bmatrix}, \qquad \text{for } k = x. \tag{3.5}$$

$$\boldsymbol{R}(\theta, k) \triangleq \begin{bmatrix} c_{\theta_k} & 0 & -s_{\theta_k} \\ 0 & 1 & 0 \\ s_{\theta_k} & 0 & c_{\theta_k} \end{bmatrix}, \qquad \text{for } k = y. \tag{3.6}$$

$$\boldsymbol{R}(\theta, k) \triangleq \begin{bmatrix} c_{\theta_k} & -s_{\theta_k} & 0 \\ s_{\theta_k} & c_{\theta_k} & 0 \\ 0 & 0 & 1 \end{bmatrix}, \qquad \text{for } k = z. \tag{3.7}$$

Thereafter, replace θ_k by $\overline{\theta_k}$ and α_k by $\overline{\alpha_k}$.

b) Second step is to, separate the real and dual part, the general structure of final matrix will be as given below:

$$\bar{M}_0^n = R_0^n[\text{Real part}] + [\text{Dual part}]. \tag{3.8}$$

The real part of final matrix describes the orientation, whereas dual part position of frame attached to end-effector.

3.3 Homogeneous Transformations

The orientation of coordinate frame attached rigidly to a body can be mapped to another coordinate frame by pure rotation matrix (3×3) in $\mathbb{R}^3$. However, the position of the same, which is changing continuously when the body is in motion cannot be defined in $\mathbb{R}^3$ by a matrix of order 3×3. Because, after rotation of frame attached to body the position of origin remains same as it is before rotation, whereas this is not true for the case of displacement of body, resulting into change in position of origin. So, in order to define the position of body-attached frame with respect to some other coordinate frame there is a need for another type of transformation, which is known as *translation* and is defined in four dimensional space ($\mathbb{R}^4$), by means of homogeneous coordinates. Homogeneous coordinates of a point (say) $\boldsymbol{p}$ in $\mathbb{R}^3$, w.r.t an orthonormal coordinate frame {A} in $\mathbb{R}^3$, are denoted as $[\boldsymbol{p}]^A$ and are given as [8]:

$$[\boldsymbol{p}]^A = \sigma[p_1, p_2, p_3, 1]^T \tag{3.9}$$

where p_1, p_2 and p_3 are components of point $\boldsymbol{p}$.

Thus, homogeneous coordinates of a point $\boldsymbol{p}$ in $\mathbb{R}^3$ can be represented by a vector in $\mathbb{R}^4$. Where, fourth component σ is a non-zero scale factor and it can have any value, which results in generation of same physical space. Hence, homogeneous coordinates are not unique.

Homogeneous transformation was introduced by Maxwell and are used to describe the transformations of point vectors in three dimensional space [13]. These transformations are the *point* transformations. Now, to transform a physical point, defined in its homogeneous coordinates in $\mathbb{R}^3$, from one coordinate frame to other coordinate frame a 4×4 homogeneous coordinate transformation matrix is used and is defined as:

$$\mathrm{T} \triangleq \begin{bmatrix} \boldsymbol{R} & \boldsymbol{p} \\ \boldsymbol{\eta}^T & \sigma \end{bmatrix} \tag{3.10}$$

where

$\boldsymbol{R}$ is a 3×3 matrix representing orientation of frame to be rotated w.r.t frame into which it is being rotated.

$\boldsymbol{p}$ is a 3×1 column vector representing position of frame to be translated w.r.t frame into which it is being translated.

$\boldsymbol{\eta}^T$ is perspective vector which specify a point of perspective for visual sensing with camera. It has non-zero value in case of overhead camera transformations.

3.3.1 Homogeneous Rotation and Translation

An elementary rotation or translation can be regarded as a special case of 4×4 homogeneous transformation matrix. Consider {A}, {B} are two orthonormal coordinate frames, initially coincident, now:

i. if we rotate frame {B} through an angle θ about i^{th} unit vector of frame {A}, the same can be represented in terms of homogeneous coordinates by 4×4 matrix denoted by Rot (θ, i) and is pronounced as i^{th} *elementary homogeneous rotation matrix*:

$$ {}^{A}_{B}[\mathbf{Rot}\ (\boldsymbol{\theta}, \boldsymbol{i})\ ] \triangleq \begin{bmatrix} & [\boldsymbol{R_i}(\boldsymbol{\theta})]_{3\times3} & & 0 \\ & & & 0 \\ & & & 0 \\ 0 & 0 & 0 & 1 \end{bmatrix} \quad 1 \leq i \leq 3; \qquad (3.11) $$

Where

$[\boldsymbol{R_i}(\boldsymbol{\theta})]_{3\times3}$ is the elementary rotation matrix about i^{th} unit vector.

ii. For elementary translation of origin of frame {B} relative to the origin of frame {A}, say by amount t_i along i^{th} unit vector of frame {A} following 4×4 homogeneous transformation matrix is used:

$$ {}^{A}_{B}[\mathbf{Trans}\,(\boldsymbol{q})] \triangleq \begin{bmatrix} 1 & 0 & 0 & | & t_i \\ 0 & 1 & 0 & | & 0 \\ 0 & 0 & 1 & | & 0 \\ \hline 0 & 0 & 0 & | & 1 \end{bmatrix} \tag{3.12} $$

iii. Simultaneous rotation and translation homogeneous transformation matrix can be written as:

$$ {}^{A}_{B}[\mathbf{T}] \triangleq \begin{bmatrix} & [\boldsymbol{R}_i(\theta)]_{3\times3} & & | & t_i \\ & & & | & t_j \\ \hline 0 & & 0 & | & t_k \\ & & & | & 1 \end{bmatrix} \tag{3.13} $$

iv. A point $\boldsymbol{p}$ defined in local coordinate frame {A}, can be defined in global coordinate frame using homogeneous transformation as:

$$ {}^{B}\boldsymbol{p} = {}^{B}_{A}\mathbf{T}\ {}^{A}\boldsymbol{p} \tag{3.14} $$

3.3.2 Limitations of Homogeneous Transformations:

1. Since, homogeneous transformations are the point transformations [60], therefore it cannot represent combination of linear and angular quantities by lines in $\mathbb{R}^3$.
2. As reported by Nicolas et al. [13]
   i. Homogeneous transformation matrix is highly redundant. Because, it uses twelve parameters to represent six degree of freedom. Out of twelve, nine parameters are used to describe orientation of body, whereas, remaining three are used to define its position in $\mathbb{R}^3$. However, other methods like based on Lie algebra and dual quaternion uses three and four parameters respectively, to describe orientation of body.
   ii. In case of manipulators with more than three degree of freedom, homogeneous transformation takes more computational time as compared to methods based on Lie algebra or dual quaternion theory.
3. Homogeneous transformations are less efficient, compact and elegant as compared to method based on quaternion theory, as pointed out by Funda, Taylor and Paul [62].

3.4 Forward Kinematics

The process of obtaining the tool configuration vector (describing position and orientation) of robotic end-effector, when joint variables are given is known as forward or direct kinematics. The objective of this formulation is to design and simulate kinematic chains [6]. Also, forward kinematics can be defined as the transformation from joint space ($\mathbb{R}^n$) to three-dimensional task space ($\mathbb{R}^3$) [8].The importance of forward kinematics lies in the fact that all practical applications of robotic manipulators are based on inverse kinematic models i.e knowing the position and orientation of robotic end-effector for a given configuration, joint variable are obtained. So, for that purpose formulation of forward kinematic model is prerequisite.

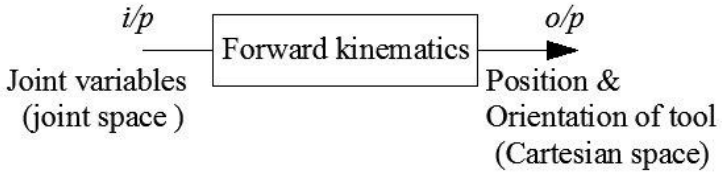

Fig. 3.2: Description of forward kinematics.

Now, to derive forward kinematic model, the most widely used method is the Denavit and Hartenberg method [31]. This is because of its minimal parameter representation. Further, this method is based on homogeneous transformations, which involves only multiplication of transformation matrices to obtain mapping from end-effector to base of the manipulator. According to this method first, an algorithm proposed by Denavit and Hartenberg is applied to line diagram of a given manipulator. Thereafter, corresponding D-H parameters are obtained and finally, *'n'* multiplications of transformation matrices according to distal variant, $(n + 1)$ multiplications according to proximal variant are performed to transform end-effector tip into base coordinates of manipulator. However, it is applicable to serial manipulators only. So, for the case of closed-loop, tree like robot structures S-U method can be used. Also, other methods discussed in previous chapter can be used for kinematic modelling.

3.5 Open-loop Robot

A kinematic chain or robotic manipulator can be stated as an open-loop if, out of its two ends, first end is connected to a link (usually fixed link) and second end (attached with an *end-effector*) is free to move in $\mathbb{R}^3$. Under this section, first, general description of open-loop robots has been presented. Thereafter, kinematic analysis of some standard industrial manipulators has been performed by two variants of original D-H parameter method and modified D-H parameter method (S-U method). The standard industrial manipulators includes 4-axis SCARA robot, 5-axis articulated robot (Microbot Alpha-2, Rhino XR-3) and 6-axis PUMA 560 etc. Corresponding schematic representations has been presented, describing the geometrical configuration of robotic structures. Also, D-H parameters describing the shape of a link and joint motion are calculated according to guidelines of a given method and are given in tabular form.

3.5.1 General Description

An open-loop robotic manipulator can be imagined as an arrangement of $(n+1)$ rigid links, as shown in Fig. 3.3. Out of total number of links, 1st one is usually a fixed link whereas remaining $'n'$ are moving links.

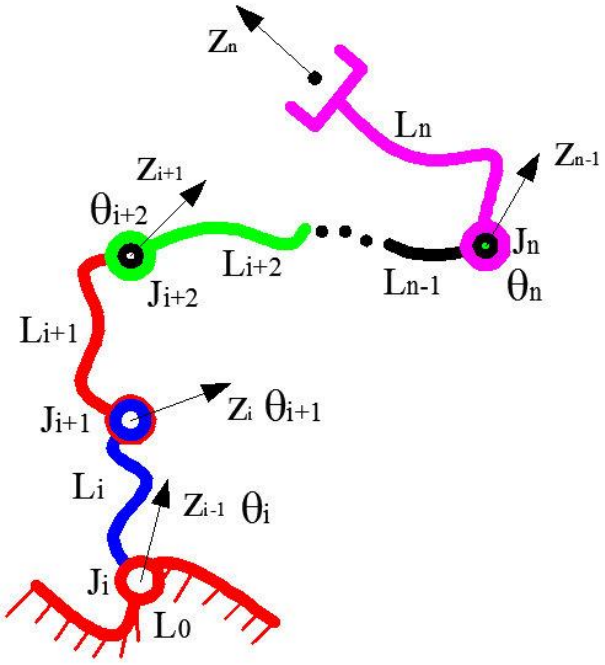

Fig. 3.3 General description of an open-loop robotic manipulator.

With reference to Figure 3.3, joint, J_i connects link L_i and L_{i-1}. Thereafter, link-frame's $z-axis$ is assigned to different links according to the distal variant of D-H parameter method. Thereafter, tool-tip frame is mapped to base frame by using homogeneous transformations [15]:

$$ {}^{0}_{n}A\,(q) \quad = \quad {}^{i-1}_{i}A\,(q_i)\ {}^{i}_{i+1}A\,(q_{i+1}) \ldots {}^{n-1}_{n}A\,(q_{j+1}) \tag{3.15} $$

3.5.2 Examples

i. Applications of Distal variant

a) Four-axis SCARA robot: - The acronym SCARA stands for *Selective Compliance Assembly Robot Arm* [8]. It consists of one fixed link (L_0, in red) and four moving links (L_1, L_2, L_3 and L_4), providing four independent motions in Cartesian space (R^3). The kinematic configuration of this robot has been described in Fig. 3.4.

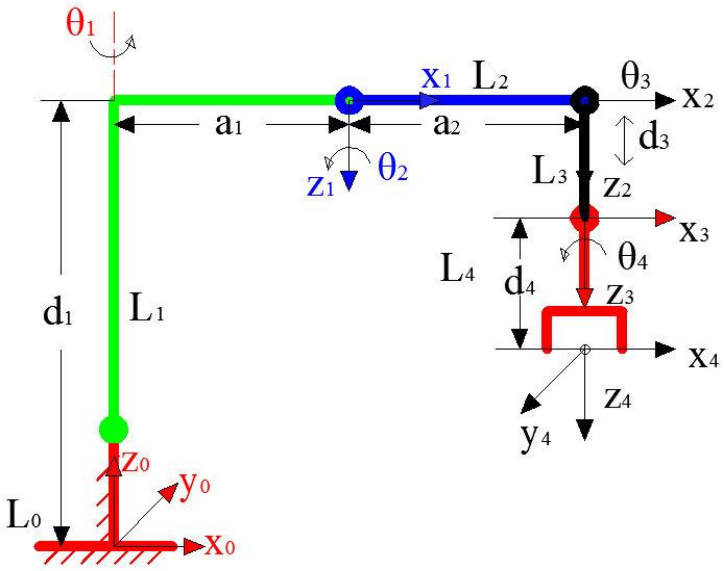

Fig. 3.4: Description of 4-axis SCARA robot according to distal variant.

There are two types of pairs between these links– i) revolute, between links $(L_0, L_1), (L_1, L_2)$ and (L_3, L_4); ii) a prismatic pair, between links L_2, L_3. Link-frames are assigned using distal variant of D-H parameter method. The corresponding link parameters and joint parameters are as shown in Fig. 3.4 and are given in Table 3.1. Major

application of this robot is pick and place operations.

Table 3.1: Distal variant D-H parameters of SCARA robot.

S. No.	Link Length (a_{i-1}) (mm)	Link Twist (α_{i-1}) (deg.)	Joint offset (d_i) (mm)	Joint angle (θ_i) (deg.)	Home position
1.	a_1	α_1 = 180;	d_1	θ_1	0
2.	a_2	α_2 = 0;	d_2 = 0;	θ_2	0
3.	a_3 = 0;	α_3 = 0;	d_3	θ_3 = fixed	d
4.	a_4 = 0;	α_4 = 0;	d_4	θ_4	0

b) Five-axis articulated robot: - A manipulator whose kinematic configuration resembles very closely to the human arm anatomy, is 5-axis articulated robot. It consists of one fixed (marked as L_0) and four moving links (L_1, L_2, L_3 and L_4). All joints are of revolute type. At last link, usually known as end-effector, two motions (pitch and roll) can be observed. Two examples of this robot can be reported, these are– i) Microbot Alpha II; ii) Rhino XR-3 [8]. Both of these manipulators has same kinematic configuration. It has been observed while calculating D-H parameters, that these parameters are same for both and are given in Table 3.2.

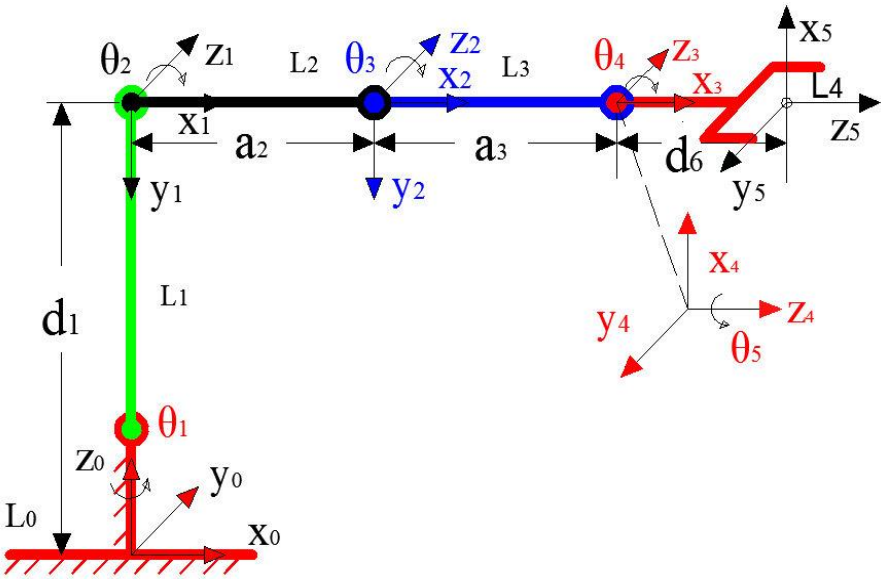

Fig. 3.5: Description of 5-axis articulated robot according to distal variant.

Table 3.2: Distal variant parameters of 5-axis articulated arm.

S. No.	Link Length (a_{i-1}) (mm)	Link Twist (α_{i-1}) (deg.)	Joint offset (d_i) (mm)	Joint angle (θ_i) (deg.)	Home position
1.	a_1 = 0;	α_1 = - 90;	d_1	θ_1	0
2.	a_2	α_2 = 0;	d_2 = 0;	θ_2	0
3.	a_3	α_3 = 0;	d_3 = 0;	θ_3	0
4.	a_4 = 0;	α_4 = - 90;	d_4 = 0;	θ_4	+ 90
5.	a_5 = 0;	α_5 = 0;	d_5	θ_5	0

ii. Applications of Proximal variant

a) Four-axis SCARA robot: - The kinematic configuration of this robot has been described in the previous section, in applications of distal variant. However, the link-frame assignment and D-H parameters calculation has been carried out in this example according to proximal variant, as shown in Fig. 3.6. The calculated D-H parameters are given in Table 3.4.

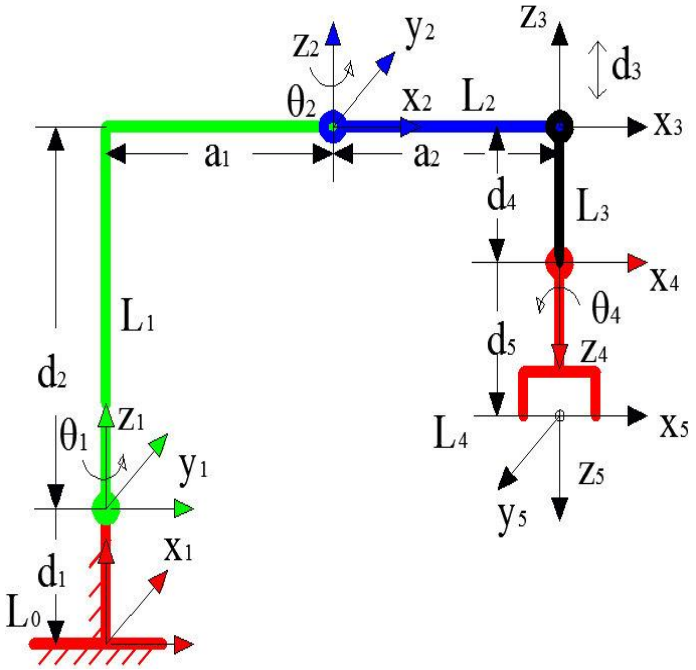

Fig. 3.6: Description of 4-axis SCARA robot according to proximal variant.

Table 3.3: Proximal variant D-H parameters of SCARA robot.

S. No.	Link Length (a_{i-1}) (mm)	Link Twist (α_{i-1}) (deg.)	Joint offset (d_i) (mm)	Joint angle (θ_i) (deg.)	Home position
1.	a_0 = 0;	α_0 = 0;	d_1	θ_1	0
2.	a_1	α_1 = 0;	d_2	θ_2	0
3.	a_2	α_2 = 0;	d_3 = variable	θ_3 = fixed	0
4.	a_3 = 0;	α_3 = 180;	d_4	θ_4	0
5.	a_4 = 0;	α_4 = 0;	d_5	–	–

b) Five-axis articulated robot: - With reference to Figure 3.7, link diagram of a 5-axis articulated arm is as shown in assumed home position. In this case, link frame assignment and D-H parameters are described using proximal variant of D-H parameter method. The corresponding D-H parameters are given in Table 3.4.

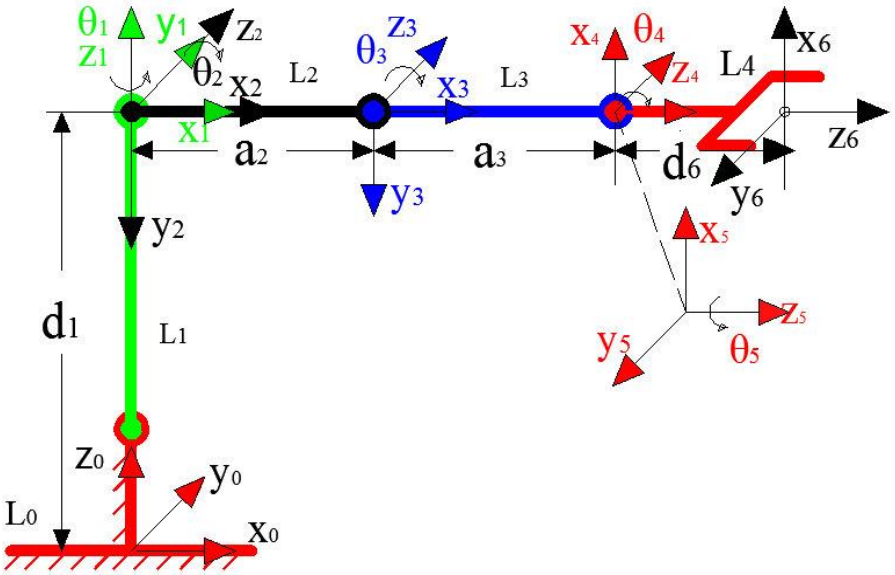

Fig. 3.7: Description of 5-axis articulated robot according to proximal variant.

Table 3.4: Proximal variant D-H parameters of articulated arm.

S. No.	Link Length (a_{i-1}) (deg.)	Link Twist (α_{i-1}) (deg.)	Joint offset (d_i) (mm)	Joint angle (θ_i) (deg.)	Home position
1.	a_0 = 0;	α_0 = 0;	d_1	θ_1	0
2.	a_1 = 0;	α_1 = -90;	d_2 = 0;	θ_2	0
3.	a_2	α_2 = 0;	d_3 = 0;	θ_3	0
4.	a_3	α_3 = 0;	d_4 = 0;	θ_4	+ 90
5.	a_4 = 0;	α_4 = -90;	d_5 = 0;	θ_5	0
6.	a_5 = 0;	α_5 = 0;	d_6;	–	–

c) Six-axis PUMA 560 robot: - The Unimation PUMA 560 is a six DOF robot [2]. It consists of one fixed (L_0) and four moving links (L_1, L_2, L_3 and L_4). All joints are of revolute type. The end-effector of this robot has Roll-Pitch-Roll motion. The axes about which these motions takes place intersect at a point and three frames one for each, are assigned at this point. Fig. 3.8, describes link-frame assignment and marked D-H parameters (refer Table 3.6) according to proximal variant.

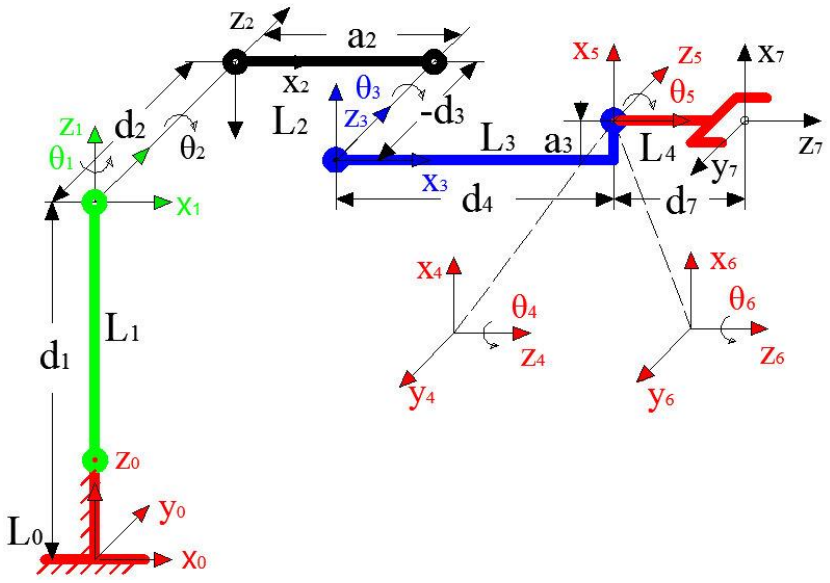

Fig. 3.8: Description of 6-axis Puma 560 robot according to proximal variant.

Table 3.5: Proximal variant D-H parameters of PUMA 560 robot.

S. No.	Link Length (a_{i-1}) (mm)	Link Twist (α_{i-1}) (deg.)	Joint offset (d_i) (mm)	Joint angle (θ_i) (deg.)	Home position
1.	$a_0 = 0$;	$\alpha_0 = 0$;	d_1	θ_1	0
2.	$a_1 = 0$;	$\alpha_1 = -90$;	d_2	θ_2	0
3.	a_2	$\alpha_2 = +90$;	$d_3 = 0$;	θ_3	-90
4.	a_3	$\alpha_3 = -90$;	d_4	θ_4	0
5.	$a_4 = 0$;	$\alpha_4 = +90$;	$d_5 = 0$;	θ_5	0
6.	$a_5 = 0$;	$\alpha_5 = -90$;	$d_6 = 0$;	θ_6	0
7.	$a_6 = 0$	$\alpha_6 = 0$	d_7	–	–

i. Applications of S-U method

a) Four-axis SCARA robot: - With reference to Figure 3.9, an example of S-U method has been presented. According to Sheth and Uicker, first, link-frames are assigned thereafter, S-U parameters are calculated given in Table 3.7. Two frames to each link has been assigned first at its proximal and second at distal ends respectively.

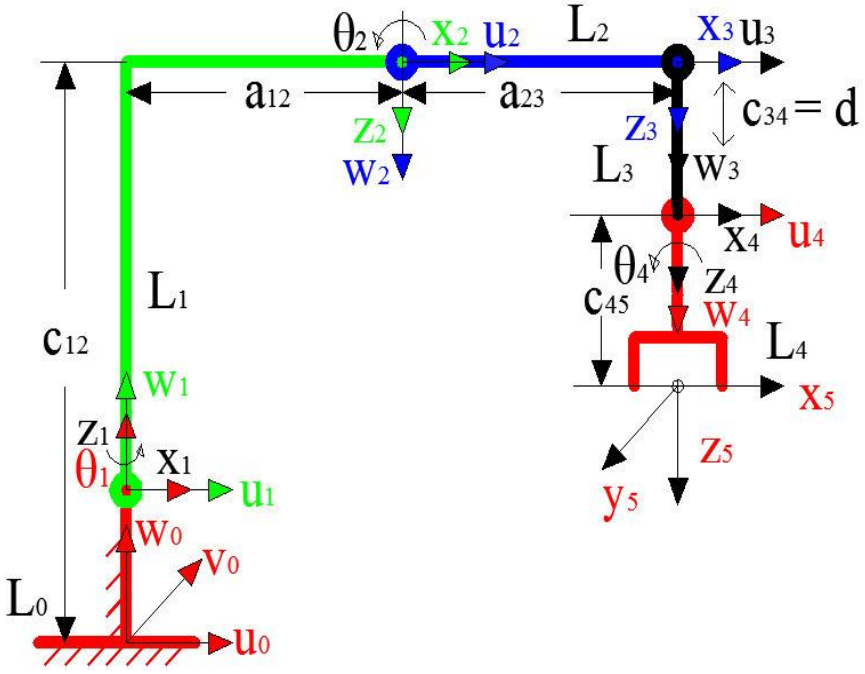

Fig. 3.9: Description of 4-axis SCARA robot according to S-U method.

Table 3.6: S-U parameters of 4-axis SCARA robot.

S. No.	(a_{jk}) (mm)	(α_{jk}) (deg.)	(b_{jk}) (mm)	(β_{jk}) (deg.)	(c_{jk}) (mm)	(γ_{jk}) (deg.)	(θ_i) (deg.)	Home position
1.	a_{12}	α_{12} = 180;	b_{12} = 0;	β_{12} = 0;	c_{12}	γ_{12} = 0;	θ_1	0
2.	a_{23}	α_{23} = 0;	b_{23} = 0;	β_{23} = 0;	c_{23} = 0;	γ_{23} = 0;	θ_2	0
3.	a_{34} = 0;	α_{34} = 0;	b_{34} = 0;	β_{34} = 0;	c_{34}	γ_{34} = 0;	θ_3 = fixed	d
4.	a_{45} = 0;	α_{45} = 0;	b_{45} = 0;	β_{45} = 0;	c_{45}	γ_{45} = 0;	θ_4	0

a) 5-axis articulated robot: - Figure 3.10, represents the application of S-U method to five-axis articulated. The link-frame assignment and S-U parameters (given in Table 3.8) are as shown.

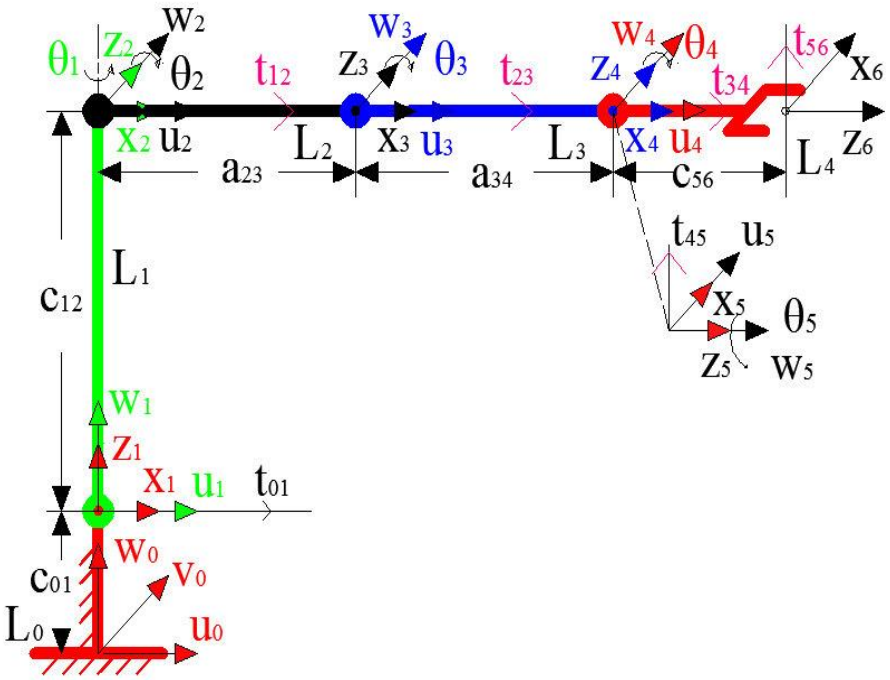

Fig. 3.10: Description of 5-axis articulated robot according to S-U method.

Table 3.7: S-U parameters of 5-axis articulated arm.

S. No.	(a_{jk}) (mm)	(α_{jk}) (deg.)	(b_{jk}) (mm)	(β_{jk}) (deg.)	(c_{jk}) (mm)	(γ_{jk}) (deg.)	(θ_i) (deg.)	Home position
1.	a_{01} = 0;	α_{01} = 0;	b_{01} = 0;	β_{01} = 0;	c_{01}	γ_{01} = 0;	–	–
2.	a_{12} = 0;	α_{12} = -90;	b_{12} = 0;	β_{12} = 0;	c_{12}	γ_{12} = 0;	θ_1	0
3.	a_{23}	α_{23} = 0;	b_{23} = 0;	β_{23} = 0;	c_{23} = 0;	γ_{23} = 0;	θ_2	0
4.	a_{34}	α_{34} = 0;	b_{34} = 0;	β_{34} = 0;	c_{34} = 0;	γ_{34} = 0;	θ_3	0
5.	a_{45} = 0;	α_{45} = -90;	b_{45} = 0;	β_{45} = -90;	c_{45} = 0;	γ_{45} = -90;	θ_4	0
6.	a_{56} = 0;	α_{56} = 0;	b_{56} = 0;	β_{56} = -90;	c_{56}	γ_{56} = 90;	θ_5	0

3.6 Closed-loop Robot

A robotic manipulator can be stated as a closed-loop manipulator, if links constituting a kinematic chain are connected in such a way so as to form closed-loop (s). The total number of loops being formed can be calculated, knowing the number of moving links and joints, according to expression given below [63]:

$$L = J - (N - 1) \tag{3.16}$$

where

L = total number of closed-loop (s) formed.

J = total number of joints.

$N = n + 1$, total number of links.

3.6.1 General Description

A closed-loop robotic manipulator may be imagined as an arrangement of $(n + 1)$ rigid links, as shown in Fig. 3.11. Out of total number of links, 1st one is usually a fixed link whereas remaining $'n'$ are moving links. As observed, in previous chapter (literature review) that conventional D-H parameter method leads to ambiguities for the case of closed-loop manipulators. However, the same can be extended to closed-loop robots by cutting it at a joint which is not actuated.

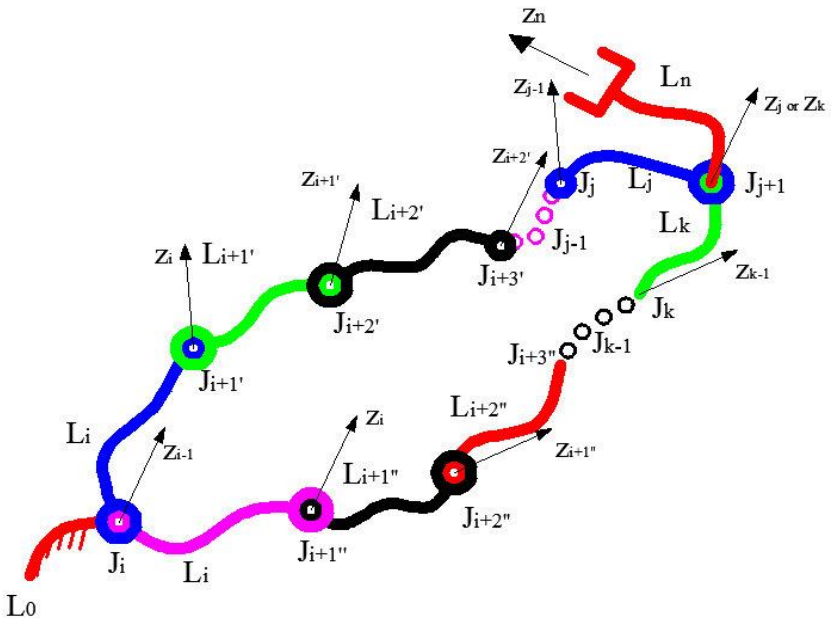

Fig. 3.11: Schematic representation of basic structure of closed-loop robot.

In other words, a closed kinematic chain may be considered as an open chain by removing a joint, one which is not actuated. So, assuming chain is cut or opened at a joint which is between links (say) 'j' and 'k'. Now, conventional D-H algorithm can be applied to it. With reference to Figure 3.11, link numbering, link-frame description and D-H parameters (refer Table) of a closed-loop robot are as shown. For the placement of link-frame, frame 'i' is placed at joint $(i+1)$ according to the D-H parameter method [15]. According to this convention frames are marked in Fig. 3.11. Thereafter, homogeneous coordinate transformations can be applied to transform tool-tip point ($n^{th}\ frame$) to base frame ($0^{th}\ frame$) and this process of transformation is as follows [15]:

i. First of all, transform either frame 'j' or 'k' to frame $(i-1)$. Eqns. (3.17) and (3.18) gives transformation of, frame *'j'* into frame $(i-1)$ and frame *'k'* into frame $(i-1)$ respectively.

$$ {}^{i-1}_{j}\boldsymbol{A}(\boldsymbol{q'}) = {}^{i-1}_{i}\boldsymbol{A}\,(q_i)\ {}^{i}_{i+1'}\boldsymbol{A}\,(q_{i+1'})\ {}^{i+1'}_{i+2'}\boldsymbol{A}\,(q_{i+2'}) \dots\dots\ {}^{j-1}_{j}\boldsymbol{A}\,(q_j) \qquad (3.17) $$

$$ {}^{i-1}_{k}\boldsymbol{A}(\boldsymbol{q'}) = {}^{i-1}_{i}\boldsymbol{A}\,(q_i)\ {}^{i}_{i+1''}\boldsymbol{A}\,(q_{i+1''})\ {}^{i+1'}_{i+2''}\boldsymbol{A}\,(q_{i+2''}) \dots\dots\ {}^{k-1}_{k}\boldsymbol{A}\,(q_k) \qquad (3.18) $$

ii. Thereafter, transform tool-tip frame (n^{th} frame) to $(i-1)^{th}$ frame as given below:

$$ {}^{i-1}_{n}\boldsymbol{A}\,(\boldsymbol{q'}) = {}^{i-1}_{j}\boldsymbol{A}\,(q')\ {}^{j}_{n}\boldsymbol{A}\,(q_{j+1}) \qquad (3.19) $$

$$ {}^{i-1}_{n}\boldsymbol{A}\,(\boldsymbol{q}') \;=\; {}^{i-1}_{k}\boldsymbol{A}\,(q')\;{}^{k}_{n}\boldsymbol{A}\,(q_{k+1}) \tag{3.20} $$

iii. And finally, transform n^{th} frame to base frame:

$$ {}^{b}_{n}\boldsymbol{A}\,(\boldsymbol{q}') \;=\; {}_{i-1}{}^{b}\boldsymbol{A}\,(q=c)\;{}^{i-1}_{n}A\,(\boldsymbol{q}') \tag{3.21} $$

The following position and orientation constraints can be observed on closed-loop robot:

If joint $(j+1)$ between links '*j'* and *'k'* is *revolute* constraints are:

$$ {}_{i-1}{}^{j}\boldsymbol{R}\,(q')\,({}^{i-1}_{j}\boldsymbol{p}\,(q') - {}^{i-1}_{k}\boldsymbol{p}\,(q'')) \;=\; [0 \quad 0 \quad d_{jk}]^{T} \tag{3.22} $$

$$ z_j^{i-1}\,(\boldsymbol{q}') \;=\; z_k^{i-1}\,(q'') \tag{3.23} $$

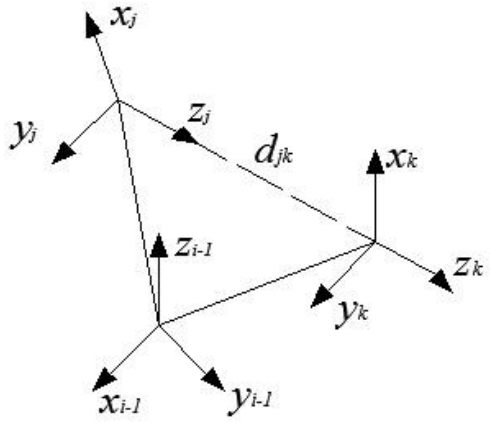

Fig. 3.12: Transformations between frames *'j'* and *'k'*.

If joint $(j+1)$ between links '*j'* and *'k'* is *prismatic* constraints are:

$$ \begin{bmatrix} x_j^{i-1}\,(q') \\ y_j^{i-1}\,(q') \end{bmatrix} (\boldsymbol{p}_j^{i-1}(\boldsymbol{q}') - \boldsymbol{p}_k^{i-1}\,(q'')) \;=\; \begin{bmatrix} 0 \\ 0 \end{bmatrix} \tag{3.24} $$

$$ z_j^{i-1}\,(q') \;=\; z_k^{i-1}\,(q'') \tag{3.25} $$

$$ x_j^{(i-1)T}\,(\boldsymbol{q}')\;x_k^{(i-1)T}\,(q'') \;=\; \cos v_{jk} \tag{3.26} $$

3.6.2 Example

An example, of a parallelogram linkage, has been presented to demonstrate the application of conventional D-H parameter method to a closed-loop robot. Figure 3.13 shows a closed-loop robot, constitutes of one fixed (L_0) and four moving links ($L_{1\prime}, L_{2\prime}, L_{3\prime}$ and $L_{1\prime\prime}$). A closed-loop can be observed between links $L_0, L_{1'}, L_{2'}, L_{3'}$ and $L_{1\prime\prime}$. In order to apply D-H algorithm, chain can be supposed to be opened at joint between links $L_{3\prime}$ and $L_{1\prime\prime}$. Thereafter, link-frames are assigned and corresponding D-H parameters are calculated by applying D-H parameter method

Next, following the transformation Eqn. given above for closed loop robot mapping between tool-tip frame and base frame can be derived [15].

i. First, transform frame $(3')$ into frame (0) given as ${}^{0}_{3'}\boldsymbol{A}\,(\boldsymbol{q}')$, where $\boldsymbol{q}' = [\theta_{1'}, \theta_{2'}, \theta_{3'}]^T$.

$$ {}^{0}_{3'}\boldsymbol{A}\,(\boldsymbol{q}') = {}^{0}_{1'}\boldsymbol{A}\,(\theta_{1'})\ {}^{1'}_{2'}\boldsymbol{A}\,(\theta_{2'})\ {}^{2'}_{3'}\boldsymbol{A}\,(\theta_{3'}) \tag{3.27} $$

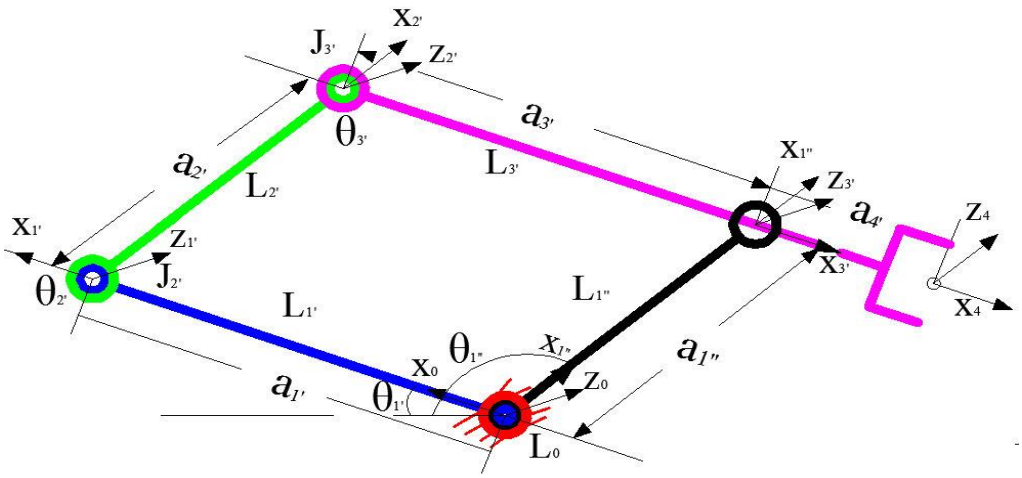

Fig. 3.13: Parallelogram Linkage with assigned link frames and marked D-H parameters.

ii. Thereafter, transform $(1'')$ into frame (0) given as

$$ {}^{0}_{1''}\boldsymbol{A}\,(\theta_{1''}) \;=\; \left[\begin{array}{ccc|c} c_{1''} & -s_{1''} & 0 & a_{1''}\,c_{1''} \\ s_{1''} & c_{1''} & 0 & a_{1''}\,s_{1''} \\ \hline 0 & 0 & 1 & 0 \\ \hline 0 & 0 & 0 & 1 \end{array}\right] \tag{3.28} $$

iii. Next, to complete the mapping, transform tool frame (4^{th}) into frame ($3'^{rd}$), which is a constant transformation as there is no any actuated joint motion at connection between links ($3'$) and ($1''$).

$$ {}^{3'}_{4}\boldsymbol{A}\,(0) \;=\; \left[\begin{array}{ccc|c} 1 & 0 & 0 & a_4 \\ 0 & 1 & 0 & 0 \\ \hline 0 & 0 & 1 & 0 \\ \hline 0 & 0 & 0 & 1 \end{array}\right] \tag{3.29} $$

iv. Since, joint between links $L_{3'}$ and $L_{1''}$ is revolute, therefore position constraints are:

$$ \left(\boldsymbol{p}^{0}_{3'}\,(\boldsymbol{q}') - \boldsymbol{p}^{0}_{1''}\,(q'')\right) \;=\; \begin{bmatrix} 0 \\ 0 \\ 0 \end{bmatrix} \tag{3.30} $$

Here, $d_{3'1''} = 0$, which is distance along $z_{1''}$ or $z_{3'}$.

v. Orientation constraints can be satisfied independent of q' and q''. Since, $a_{1'} = a_{3''}$ and $a_{2'} = a_{1''}$, so following two independent constraints can be extracted:

$$ a_{1'}\,(c_{1'} + c_{1'2'3'}) + a_{1''}\,(c_{1'2'} - c_{1''}) \;=\; 0 \tag{3.31} $$

$$ a_{1'}\,(s_{1'} + s_{1'2'3'}) + a_{1''}\,(s_{1'2'} - s_{1''}) \;=\; 0 \tag{3.32} $$

Now, in order to satisfy above constraints for any value of $a_{1'}$ or $a_{1''}$. From Figure. 3.13, it can be observed that:

$$ \theta_{2'} \;=\; (\theta_{1''} - \theta_{1'}) \tag{3.33} $$

$$ \theta_{3'} \;=\; \pi - \theta_{2'} = \pi - \theta_{1''} + \theta_{1'} \tag{3.34} $$

From expressions of $\theta_{2'}$ and $\theta_{3'}$, it can be observed that both depends upon $\theta_{1'}$ and $\theta_{1''}$.

Thus, joint vector $\boldsymbol{q'} = [\theta_{1'} \quad \theta_{1''}]$. Substituting (17, 18) in ${}^{0}_{3'}\boldsymbol{A}\,(\boldsymbol{q'})$ and deriving final transformation matrix ${}^{0}_{4}A\,(q')$:

$$ {}^{0}_{4}\boldsymbol{A}\,(\boldsymbol{q'}) \quad = \quad {}^{0}_{3'}\boldsymbol{A}\,(\boldsymbol{q'})\ {}^{3'}_{4}\boldsymbol{A}\,(0) \tag{3.35}$$

Table 3.8: D-H parameter of parallelogram linkage.

S. No.	Link Length (a_i)	Link Twist (α_i) (deg.)	Joint offset (d_i)	Joint angle (θ_i)	Home (deg.)
1.	$a_{1'}$	$\alpha_1 = 0$;	$d_1 = 0$;	$\theta_{1'}$	0
2.	$a_{2'}$	$\alpha_2 = 0$;	$d_2 = 0$;	$\theta_{2'}$	-30
3.	$a_{3'}$	$\alpha_3 = 0$;	$d_3 = 0$;	$\theta_3{}'$	-60
4.	$a_{1''}$	$\alpha_{1''} = 180$;	$d_{1''} = 0$;	$\theta_{1''}$	-120
5.	$a_{4'}$	$\alpha_{4'} = 0$;	$d_{4'} = 0$;	–	–

3.7 Observations

The following observations can be drawn from above illustrated schematic diagrams of standard manipulators:

1. Both, proximal and distal variants of D-H parameter method use one frame per link. However, S-U method uses two frames per link.
2. To provide geometric description to a manipulator having *n*-DOFs the number of coordinate frames required according to distal, proximal variants and S-U method are $n,\ n+1\ \ and\ (n \times 2 + 2)$ respectively.
3. A contradiction between two statements has been observed in case of distal variant when being applied to PUMA 560 manipulator. However, both statements are satisfied in case of proximal variant of D-H notation. These statements are as follow [2]:
   i. The point on **body** whose position needs to be described, can be chosen arbitrarily. However, for our convenience, point on body whose position we want to describe is chosen as body-attached frame.
   ii. Find the common perpendicular between i^{th} and $(i+1)^{th}$ joint axes, or their point of intersection. At the point of intersection or at the point where common perpendicular meets the i^{th} axis, assign the link-frame origin.

Table 3.9: Comparison of different robot kinematics methods.

Parameter (s)	Method (s)				
	Distal variant	**Proximal variant**	**S-U method**	**K-K method [31]**	**Screw Based method**
f	n	$(n+1)$	$(n \times 2 + 2)$		2
p	4	4	7	4 or 6	7
r	Serial	Serial	Any	Any	–
c	Less	Less	More	Less	

In above table,

f = Number of frames for given manipulator.

p = Number of parameters used by a method to describe a manipulator.

r = Range of applicability.

c = Complexity of method.

4. Both, proximal and distal variants of D-H parameter method use four parameters to describe link-shape and joint motion in three dimensional Cartesian space. However, S-U method uses seven parameters to describe the same.
5. Because of more number of parameters used S-U method is more time consuming as compared to other methods, that is why used only for closed loop robots.

3.8 Summary

In this chapter, forward kinematics of open- as well as closed-loop robotic manipulators has been presented. First, general description of these manipulators has been given, using two variants (distal and proximal) of D-H parameter method and S-U method. Thereafter, illustrative examples of both classes of manipulators has been presented. A comparison of these methods can be observed in Section 3.7. This discussion will be helpful in describing

the kinematics of a hybrid manipulator, which is a combination of open- and closed-loop chains. Based on the discussion in this chapter, the complete kinematic model of a hybrid manipulator is developed in Chapter 4.

Chapter 4

Kinematic Study of Spatial Hybrid Manipulators

4.1 Introduction

In the last chapter, kinematic analysis of open- as well as closed-loop robotic manipulators has been presented. Based on discussion reported in Chapter 3, is it possible to derive the forward kinematics of a spatial hybrid manipulator, which is a combination of open and closed chains with planar as well as spatial links? In the present chapter, the main focus is to answer this question and to develop a forward kinematic model for a spatial hybrid manipulator. It has been reported by Siciliano [15] that deriving the forward kinematic model of a closed-loop robotic manipulator may or may not be feasible. So, from reported information, it can be concluded that dealing with kinematic problem of a spatial hybrid manipulator is undoubtedly a challenging task. In the present work, a recognizable deficiency in D-H parameter method has been observed and in order to eliminate the same, the concept of *dummy frame*s has been proposed. The efficacy of proposed concept is demonstrated both analytically as well as physically for the case of Manipulator for Medical Applications (MMA).

4.2 Spatial Hybrid Manipulator

A spatial hybrid manipulator may be considered as a combination of, an open-loop (s), closed-loop (s) robotic structure (s) containing *planar*, *spatial* or combination of both types of links. The geometric structure of a spatial hybrid manipulator is quite complicated as compared to an open- as well as a closed-loop robots. Also, the degree of complexity will depends upon the type of the links contained by the structure of same. Figure 4.1, represents the general structure of a spatial hybrid manipulator, consists of planar links $L_i, L_{i+1'}, L_{i+1''}, L_{i+2'}, L_{i+2''},$ and L_j, spatial links, $L_k, L_{k+1}, \dots L_{k+n}$ and a closed-loop kinematic chain between links $L_{i+1'}, L_{i+2'}, \dots \dots \dots . L_j$ and $L_{i+1''}, L_{i+2''}, \dots . L_k$. Since, D-H

parameter method is applicable to serial manipulators. However, in the present work, an effort has been made to extend its utility to spatial hybrid manipulators. The kinematic structure of MMA is described in Section 4.4.

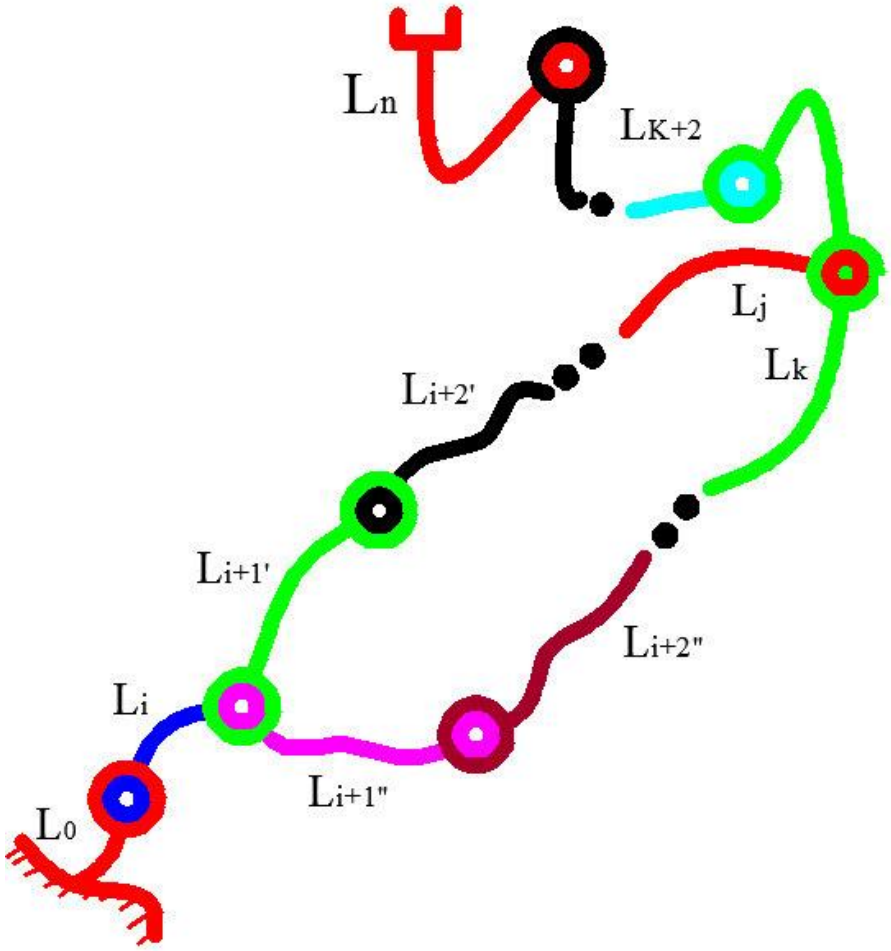

Fig. 4.1: General representation of kinematic structure of a spatial hybrid manipulator.

4.3 Manipulator for Medical Applications (MMA)

Manipulator for medical applications is a spatial hybrid manipulator, intended to serve the medical surgical operations. With reference to Figure 4.2, the basic kinematic structure of MMA consists of planar links, spatial links and a closed-loop kinematic chain. Further, thes closed-loop chain is formed by one spatial and three planar links. The detailed description is given is Section 4.4. As reported in Section 4.2 that geometric structure of a spatial hybrid manipulator is quite complex, the same can be observed here.

Moreover, MMA is a device, being operated by the surgeon during a surgical task. While sitting on surgeon console as the surgeon make some hand movements, the same were recorded by the sensors equipped to the manipulator. Thereafter, recorded motion is transferred to patient side manipulator, which actually performs the surgery.

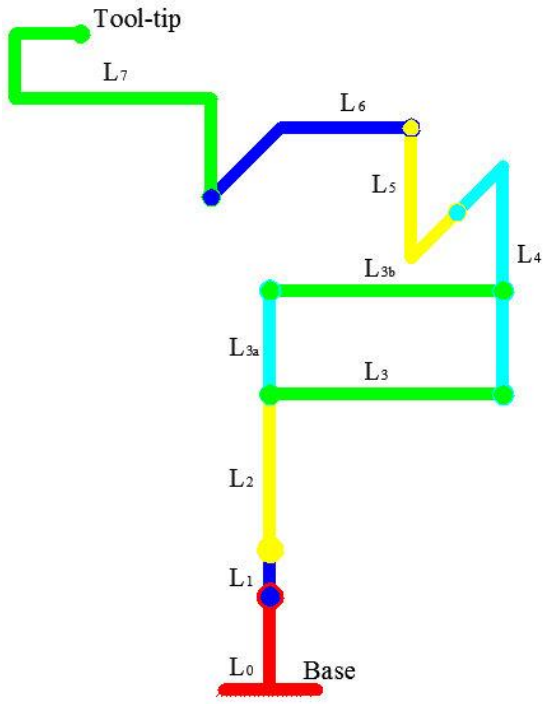

Fig. 4.2: Basic kinematic structure of manipulator for medical applications (MMA).

4.4 Kinematic Study of MMA

The detailed kinematic analysis of MMA is presented in Figs. 4.3-(a) and 4.3-(b). First, the links and frames description is given in Fig. 4.3-(a), thereafter, shape of links and joint motions are described in Fig. 4.3-(b), using proximal variant of original D-H parameter method. The MMA consists of 1 fixed link (shown in red color), known as base link, and 9 moving rigid-links, out of which links numbered as L_1, L_2, L_3, L_{3a}, and L_{3b} are planar, while L_4, L_5, L_6, and L_7 are spatial links. Kinematic chain contains two types of joints: i) a ternary joint between links L_2, L_3 and L_{3a}. ii) binary joints between rests of links. All joints are of revolute type. The DOF of MMA is seven and it provides the surgeon with all of the independent motions that a human arm can. In general, to provide the geometric description

of a kinematic chain, methods like distal and proximal variants of D-H notation, screw based displacement method, simple and systematic method to generate D-H parameters, S-U method, modified D-H method etc. are available in the literature. Due to minimal parameters representation, proximal variant of D-H notation has been preferred in the present work to assign reference coordinates frames to the links of MMA as shown in Fig. 4.3-(a). Thereafter, corresponding D-H parameters are calculated, as shown in Fig. 4.3-(b) and are given in Table 4.1.

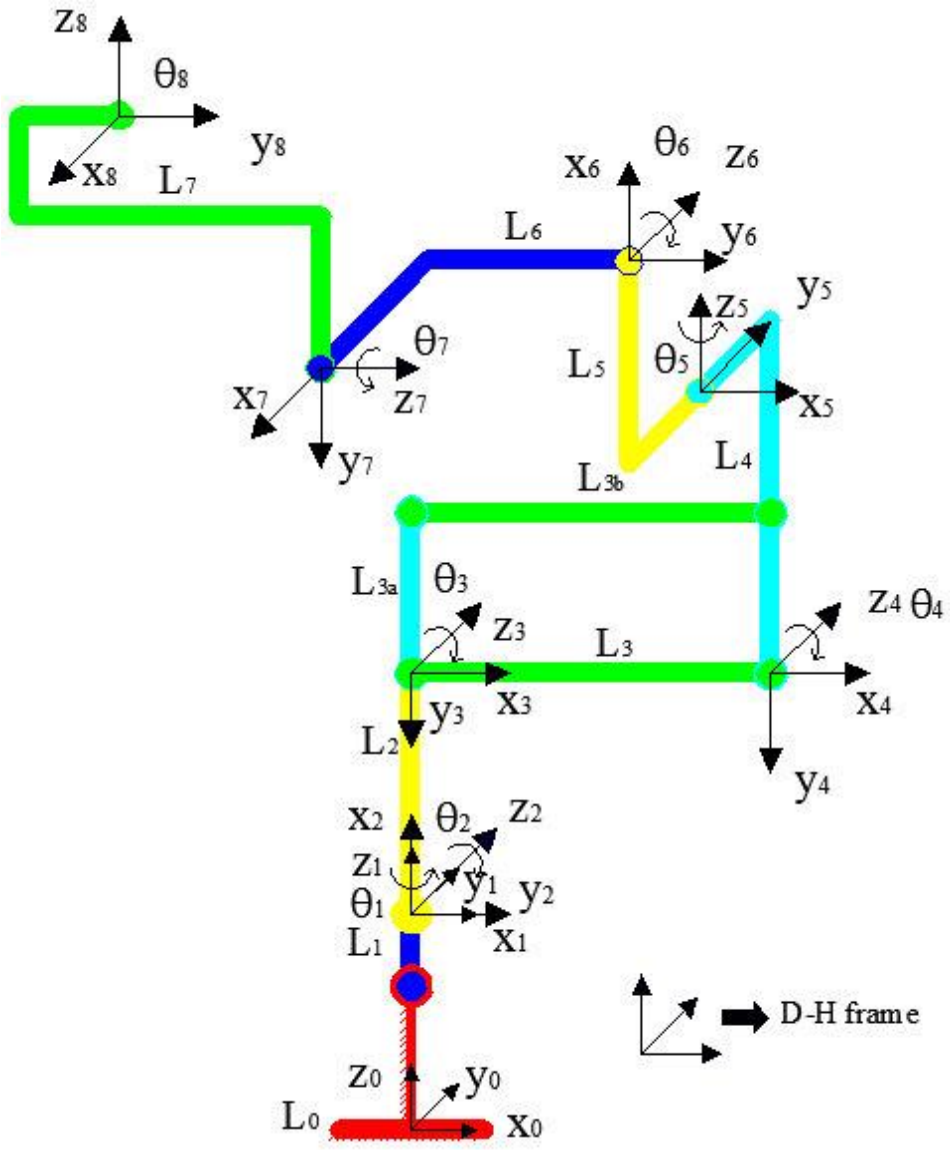

Fig. 4.3-(a): Line diagram of the MMA in assumed home position with assigned link-frames according to proximal variant of D-H parameter method.

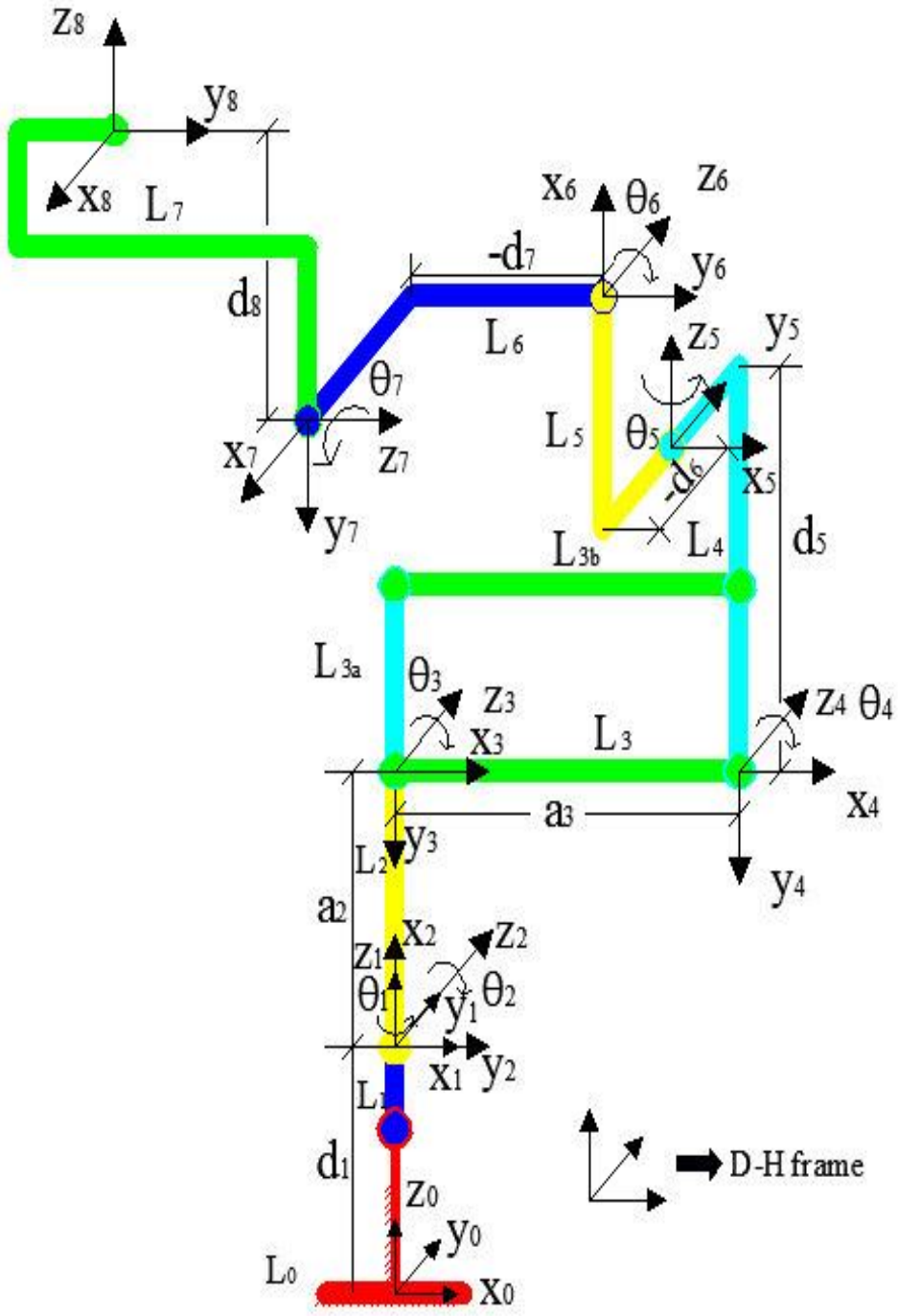

Fig. 4.3-(b): Line diagram of MMA with marked D-H parameters.

Table 4.1: D-H Parameters of MMA in assumed home position.

S.No	Link Length (a_{i-1}) (mm)	Joint Distance (d_i) (mm)	Link Twist (α_{i-1}) (deg.)	Joint Variable (θ_i) (deg.)	Home Position
1.	$a_0 = 0$	d_1 = 137.77	α_0 = 0	θ_1	0
2.	$a_1 = 0$	d_2 = 0	α_1 = -90	θ_2	-90
3.	a_2 = 187.46	d_3 = 0	α_2 = 0	θ_3	90
4.	a_3 = 160.76	$d_4 = 0$	α_3 = 0	θ_4	0
5.	a_4 = 0	d_5 = 67.82	α_4 = 90	θ_5	0
6.	$a_5 = 0$	d_6 = -35.07	α_5 = -90	θ_6	-90
7.	a_6 = 0	d_7 = -38.40	α_6 = -90	θ_7	90
8.	a_7 = 0	d_8 = 63.79	α_7 = 90	-	-

4.5 Development of the Forward Kinematic Model of MMA

In this section, forward kinematic model of the manipulator for medical applications has been developed using homogeneous coordinate transformations. The matrix, ${}^{i-1}_{i}\boldsymbol{A}$ represents the homogeneous transformation matrix, mapping i^{th} frame to $(i-1)^{th}$ frame for $i =$ 1 to 8, as given below:

$$ {}^{i-1}_{i}\boldsymbol{A} = \left[\begin{array}{ccc|c} c_{\theta_i} & -s_{\theta_i} & 0 & a_{i-1} \\ s_{\theta_i}c_{\alpha_{i-1}} & c_{\theta_i}c_{\alpha_{i-1}} & -s_{\alpha_{i-1}} & -s_{\alpha_{i-1}}d_i \\ s_{\theta_i}s_{\alpha_{i-1}} & c_{\theta_i}s_{\alpha_{i-1}} & c_{\alpha_{i-1}} & c_{\alpha_{i-1}}d_i \\ \hline 0 & 0 & 0 & 1 \end{array}\right] \quad (4.1) $$

By using Eqn. (4.1), the tool-tip of MMA can be transformed to its base, as given below:

$$ {}^{0}_{8}\boldsymbol{A} = {}^{0}_{1}\boldsymbol{A}\,{}^{1}_{2}\boldsymbol{A}\,{}^{2}_{3}\boldsymbol{A}\,{}^{3}_{4}\boldsymbol{A}\,{}^{4}_{5}\boldsymbol{A}\,{}^{5}_{6}\boldsymbol{A}\,{}^{6}_{7}\boldsymbol{A}\,{}^{7}_{8}\boldsymbol{A}. \quad (4.2) $$

where

$$ {}^{0}_{1}\boldsymbol{A} = \left[\begin{array}{ccc|c} c_1 & -s_1 & 0 & 0 \\ s_1 & c_1 & 0 & 0 \\ 0 & 0 & 1 & d_1 \\ \hline 0 & 0 & 0 & 1 \end{array}\right] \tag{4.3} $$

$$ {}^{1}_{2}\boldsymbol{A} = \left[\begin{array}{ccc|c} c_2 & -s_2 & 0 & 0 \\ 0 & 0 & 1 & 0 \\ -s_2 & -c_2 & 0 & 0 \\ \hline 0 & 0 & 0 & 1 \end{array}\right] \tag{4.4} $$

$$ {}^{2}_{3}\boldsymbol{A} = \left[\begin{array}{ccc|c} c_3 & -s_3 & 0 & a_2 \\ s_3 & c_3 & 0 & 0 \\ 0 & 0 & 1 & 0 \\ \hline 0 & 0 & 0 & 1 \end{array}\right] \tag{4.5} $$

$$ {}^{3}_{4}\boldsymbol{A} = \left[\begin{array}{ccc|c} c_4 & -s_4 & 0 & a_3 \\ s_4 & c_4 & 0 & 0 \\ 0 & 0 & 1 & 0 \\ \hline 0 & 0 & 0 & 1 \end{array}\right] \tag{4.6} $$

After multiplying these matrices the key result is ${}^{0}_{4}\boldsymbol{A}$, which is given as,

$$ {}^{0}_{4}\boldsymbol{A} = \left[\begin{array}{ccc|c} c_1c_{234} & -c_1s_{234} & -s_1 & c_1(c_2a_2 + c_{23}a_3) \\ s_1c_{234} & -s_1s_{234} & c_1 & s_1(c_2a_2 + c_{23}a_3) \\ -s_{234} & -c_{234} & 0 & d_1 - a_2s_2 - a_3s_{23} \\ \hline 0 & 0 & 0 & 1 \end{array}\right] \tag{4.7} $$

Now, the transformation ${}^{4}_{8}\boldsymbol{A}$, can be obtained as,

$$ {}^{4}_{8}\boldsymbol{A} = {}^{4}_{5}\boldsymbol{A}\,{}^{5}_{6}\boldsymbol{A}\,{}^{6}_{7}\boldsymbol{A}\,{}^{7}_{8}\boldsymbol{A} \tag{4.8} $$

where

$$ {}^{4}_{5}\boldsymbol{A} = \left[\begin{array}{ccc|c} c_5 & -s_5 & 0 & 0 \\ 0 & 0 & -1 & -d_5 \\ s_5 & c_5 & 0 & 0 \\ \hline 0 & 0 & 0 & 1 \end{array}\right] \tag{4.9} $$

$$
{}^{5}_{6}\boldsymbol{A} = \left[\begin{array}{ccc|c} c_6 & -s_6 & 0 & 0 \\ 0 & 0 & 1 & -d_6 \\ -s_6 & -c_6 & 0 & 0 \\ \hline 0 & 0 & 0 & 1 \end{array}\right] \tag{4.10}
$$

$$
{}^{6}_{7}\boldsymbol{A} = \left[\begin{array}{ccc|c} c_7 & -s_7 & 0 & 0 \\ 0 & 0 & 1 & -d_7 \\ -s_7 & -c_7 & 0 & 0 \\ \hline 0 & 0 & 0 & 1 \end{array}\right] \tag{4.11}
$$

$$
{}^{7}_{8}\boldsymbol{A} = \left[\begin{array}{ccc|c} 1 & 0 & 0 & 0 \\ 0 & 0 & -1 & -d_8 \\ 0 & 1 & 0 & 0 \\ \hline 0 & 0 & 0 & 1 \end{array}\right] \tag{4.12}
$$

After, multiplying these four matrices the resultant matrix is,

$$
{}^{4}_{8}\boldsymbol{A} = \left[\begin{array}{ccc|c} \tilde{a}_{11} & \tilde{a}_{12} & \tilde{a}_{13} & \tilde{a}_{14} \\ \tilde{a}_{21} & \tilde{a}_{22} & \tilde{a}_{23} & \tilde{a}_{24} \\ \tilde{a}_{31} & \tilde{a}_{32} & \tilde{a}_{33} & \tilde{a}_{34} \\ \hline 0 & 0 & 0 & 1 \end{array}\right] \tag{4.13}
$$

where

$$\tilde{a}_{11} = c_5 c_6 c_7$$

$$\tilde{a}_{12} = -c_5 s_6$$

$$\tilde{a}_{13} = c_5 c_6 s_7 - s_5 c_7$$

$$\tilde{a}_{14} = s_5 d_6 + c_5 s_6 d_7 - d_8(s_5 c_7 - c_5 c_6 s_7)$$

$$\tilde{a}_{21} = s_6 c_7$$

$$\tilde{a}_{22} = c_6$$

$$\tilde{a}_{23} = s_6 s_7$$

$$\tilde{a}_{24} = -d_5 - c_6 d_7 + s_6 s_7 d_8$$

$$\tilde{a}_{31} = s_5 c_6 c_7 - c_5 s_7$$

$$\tilde{a}_{32} = -s_5 s_6$$

$$\tilde{a}_{33} = s_5 c_6 s_7 + c_5 c_7$$

$$\tilde{a}_{34} = -c_5 d_6 + s_5 s_6 d_7 + d_8(s_5 c_6 s_7 + c_5 c_7)$$

The transformation matrix which transforms the tool-tip frame into base frame can be evaluated by multiplying Eqns. (4.7) and (4.13) as

$$ {}^{0}_{8}\boldsymbol{A} = {}^{0}_{4}\boldsymbol{A}\,{}^{4}_{8}\boldsymbol{A} = \begin{bmatrix} \tilde{b}_{11} & \tilde{b}_{12} & \tilde{b}_{13} & | & \tilde{b}_{14} \\ \tilde{b}_{21} & \tilde{b}_{22} & \tilde{b}_{23} & | & \tilde{b}_{24} \\ \tilde{b}_{31} & \tilde{b}_{32} & \tilde{b}_{33} & | & \tilde{b}_{34} \\ - & - & - & | & - \\ 0 & 0 & 0 & | & 1 \end{bmatrix} \quad (4.14)$$

where

$$\tilde{b}_{11} = c_7\{c_6(c_1 c_{234} c_5 - s_1 s_5) - c_1 s_{234} s_6\} + s_7(c_1 c_{234} s_5 + s_1 c_5)$$

$$\tilde{b}_{12} = -s_6(c_1 c_{234} c_5 - s_1 s_5) - c_1 c_6 s_{234}$$

$$\tilde{b}_{13} = s_7\{c_6(c_1 c_{234} c_5 - s_1 s_5) - c_1 s_{234} s_6\} - c_7(c_1 c_{234} s_5 + s_1 c_5)$$

$$\begin{aligned}\tilde{b}_{14} = {} & d_8 s_7\{c_6(c_1 c_{234} c_5 - s_1 s_5) - c_1 s_{234} s_6\} - d_8 c_7(c_1 c_{234} s_5 + s_1 c_5) \\ & + d_7 s_6(c_1 c_{234} c_5 - s_1 s_5) + c_1 s_{234} c_6 d_7 + d_6(c_1 c_{234} s_5 + s_1 c_5) \\ & + c_1 s_{234} d_5 + c_1(c_{23} a_3 + c_2 a_2)\end{aligned}$$

$$\tilde{b}_{21} = c_7\{c_6(s_1 c_{234} c_5 + c_1 s_5) - s_1 s_{234} s_6\} + s_7(s_1 c_{234} s_5 - c_1 c_5)$$

$$\tilde{b}_{22} = -s_6(s_1 c_{234} c_5 + c_1 s_5) - s_1 c_6 s_{234}$$

$$\tilde{b}_{23} = s_7\{c_6(s_1 c_{234} c_5 + c_1 s_5) - s_1 s_{234} s_6\} - c_7(s_1 c_{234} s_5 + c_1 c_5)$$

$$\begin{aligned}\tilde{b}_{24} = {} & d_8[s_7\{c_6(s_1 c_{234} c_5 + c_1 s_5) - s_1 s_{234} s_6\} - c_7(s_1 c_{234} s_5 + c_1 c_5)] \\ & + s_1(c_{23} a_3 + c_2 a_2) + s_1 s_{234} d_5 + d_6(c_1 c_{234} s_5 + s_1 c_5) + d_7\{s_6\end{aligned}$$

$$(c_1 c_{234} c_5 - s_1 s_5) + c_1 s_{234} c_6\}$$

$$\tilde{b}_{31} = c_7(-s_{234} c_5 c_6 - c_{234} s_6) - s_{234} s_5 s_7$$

$$\tilde{b}_{32} = s_{234} c_5 s_6 - c_{234} c_6$$

$$\tilde{b}_{33} = s_7(-s_{234} c_5 c_6 - c_{234} s_6) + s_{234} s_5 c_7$$

$$\tilde{b}_{34} = d_8 s_7(-s_{234} c_5 c_6 - c_{234} s_6) + s_{234} s_5 c_7 d_8 - d_7(s_{234} c_5 s_6 - c_{234} c_6) - d_6 s_{234} s_5 + c_{234} d_5 - a_2 s_2 - a_3 s_{23} + d_1$$

4.6 Ambiguity in D-H Parameter Method

A forward kinematic model is developed in Section 4.5. The developed model gives the position and orientation of the tool-tip, given the joint angles. Thereafter, D-H parameters calculated in Section 2 are substituted in the derived model. However, discrepancies has been observed in tool-tip position obtained from kinematic model as compared to one obtained from physical prototype of MMA. This geometrical inconsistency arises because all the segments of spatial links L_4, L_5, L_6, and L_7 does not get accounted for into corresponding D-H parameters Table 4.1, as can be seen in Fig. 4.3-(b). This leads to *recognizable deficiency* of D-H notation in case of spatial links, where two consecutive joint axes at right angles to each other. A detailed analysis has been made by considering a spatial link L_4 taken from Fig. 4.3-(b), separately with two possible joint axes orientations, as can be seen in Figs. 4.5-(b) and 4.5-(c). Figure 4.5-(a) shows a solid spatial link to which joint axes are assigned with two possibilities– a) parallel to each other, b) at right angles to each other.

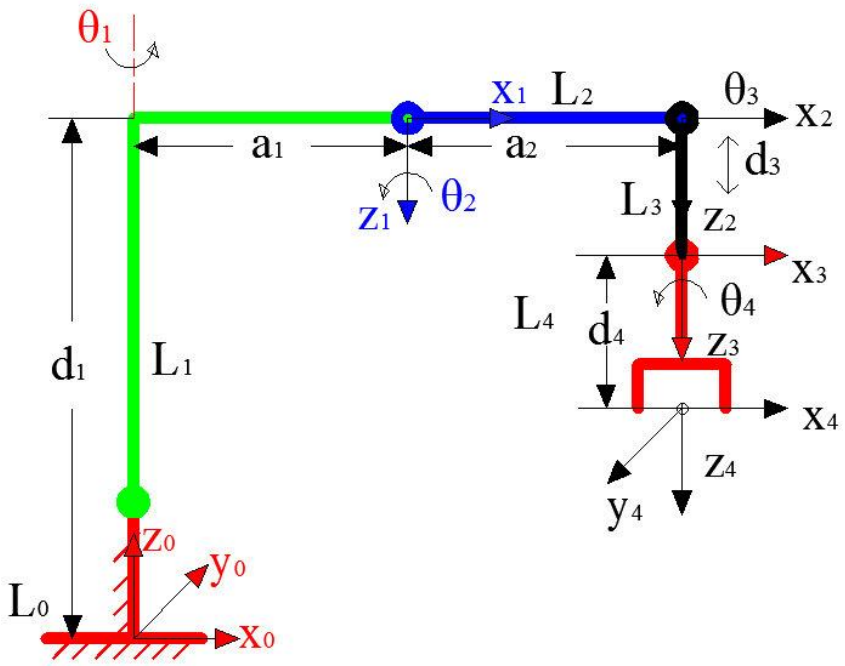

Fig. 4.4: Four-axis SCARA robot with assigned link-frames and marked D-H parameters.

Now, if a mechanism contains a spatial link with parallel joint axes, as in case of four-axis SCARA robot (refer Fig. 4.4) [8], D-H notation comes geometrically consistent as both segments of spatial link get accounted for into corresponding D-H parameters. However, in case of a spatial link with two consecutive joint axes at right angle to each other, all the segments of spatial link does not get accounted for into corresponding D-H parameter table (refer Table 4.2).

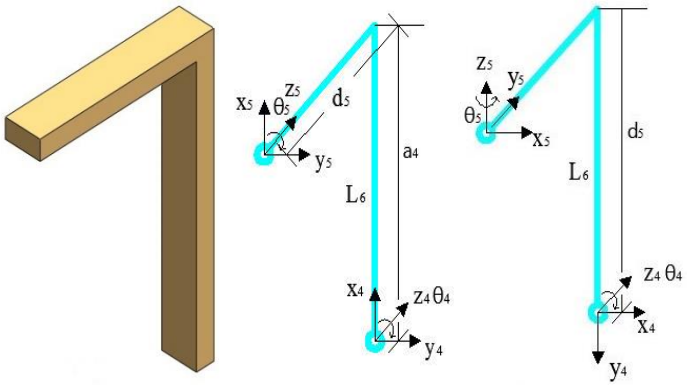

Fig. 4.5-(a) Geometry of a solid spatial link L_4, Fig. 4.5-(b): Spatial link L_4 with parallel joint axes and Fig. 4.5-(c) Spatial link L_4 with perpendicular joint axes describing the recognizable deficiency of proximal variant of original D-H parameter method.

Table 4.2: D-H parameters of link L_4, shown in fig. 4.5-(c).

S.No	Link Length (a_{i-1})	Joint Distance (d_i)	Link Twist (α_{i-1}) (deg.)	Joint Variable (θ_i)	Home Position (deg.)
1.	$a_4 = 0$	d_5	-90	θ_5	0

On the similar basis, if the remaining spatial links of the MMA are observed, geometrical inconsistency is found in all of them. This inconsistency can be observed from Table 4.1, where the entries a_5, a_6 and a_7 are coming as zero, describing that all the parameters of spatial links L_4, L_5, L_6 and L_7 are not accounted for. The geometric validation of this inconsistency is given in later section.

4.7 Improvement in D-H Parameter Method

4.7.1 Concept of a Virtual-Link

Now, in order to eliminate the deficiency of D-H notation as reported in Section 3, the *concept of virtual link* has been applied. According to the fundamentals of kinematics that motion study does not depend upon shape of link. So, a virtual link is generally assumed by joining end points of a spatial link. An attempt is made to use virtual link because both of the segments of spatial link get accounted for into corresponding length calculation as s $=\sqrt[2]{(a^2 + b^2)}$, according to Pythagoras theorem.

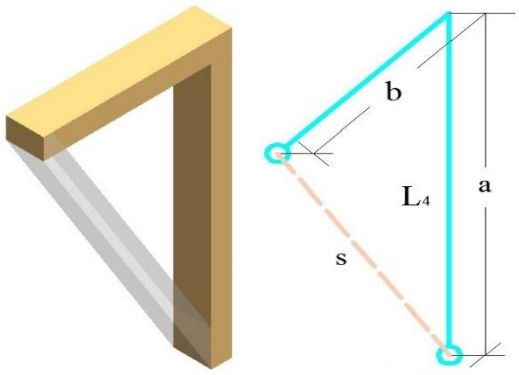

Fig. 4.6-(a) A solid spatial link with its corresponding virtual link, and Fig.4.6-(b) Geometric description of spatial link.

Taking virtual link in account, the plane of motion of original spatial link got changed, which is not desirable in surgical applications. That is why, the concept of virtual link has not been applied.

4.7.2 Concept of a Dummy Frame

However, the reported deficiency can be successfully eliminated by introducing a new concept, which is to the best of authors knowledge, has not been used before in literature. The introduced concept is coined as the concept of ***Dummy Frames.***

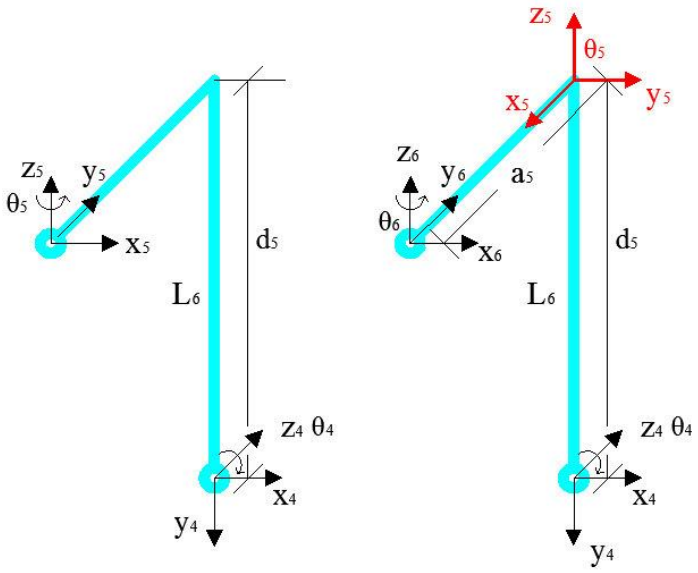

Fig. 4.7-(a): A Spatial link L_4 considered separately from Fig. 4.3-(b), and Fig. 4.7-(b) A spatial link L_4 with dummy frame (in red color) assignment.

When this concept is applied to a spatial link, as shown in Fig. 4.7-(b), it accounts for all the segments of spatial link into corresponding D-H parameters (refer Table 4.3) and eliminates the deficiency of D-H notation. Dummy frame is different from D-H frame in the sense that it is placed at a point where there is no motion, whereas a D-H frame is placed at a point where motion is taking place. Absence of motion at dummy frame does not imply that joint angle corresponding to dummy frame vanishes rather it becomes a constant, whose value can be determined (as angle from x_{i-1} to x_i about z_i) according to D-H algorithm.

Table 4.3: D-H parameters of spatial link L_4 augmented with dummy frame, shown in fig. 4.7-(b).

S.No	Link Length (a_{i-1})	Joint Distance (d_i)	Link Twist (α_{i-1}) (deg.)	Joint Variable (θ_i) (deg.)	Home Position (deg.)
1.	a_5	d_5	0	θ_5	-90

Rules to Assign Dummy Frames:

1. First of all, z-axis is assigned in the appropriate direction.
2. Next, assign x-axis according to D-H notation.
3. Use right hand thumb rule to assign y-axis.

Figure 4.7-(b) shows the demonstration of concept of dummy frame (shown in red color). In the present work, four dummy frames are attached to Manipulator for Medical Application. Hence, four constants are present in Table 4.4. As there is no motion taking place about any of the axis of assigned dummy frame, that is why, they are known as dummy frames.

4.8 D-H parameters of MMA Augmented with Dummy Frames

Figure 4.8-(a) shows the line diagram of Manipulator for Medical Application with assigned dummy frames (shown in red) in addition to D-H frames and Fig. 4.8-(b) shows the line diagram with marked new D-H parameters, which are given in Table 4.4. At this point, a comparison of Figs. 4.3-(b) and 4.8-(b) can be made and it can be observed that segments of spatial links L_4, L_5, L_6, and L_7 which are not get accounted for into corresponding D-H parameters with conventional D-H notation, are now get accounted into D-H parameters. Thereafter, again, a forward kinematic model is developed as developed in Section 4.5, however augmented with dummy frames.

Table 4.4: D-H Parameters of MMA with augmented dummy frames.

S.No	Link Length (a_{i-1}) (mm)	Joint Distance (d_i) (mm)	Link Twist (α_{i-1}) (deg.)	Joint Var. (θ_i) (deg.)	Home Postn.
1.	$a_0 = 0$	d_1 = 137.77	α_0 = 0	θ_1	0
2.	$a_1 = 0$	d_2 = 0	α_1 = -90	θ_2	-90
3.	a_2 = 187.46	d_3 = 0	α_2 = 0	θ_3	90

4.	a_3 = 160.76	d_4 = 0	α_3 = 0	θ_4	0
5.	$a_4 = 0$	d_5 = 67.82	α_4 = 90	θ_5 = C	-90
6.	a_5 = 20.11	d_6 = 0	α_5 = 0	θ_6	90
7.	$a_6 = 0$	d_7 = -35.07	α_6 = -90	θ_7 = C	-90
8.	a_7 = 25.24	d_8 = 0	α_7 = 0	θ_8	0
9.	$a_8 = 0$	d_9 = -38.40	α_8 = -90	θ_9 = C	90
10.	a_9 = 16.09	d_{10} = 0	α_9 = 0	θ_{10}	0
11.	a_{10} = 0	d_{11}= 27.29	α_9 = 90	θ_{11}= C	-90
12	$a_{11} = 118.73$	d_{12} = 36.50	α_{10} = 90	-	-

The tip of the MMA can be transformed to base frame according to,

$$ {}^{0}_{12}\boldsymbol{A} = {}^{0}_{1}\boldsymbol{A}\,{}^{1}_{2}\boldsymbol{A}\,{}^{2}_{3}\boldsymbol{A}\,{}^{3}_{4}\boldsymbol{A}\,{}^{4}_{5}\boldsymbol{A}\,{}^{5}_{6}\boldsymbol{A}\,{}^{6}_{7}\boldsymbol{A}\,{}^{7}_{8}\boldsymbol{A}\,{}^{8}_{9}\boldsymbol{A}\,{}^{9}_{10}\boldsymbol{A}\,{}^{10}_{11}\boldsymbol{A}\,{}^{11}_{12}\boldsymbol{A} \qquad (4.15) $$

Since, even after augmentation of dummy frames, the description of chain remains same up-to joint variable θ_4. So, the transformation matrix ${}^{0}_{4}\boldsymbol{A}$, will be same as given by Eqn. (4.5).

The Eqn. (4.15) can be written as

$$ {}^{0}_{12}\boldsymbol{A} = {}^{0}_{4}\boldsymbol{A}\,{}^{4}_{8}\boldsymbol{A}\,{}^{8}_{12}\boldsymbol{A} \qquad (4.16) $$

where

$$ {}^{0}_{4}\boldsymbol{A} = \left[\begin{array}{ccc|c} c_1c_{234} & -c_1s_{234} & -s_1 & c_1(c_{23}a_3 + c_2a_2) \\ s_1c_{234} & -s_1s_{234} & c_1 & s_1(c_{23}a_3 + c_2a_2) \\ -s_{234} & -c_{234} & 0 & d_1 - a_2s_2 - a_3s_{23} \\ \hline 0 & 0 & 0 & 1 \end{array}\right] \qquad (4.17) $$

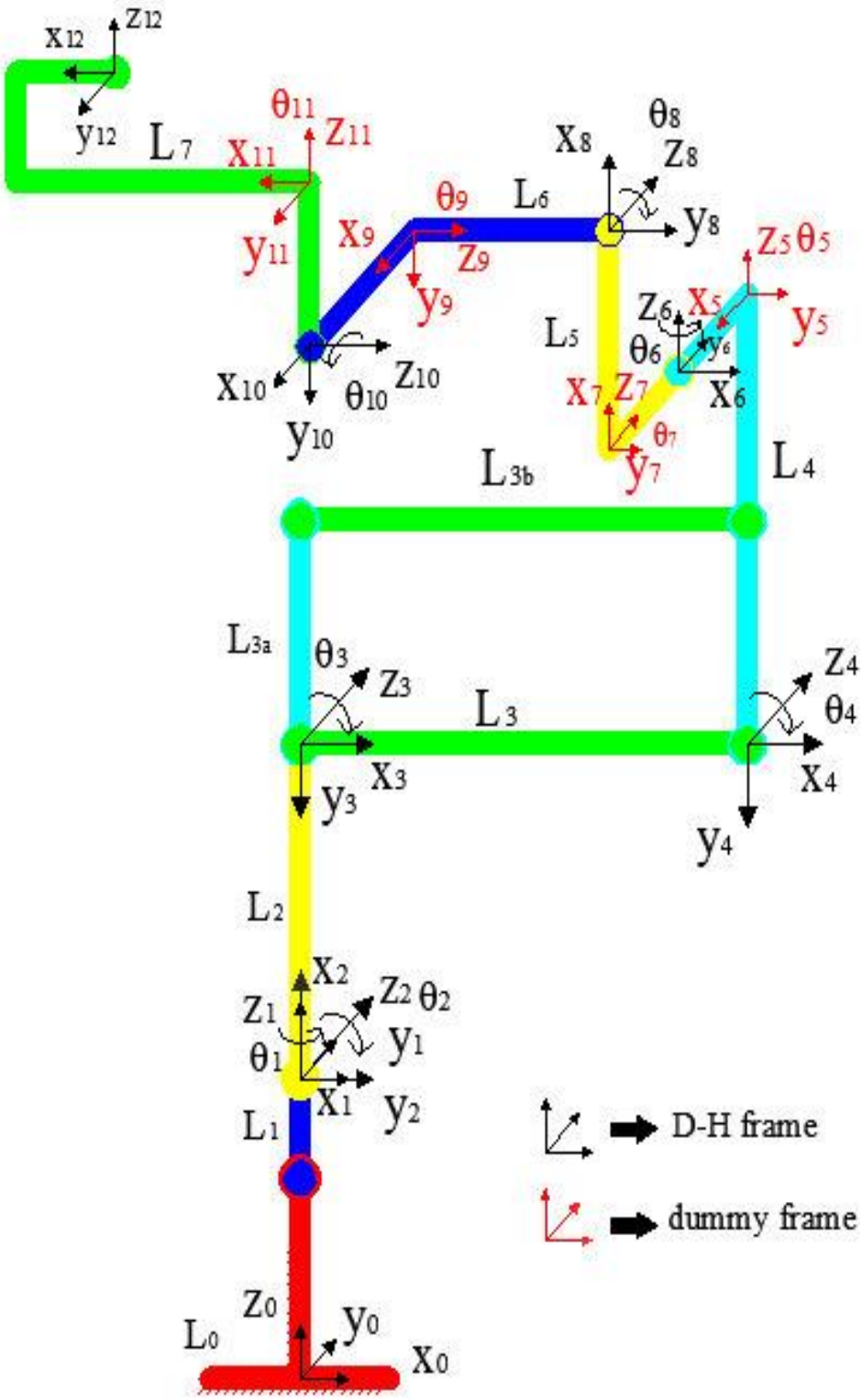

Fig. 4.8-(a) Link-frame assignment to MMA augmented with dummy frames.

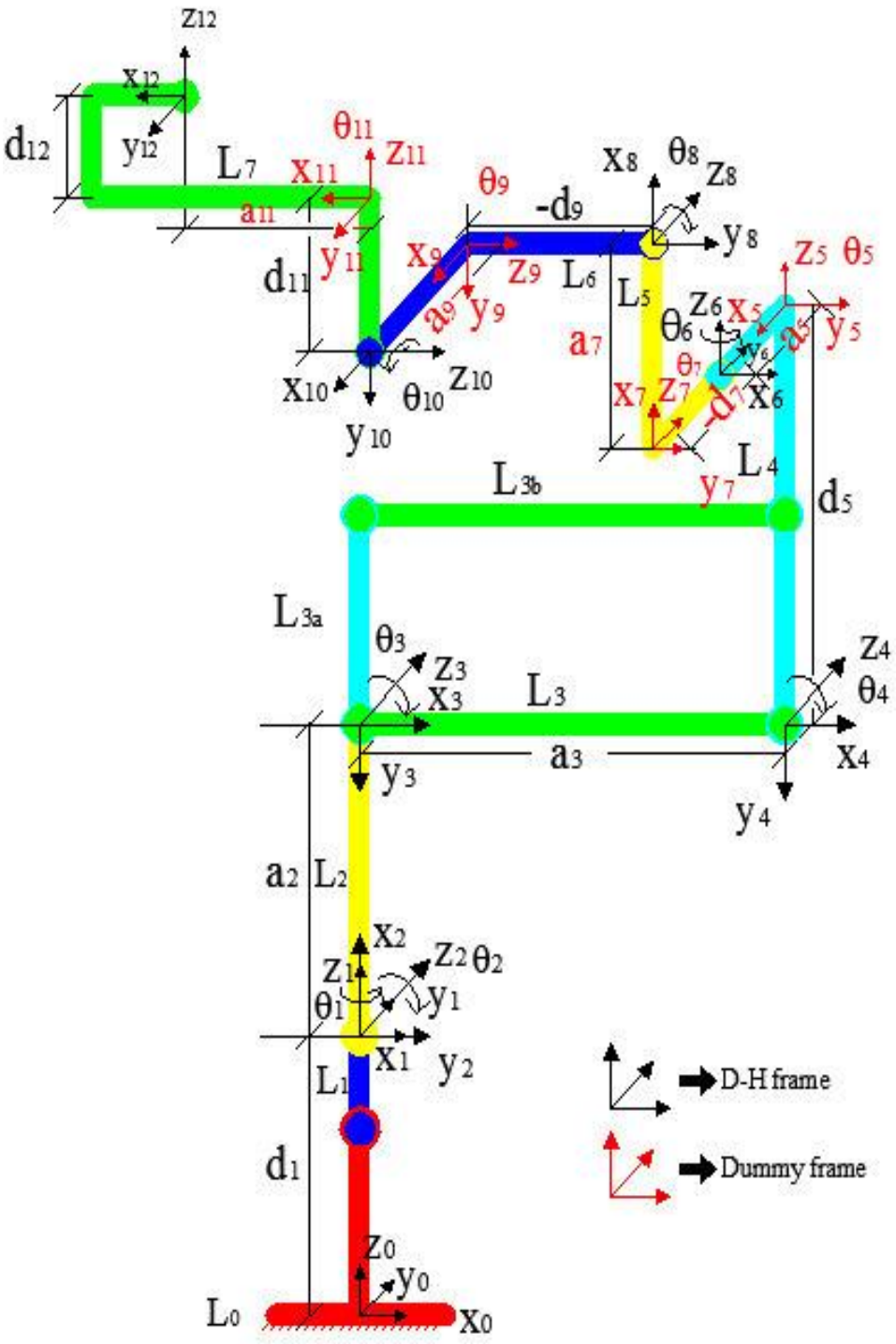

Fig. 4.8-(b) D-H parameters of MMA augmented with dummy frames.

$$ {}^{4}_{8}\boldsymbol{A} = {}^{4}_{5}\boldsymbol{A}\,{}^{5}_{6}\boldsymbol{A}\,{}^{6}_{7}\boldsymbol{A}\,{}^{7}_{8}\boldsymbol{A} \tag{4.18} $$

and

$$ {}^{4}_{5}\boldsymbol{A} = \begin{bmatrix} 0 & 1 & 0 & 0 \\ 0 & 0 & -1 & -d_5 \\ -1 & 0 & 0 & 0 \\ - & - & - & - \\ 0 & 0 & 0 & 1 \end{bmatrix} \tag{4.19} $$

$$ {}^{5}_{6}\boldsymbol{A} = \begin{bmatrix} c_6 & -s_6 & 0 & a_5 \\ s_6 & c_6 & 0 & 0 \\ 0 & 0 & 1 & 0 \\ - & - & - & - \\ 0 & 0 & 0 & 1 \end{bmatrix} \tag{4.20} $$

$$ {}^{6}_{7}\boldsymbol{A} = \begin{bmatrix} 0 & 1 & 0 & 0 \\ 0 & 0 & 1 & -d_7 \\ 1 & 0 & 0 & 0 \\ - & - & - & - \\ 0 & 0 & 0 & 1 \end{bmatrix} \tag{4.21} $$

$$ {}^{7}_{8}\boldsymbol{A} = \begin{bmatrix} c_8 & -s_8 & 0 & a_7 \\ s_8 & c_8 & 0 & 0 \\ 0 & 0 & 1 & 0 \\ - & - & - & - \\ 0 & 0 & 0 & 1 \end{bmatrix} \tag{4.22} $$

$$ {}^{4}_{8}\boldsymbol{A} = \begin{bmatrix} s_6 s_8 & s_6 c_8 & c_6 & -c_6 d_7 \\ -c_8 & s_8 & 0 & -d_5 - a_7 \\ -c_6 s_8 & -c_6 c_8 & s_6 & -a_5 - s_6 d_7 \\ - & - & - & - \\ 0 & 0 & 0 & 1 \end{bmatrix} \tag{4.23} $$

Now, ${}^{8}_{12}\boldsymbol{A}$ is obtained as

$$ {}^{8}_{12}\boldsymbol{A} = {}^{8}_{9}\boldsymbol{A}\,{}^{9}_{10}\boldsymbol{A}\,{}^{10}_{11}\boldsymbol{A}\,{}^{11}_{12}\boldsymbol{A} \tag{4.24} $$

where

$$ {}^{8}_{9}\boldsymbol{A} = \left[\begin{array}{ccc|c} 0 & -1 & 0 & 0 \\ 0 & 0 & 1 & -d_9 \\ -1 & 0 & 0 & 0 \\ \hline 0 & 0 & 0 & 1 \end{array}\right] \tag{4.25} $$

$$ {}^{9}_{10}\boldsymbol{A} = \left[\begin{array}{ccc|c} c_{10} & -s_{10} & 0 & a_9 \\ s_{10} & c_{10} & 0 & 0 \\ 0 & 0 & 1 & 0 \\ \hline 0 & 0 & 0 & 1 \end{array}\right] \tag{4.26} $$

$$ {}^{10}_{11}\boldsymbol{A} = \left[\begin{array}{ccc|c} 0 & 1 & 0 & 0 \\ 0 & 0 & -1 & -d_{11} \\ -1 & 0 & 0 & 0 \\ \hline 0 & 0 & 0 & 1 \end{array}\right] \tag{4.27} $$

$$ {}^{11}_{12}\boldsymbol{A} = \left[\begin{array}{ccc|c} 1 & 0 & 0 & a_{11} \\ 0 & 1 & 0 & 0 \\ 0 & 0 & 1 & -d_{12} \\ \hline 0 & 0 & 0 & 1 \end{array}\right] \tag{4.28} $$

Therefore

$$ {}^{8}_{12}\boldsymbol{A} = \left[\begin{array}{ccc|c} 0 & -s_{10} & c_{10} & c_{10}(d_{11}+d_{12}) \\ -1 & 0 & 0 & -a_{11}-d_9 \\ 0 & -c_{10} & -s_{10} & -a_9 - s_{10}(d_{11}+d_{12}) \\ \hline 0 & 0 & 0 & 1 \end{array}\right] \tag{4.29} $$

Substituting for Eqns. (4.17), (4.23) and (4.29) in Eqn. (4.16),

$$ {}^{0}_{12}\boldsymbol{A} = \left[\begin{array}{ccc|c} \tilde{c}_{11} & \tilde{c}_{12} & \tilde{c}_{13} & \tilde{c}_{14} \\ \tilde{c}_{21} & \tilde{c}_{22} & \tilde{c}_{23} & \tilde{c}_{24} \\ \tilde{c}_{31} & \tilde{c}_{32} & \tilde{c}_{33} & \tilde{c}_{34} \\ \hline 0 & 0 & 0 & 1 \end{array}\right] \tag{4.30} $$

where

$$ \tilde{c}_{11} = c_1 s_{234} s_8 - c_8(s_1 c_6 + c_1 c_{234} s_6) $$

$$ \tilde{c}_{12} = (s_1 s_6 - c_1 c_{234} c_6) $$

$$ \tilde{c}_{13} = \{c_1 s_{234} c_8 + s_8(s_1 c_6 + c_1 c_{234} s_6)\} $$

$$\tilde{c}_{14} = c_1(c_2a_2 + c_{23}a_3) + s_1a_5 + c_1s_{234}d_5 - d_7(-s_1s_6 + c_1c_{234}c_6) + a_7c_1s_{234} - d_9\{-c_1s_{234}s_8 + c_8(s_1c_6 + c_1c_{234}s_6)\} + a_9(s_1s_6 - c_1c_{234}c_6) + d_{11}\{c_1 s_{234}c_8 + s_8(s_1c_6 + c_1c_{234}s_6)\} + a_{11}\{c_1s_{234}s_8 - c_8(s_1c_6 + c_1c_{234}s_6)\} + d_{12}\{c_1s_{234}c_8 + s_8(s_1c_6 + c_1c_{234}s_6)\}$$

$$\tilde{c}_{21} = s_1s_{234}s_8 - c_8(-c_1c_6 + s_1c_{234}s_6)$$

$$\tilde{c}_{22} = (-c_1s_6 - s_1c_{234}c_6)$$

$$\tilde{c}_{23} = \{s_1s_{234}c_8 + s_8(-c_1c_6 + s_1c_{234}s_6)\}$$

$$\tilde{c}_{24} = s_1(c_2a_2 + c_{23}a_3) - c_1a_5 + s_1s_{234}d_5 - d_7(c_1s_6 + s_1c_{234}c_6) + a_7s_1s_{234} - d_9\{-s_1s_{234}s_8 + c_8(-c_1c_6 + s_1c_{234}s_6)\} + a_9(-c_1s_6 - s_1c_{234}c_6) + d_{11}\{s_1s_{234}c_8 + s_8(-c_1c_6 + s_1c_{234}s_6)\}$$

$$\tilde{c}_{31} = c_{234}s_8 + s_{234}s_6c_8$$

$$\tilde{c}_{32} = s_{234}c_6$$

$$\tilde{c}_{33} = (c_{234}c_8 - s_6s_{234}s_8)$$

$$\tilde{c}_{34} = d_1 - a_2s_2 - a_3s_{23} + c_{234}d_5 + s_{234}c_6d_7 + a_7c_{234} - d_9(-c_{234}s_8 - s_{234}s_6c_8) + a_9s_{234}c_6 + d_{11}(c_{234}c_8 - s_6s_{234}s_8) + a_{11}(c_{234}s_8 + s_{234}s_6c_8) + d_{12}(c_{234}c_8 - s_6s_{234}s_8).$$

4.9 Validation

4.9.1 Geometrical Validation

To ensure the efficacy of the proposed concept (dummy frame), a kinematic model is developed in the Matlab environment. D-H parameters augmented with dummy frames are substituted to kinematic model, gives position and orientation of the tool-tip. The geometrical validation first without dummy frames, thereafter, with dummy frames, is presented:

i. Geometrical Validation with D-H parameters method:

To validate the D-H parameter table, the tip coordinates of MMA are geometrically calculated, as shown in Fig. 6-(b) and are given as,

Table 4.5: Geometrical validation with D-H parameter method.

Coordinate	Desirable tip coordinate obtained geometrically from Fig. 6-(b).	Position of tip given by forward kinematic model
X	$a_3 - d_9 - a_{11}$	$a_3 - d_7$
Y	$-(a_5 + d_7 + a_9)$	$-d_6$
Z	$d_1 + a_2 + d_5 + a_7 + d_{11} + d_{12}$	$d_1 + a_2 + d_5 + d_8$

It can be seen from Figs. 4.3-(b) and 4.8-(b) that $d_8 = d_{11} + d_{12}$.

$$ {}^{0}_{4}\boldsymbol{A} = \begin{bmatrix} 1 & 0 & 0 & a_3 \\ 0 & 0 & 1 & 0 \\ 0 & -1 & 0 & d_1 + a_2 \\ 0 & 0 & 0 & 1 \end{bmatrix} \tag{4.31} $$

$$ {}^{0}_{8}\boldsymbol{A} = \begin{bmatrix} 0 & 1 & 0 & a_3 - d_7 \\ -1 & 0 & 0 & -d_6 \\ 0 & 0 & 1 & d_1 + a_2 + d_5 + d_8 \\ 0 & 0 & 0 & 1 \end{bmatrix} \tag{4.32} $$

ii. Geometrical Validation with Concept of Dummy Frames

Table 4.6: Geometrical validation with improved (Dummy frame) D-H parameter method.

Coord.	Desirable tip coordinate obtained geometrically from Fig. 6-(b).	Position of tip given by forward kinematic model
X	$a_3 - d_9 - a_{11}$	$a_3 - d_9 - a_{11}$
Y	$-(a_5 + d_7 + a_9)$	$-(a_5 + d_7 + a_9)$
Z	$d_1 + a_2 + d_5 + a_7 + d_{11} + d_{12}$	$d_1 + a_2 + d_5 + a_7 + d_{11} + d_{12}$

$$ {}^{0}_{4}\boldsymbol{A} = \left[\begin{array}{ccc|c} 1 & 0 & 0 & a_3 \\ 0 & 0 & 1 & 0 \\ 0 & -1 & 0 & d_1 + a_2 \\ \hline 0 & 0 & 0 & 1 \end{array}\right] \tag{4.33} $$

$$ {}^{0}_{8}\boldsymbol{A} = \left[\begin{array}{ccc|c} 0 & 1 & 0 & a_3 \\ 0 & 0 & 1 & -a_5 - d_7 \\ 1 & 0 & 0 & d_1 + a_2 + d_5 + a_7 \\ \hline 0 & 0 & 0 & 1 \end{array}\right] \tag{4.34} $$

$$ {}^{0}_{12}\boldsymbol{A} = \left[\begin{array}{ccc|c} 1 & 0 & 0 & a_3 - d_9 - a_{11} \\ 0 & -1 & 0 & -a_5 - d_7 - a_9 \\ 0 & 0 & 1 & d_1 + a_2 + d_5 + a_7 + d_{11} + d_{12} \\ \hline 0 & 0 & 0 & 1 \end{array}\right] \tag{4.35} $$

Tables 4.5 and 4.6, shows the geometrical validation results with, conventional D-H parameter method and D-H parameters method incorporated with dummy frames. From Table 4.5 it can be observed that position given by forward kinematic model is inconsistent with one obtained from geometric line diagram (Fig. 4.8-(b)). As the all segments are not marked in Fig. 4.3-(b), so desirable tip position is obtained from Fig. 4.8-(b). However, when concept of dummy frames is implemented, as seen in Fig. 4.8-(a), position given by the kinematic model is completely consistent with one obtained from geometric line diagram (Fig. 4.8-(b)).

4.9.2 Validation with Physical Prototype

Also, a physical prototype of Manipulator for Medical Application has been made at **CSIR-CSIO** Chandigarh and position and orientation are measured with physical prototype. It has been observed that results given by kinematic model and physical prototype, found with close agreement with each other.

The comparison of both the results is given in Table 4.7. The slight variation found in the coordinates is due to the human error involved while measuring the MMA coordinates manually. It is expected that the above mentioned error will reduce significantly if more sensitive measuring techniques were adopted like Coordinate Measuring Machine (CMM) or vision-based techniques. Figure 4.9, shows the MMA prototype modeled in SolidWorks environment. Because, this manipulator is under patent process that is why physical

prototype is not shown in this thesis. However, experimentation has been performed on physical prototype.

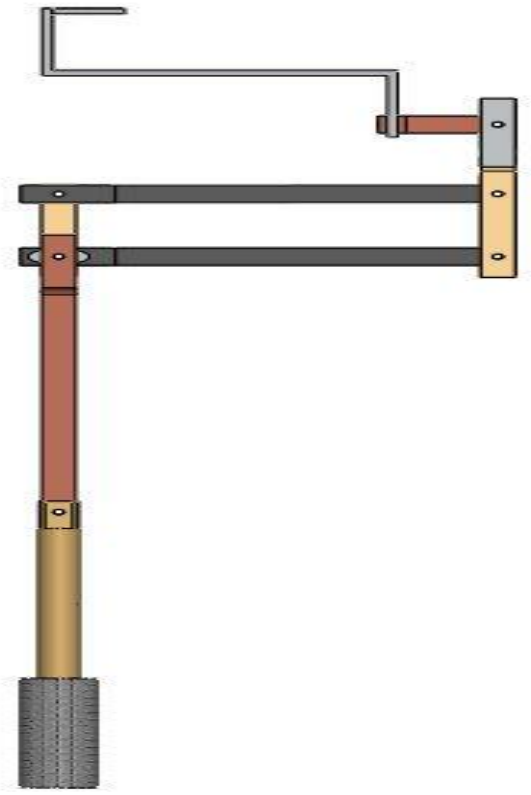

Fig. 4.9: Prototype of MMA modeled in SolidWorks environment.

Table 4.7: Comparison of Validations results.

Mapping		**With Kinematic Model**			**With Physical Prototype**		
From	**To**	**X (mm)**	**Y (mm)**	**Z (mm)**	**X (mm)**	**Y (mm)**	**Z (mm)**
4^{th}	0^{th}	160.7	0	325.2	158.5	0	323.5
5^{th}	0^{th}	160.7	0	393.1	158.5	0	391.0
6^{th}	0^{th}	160.7	-20.1	393.1	158.5	-22.9	391.0
8^{th}	0^{th}	160.7	-55.2	418.3	158.5	-56.6	417.2

9^{th}	0^{th}	122.4	-55.2	418.3	124	-56.6	417.5
12^{th}	0^{th}	3.6	-71.3	482.1	3.6	-72.9	481.5

4.10 CASE STUDY: Complete Kinematic Model of MMA

In this section, complete forward kinematic model of MMA is developed. The development of model is presented in four stages. In the first stage (Section 4.10.1), the kinematic position constraints imposed by closed-loop part of the spatial hybrid manipulator, are developed. In the second stage (Section 4.10.2), an attempt is made to derive the prescribed model for the same, using the kinematic analysis made in the previous section. However, derivation the model is not feasible using the proximal variant of D-H parameter method. This is due to the two reasons. First, D-H parameter method is applicable to serial chains only, whereas MMA is a spatial hybrid manipulator. Second, complex kinematic configuration of MMA which leads to a strong disagreement/inconsistency between orientation of frames assigned to the parallelogram linkage and a spatial link. However, the concept of D-H parameter method is extended to model the spatial hybrid manipulators by using the concept of dummy frames in Section 4.10.3. Thereafter finally, in Section 4.10.4, this extension is successfully implemented on the case study of MMA.

4.10.1 Development of the Closed-loop Constraints

As already mentioned, the spatial hybrid manipulator contains both open- as well as closed-loop chains, this section presents the development of kinematic position constraints, imposed by the closed-loop part (parallelogram linkage) of the hybrid manipulator. As shown in Fig. 4.10, the frame, ($f_{4''}$) is attached to proximal end of spatial link L_4 and ($f_{4'''}$) is attached to the distal end of link L_3. Both these frames represent the same point in Cartesian space. Now, $f_{4''}$ and $f_{4'''}$ can be transformed to base frame (f_0) by considering serial chains SC_1 and SC_2 respectively. The serial chain SC_1 consists of links $L_0, L_1, L_2, L_{3a}, L_{3b}$ and L_4 whereas, SC_2 is formed by links L_0, L_1, L_2, L_3 and L_4. Both of these possibilities are discussed separately as Case-I and Case-II respectively.

Case-I

In this case, the frame $f_{4''}$ is transformed to frame f_0 by considering the serial chain SC_1. The link-frames are assigned using proximal variant of D-H parameter method. Both link-frame assignment and marked D-H parameters are shown in Fig. 4.10 and these parameters are given in Table 4.8.

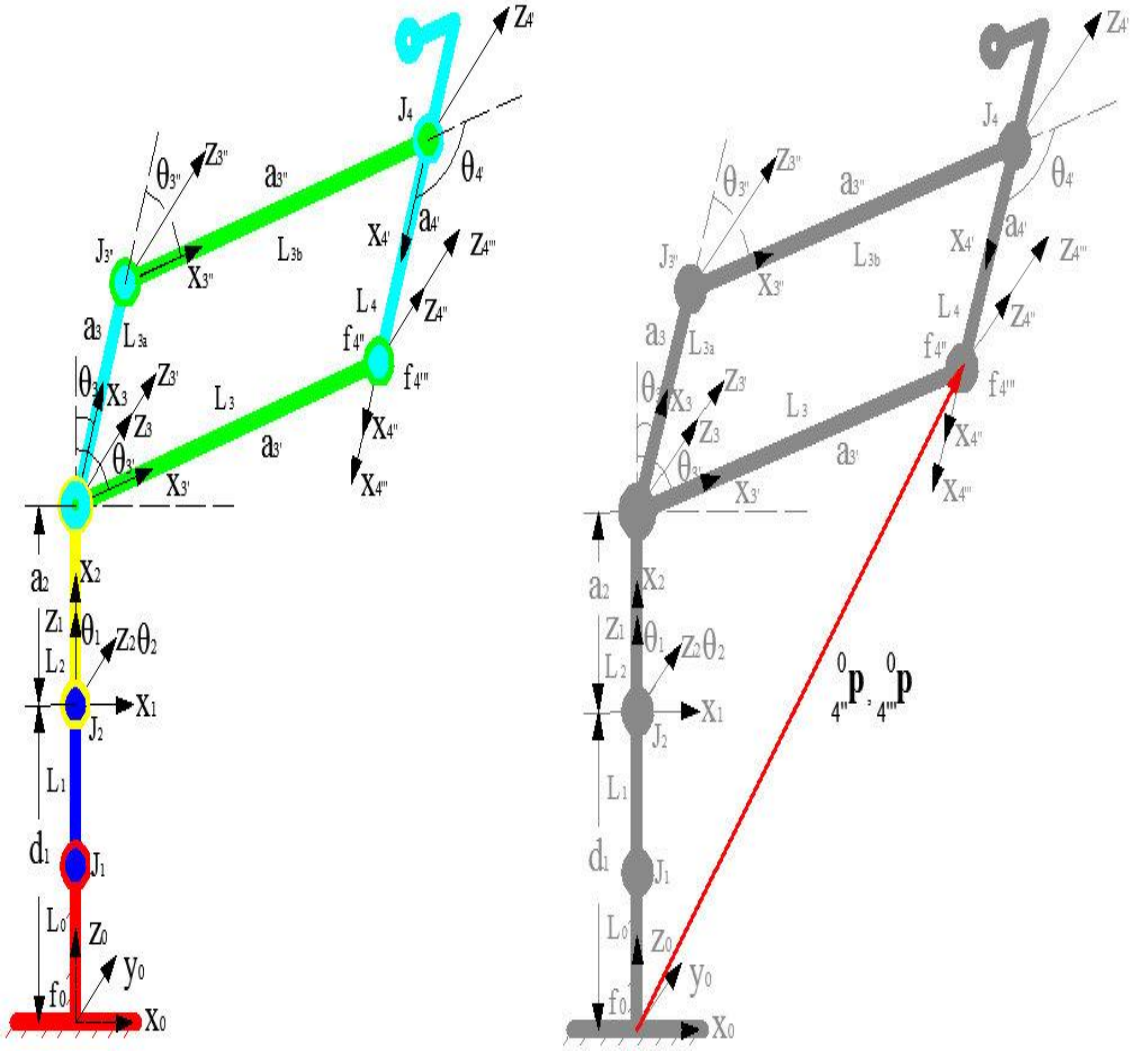

Fig. 4.10-(a): Constraint development diagram of parallelogram linkage, and Fig. 4.10-(b) point of interest is shown with respect to two chains SC_1 and SC_2.

Table 4.8: D-H parameters of serial chain SC_1.

S.No.	Link length (a_{i-1})	Link twist (α_{i-1})	Joint offset (d_i)	Joint angle (θ_i)	Home position
1.	$a_0 = 0$	$\alpha_0 = 0$	d_1	θ_1	0
2.	$a_1 = 0$	$\alpha_1 = -90$	$d_2 = 0$	θ_2	-90
3.	a_2	$\alpha_2 = 0$	$d_3 = 0$	θ_3	θ_3
$3''$	a_3	$\alpha_3 = 0$	$d_{3''} = 0$	$\theta_{3''}$	$\theta_{3''}$
$4'$	$a_{3''}$	$\alpha_{3''} = 0$	$d_{4'} = 0$	$\theta_{4'}$	$\theta_{4'}$
$4''$	$a_{4'}$	$\alpha_{4'} = 0$	$d_{4''} = 0$	–	0

Now, desired transformation can be obtained as

$$ {}^{0}_{4''}\boldsymbol{A} = {}^{0}_{1}\boldsymbol{A}\,{}^{1}_{2}\boldsymbol{A}\,{}^{2}_{3}\boldsymbol{A}\,{}^{3}_{3''}\boldsymbol{A}\,{}^{3''}_{4'}\boldsymbol{A}\,{}^{4'}_{4''}\boldsymbol{A} \tag{4.36} $$

or

$$ {}^{0}_{4''}\boldsymbol{A} = {}^{0}_{3}\boldsymbol{A}\,{}^{3}_{4''}\boldsymbol{A} \tag{4.37} $$

where

$$ {}^{0}_{3}\boldsymbol{A} = {}^{0}_{1}\boldsymbol{A}\,{}^{1}_{2}\boldsymbol{A}\,{}^{2}_{3}\boldsymbol{A} \tag{4.38} $$

$$ {}^{3}_{4''}\boldsymbol{A} = {}^{3}_{3''}\boldsymbol{A}\,{}^{3''}_{4'}\boldsymbol{A}\,{}^{4'}_{4''}\boldsymbol{A} \tag{4.39} $$

and

$$ {}^{3}_{3''}\boldsymbol{A} = \left[\begin{array}{ccc|c} c_{3''} & -s_{3''} & 0 & a_3 \\ s_{3''} & c_{3''} & 0 & 0 \\ 0 & 0 & 1 & 0 \\ \hline 0 & 0 & 0 & 1 \end{array}\right] \tag{4.40} $$

$$
{}^{3''}_{4'}\boldsymbol{A} = \begin{bmatrix} c_{4'} & -s_{4'} & 0 & | & a_{3''} \\ s_{4'} & c_{4'} & 0 & | & 0 \\ 0 & 0 & 1 & | & 0 \\ - & - & - & | & - \\ 0 & 0 & 0 & | & 1 \end{bmatrix} \tag{4.41}
$$

$$
{}^{4'}_{4''}\boldsymbol{A} = \begin{bmatrix} 1 & 0 & 0 & | & a_{4'} \\ 0 & 1 & 0 & | & 0 \\ 0 & 0 & 1 & | & 0 \\ - & - & - & | & - \\ 0 & 0 & 0 & | & 1 \end{bmatrix} \tag{4.42}
$$

Using Eqns. (4.3), (4.4), (4.5), and (4.40), (4.41), (4.42), the transformation matrices are calculated as

$$
{}^{0}_{3}\boldsymbol{A} = \begin{bmatrix} c_1c_{23} & -c_1s_{23} & -s_1 & | & c_1c_2a_2 \\ s_1c_{23} & -s_1s_{23} & c_1 & | & s_1c_2a_2 \\ -s_{23} & -c_{23} & 0 & | & (d_1 - s_2a_2) \\ - & - & - & | & - \\ 0 & 0 & 0 & | & 1 \end{bmatrix} \tag{4.43}
$$

$$
{}^{3}_{4''}\boldsymbol{A} = \begin{bmatrix} c_{3''4''} & -s_{3''4''} & 0 & | & (a_3 + c_{3''}a_{3''} + a_{4'}c_{3''4'}) \\ s_{3''4''} & c_{3''4''} & 0 & | & s_{3''}a_{3''} + a_{4'}s_{3''4'} \\ 0 & 0 & 1 & | & 0 \\ - & - & - & | & - \\ 0 & 0 & 0 & | & 1 \end{bmatrix} \tag{4.44}
$$

Therefore

$$
{}^{0}_{4''}\boldsymbol{A} = \begin{bmatrix} \check{d}_{11} & \check{d}_{12} & \check{d}_{13} & | & \check{d}_{14} \\ \check{d}_{21} & \check{d}_{22} & \check{d}_{23} & | & \check{d}_{24} \\ \check{d}_{31} & \check{d}_{32} & \check{d}_{33} & | & \check{d}_{34} \\ - & - & - & | & - \\ 0 & 0 & 0 & | & 1 \end{bmatrix} \tag{4.45}
$$

where

$$
\check{d}_{11} = c_1c_{233''4'}
$$

$$
\check{d}_{12} = -c_1s_{233''4'}
$$

$$\check{d}_{13} = -s_1$$

$$\check{d}_{14} = c_1(c_2a_2 + c_{23}a_3 + c_{233''}a_{3''} + c_{233''4'}a_{4'})$$

$$\check{d}_{21} = s_1c_{233''4'}$$

$$\check{d}_{22} = -s_1s_{233''4'}$$

$$\check{d}_{23} = c_1$$

$$\check{d}_{24} = s_1(c_2a_2 + c_{23}a_3 + c_{233''}a_{3''} + c_{233''4'}a_{4'})$$

$$\check{d}_{31} = -s_{233''4'}$$

$$\check{d}_{32} = -c_{233''4'}$$

$$\check{d}_{33} = 0$$

$$\check{d}_{34} = (d_1 - s_2a_2 - s_{23}a_3 - s_{233''}a_{3''} - s_{233''4'}a_{4'})$$

The Eqn. (4.45) gives the position and orientation (pose) of frame $f_{4''}$ relative to f_0. The position vector corresponding to this can be written as

$$\left[{}^{0}_{4''}\boldsymbol{p}\right]_{SC_1} = \begin{bmatrix} {}^{0}_{4''}x \\ {}^{0}_{4''}y \\ {}^{0}_{4''}z \\ 1 \end{bmatrix} = \begin{bmatrix} c_1(c_2a_2 + c_{23}a_3 + c_{233''}a_{3''} + c_{233''4'}a_{4'}) \\ s_1(c_2a_2 + c_{23}a_3 + c_{233''}a_{3''} + c_{233''4'}a_{4'}) \\ (d_1 - s_2a_2 - s_{23}a_3 - s_{233''}a_{3''} - s_{233''4'}a_{4'}) \\ 1 \end{bmatrix} \quad (4.45\text{-a})$$

Case-II

Now, the frame $f_{4'''}$ can be transformed to f_0, when serial chain SC_2 is considered. The frame assignment and D-H parameters calculation is done by same method as in Case-I. The D-H parameters are given in Table 4.9.

The desired pose can be obtained as

$${}^{0}_{4'''}\boldsymbol{A} = {}^{0}_{1}\boldsymbol{A}\,{}^{1}_{2}\boldsymbol{A}\,{}^{2}_{3'}\boldsymbol{A}\,{}^{3'}_{4'''}\boldsymbol{A} \quad (4.46)$$

or

$${}^{0}_{4'''}\boldsymbol{A} = {}^{0}_{3'}\boldsymbol{A}\,{}^{3'}_{4'''}\boldsymbol{A} \quad (4.47)$$

where

$${}^{0}_{3'}\boldsymbol{A} = {}^{0}_{1}\boldsymbol{A}\,{}^{1}_{2}\boldsymbol{A}\,{}^{2}_{3'}\boldsymbol{A} \quad (4.48)$$

Table 4.9: D-H parameters of serial chain SC_2.

S.No.	Link length (a_{i-1}) (mm)	Link twist (α_{i-1}) (deg.)	Joint offset (d_i) (mm)	Joint angle (θ_i) (deg.)	Home position.
1.	$a_0 = 0$	$\alpha_0 = 0$	d_1	θ_1	0
2.	$a_1 = 0$	$\alpha_1 = -90$	$d_2 = 0$	θ_2	-90
$3'$	a_2	$\alpha_2 = 0$	$d_{3'} = 0$	$\theta_{3'}$	$\theta_{3'}$
$4'''$	$a_{3'}$	$\alpha_{3'} = 0$	$d_{4'''} = 0$	$-$	90

The transformation matrix, which transform frame $f_{3'}$ into f_2 can be written as

$$ {}^{2}_{3'}\boldsymbol{A} = \left[\begin{array}{ccc|c} c_{3'} & -s_{3'} & 0 & a_2 \\ s_{3'} & c_{3'} & 0 & 0 \\ 0 & 0 & 1 & 0 \\ - & - & - & - \\ 0 & 0 & 0 & 1 \end{array}\right] \tag{4.49} $$

Referring Eqns. (4.3), (4.4) and (4.49)

$$ {}^{0}_{3'}\boldsymbol{A} = {}^{0}_{1}\boldsymbol{A}\ {}^{1}_{2}\boldsymbol{A}\ {}^{2}_{3'}\boldsymbol{A} = \left[\begin{array}{ccc|c} c_1c_{23'} & -c_1s_{23'} & -s_1 & c_1c_2a_2 \\ s_1c_{23'} & -s_1s_{23'} & c_1 & s_1c_2a_2 \\ -s_{23'} & -c_{23'} & 0 & (d_1 - s_2a_2) \\ - & - & - & - \\ 0 & 0 & 0 & 1 \end{array}\right] \tag{4.50} $$

Since, the transformation of $f_{4'''}$ into $f_{3'}$ is a constant transformation which is given by

$$ {}^{3'}_{4'''}\boldsymbol{A} = \left[\begin{array}{ccc|c} c_{4'''} & -s_{4'''} & 0 & a_{3'} \\ s_{4'''} & c_{4'''} & 0 & 0 \\ 0 & 0 & 1 & 0 \\ - & - & - & - \\ 0 & 0 & 0 & 1 \end{array}\right] \tag{4.51} $$

$\theta_{4'''} = \text{constant} = 90^{\circ}$.

$$ {}^{3'}_{4'''}\boldsymbol{A} = \left[\begin{array}{ccc|c} 0 & -1 & 0 & a_{3'} \\ 1 & 0 & 0 & 0 \\ 0 & 0 & 1 & 0 \\ \hline 0 & 0 & 0 & 1 \end{array}\right] \tag{4.52} $$

Therefore,

$$ {}^{0}_{4'''}\boldsymbol{A} = \left[\begin{array}{ccc|c} -c_1 s_{23'} & -c_1 c_{23'} & -s_1 & c_1(c_2 a_2 + c_{23'} a_{3'}) \\ -s_1 s_{23'} & -s_1 c_{23'} & c_1 & s_1(c_2 a_2 + c_{23'} a_{3'}) \\ -c_{23'} & s_{23'} & 0 & (d_1 - s_2 a_2 + s_{23'} a_{3'}) \\ \hline 0 & 0 & 0 & 1 \end{array}\right] \tag{4.53} $$

The Eqn. (4.53), transforms the frame $f_{4'''}$ to base frame f_0. Both, Eqns. (4.45) and (4.53) represents the same point in Cartesian space for the given values of D-H parameters. From Eqn. (4.53), the position of the frame $f_{4'''}$ can be written as

$$ \left[{}^{0}_{4'''}\boldsymbol{p}\right]_{SC_2} = \begin{bmatrix} {}^{0}_{4'''}x \\ {}^{0}_{4'''}y \\ {}^{0}_{4'''}z \\ 1 \end{bmatrix} = \begin{bmatrix} c_1(c_2 a_2 + c_{23'} a_{3'}) \\ s_1(c_2 a_2 + c_{23'} a_{3'}) \\ (d_1 - s_2 a_2 + s_{23'} a_{3'}) \\ \hline 1 \end{bmatrix} \tag{4.53-a} $$

Now, as reported by Siciliano [15], for a closed-loop robot having last joint as revolute, the position constraints of a parallelogram linkage can be obtained as

$$ \left(\left[{}^{0}_{4''}\boldsymbol{p}\right]_{SC_1} - \left[{}^{0}_{4'''}\boldsymbol{p}\right]_{SC_2}\right) = \begin{bmatrix} 0 \\ 0 \\ 0 \end{bmatrix} \tag{4.54} $$

Which can be written in expanded form as

$$ \left(\begin{bmatrix} {}^{0}_{4''}x \\ {}^{0}_{4''}y \\ {}^{0}_{4''}z \\ 1 \end{bmatrix} - \begin{bmatrix} {}^{0}_{4'''}x \\ {}^{0}_{4'''}y \\ {}^{0}_{4'''}z \\ 1 \end{bmatrix}\right) = \begin{bmatrix} 0 \\ 0 \\ 0 \end{bmatrix} \tag{4.55} $$

Using Eqns. (4.45-a), (4.53-a) and (4.55), the position constraints can be written as

$$(c_1(c_2a_2 + c_{23}a_3 + c_{233''}a_{3''} + c_{233''4'}a_{4'}) - c_1(c_2a_2 + c_{23'}a_{3'})) = 0$$

$$(s_1(c_2a_2 + c_{23}a_3 + c_{233''}a_{3''} + c_{233''4'}a_{4'}) - s_1(c_2a_2 + c_{23'}a_{3'})) = 0$$

$$((d_1 - s_2a_2 - s_{23}a_3 - s_{233''}a_{3''} - s_{233''4'}a_{4'}) - (d_1 - s_2a_2 + s_{23'}a_{3'})) = 0$$

From the parallelogram linkage ($L_3, L_{3a}, L_{3b},$ and L_4), it can be found that

$$a_{4'} = a_3 \quad (4.56)$$

$$a_{3''} = a_{3'} \quad (4.57)$$

By simplifying the above equations the constraints are given as

$$a_3(c_{23} + c_{233''4'}) + a_{3'}(c_{233''} - c_{23'}) = 0 \quad (4.58)$$

$$a_3(c_{23} + c_{233''4'}) + a_{3'}(c_{233''} - c_{23'}) = 0 \quad (4.59)$$

$$-a_3(s_{23} + s_{233''4'}) + a_{3'}(s_{23'} - s_{233''}) = 0 \quad (4.60)$$

The Eqns. (4.58), (4.59) and (4.60), gives the position constraints of the parallelogram linkage for the case of manipulator for medical applications. Out of three, two are independent, as first two of them are same. It is expected also, as the parallelogram linkage is planer in X-Z plane. Thus, the constraint in y-direction does not exist.

In order to satisfy these constraints for any choice of a_3 and $a_{3'}$, it follows that

$$\theta_{3''} = (\theta_{3'} - \theta_3) \quad (4.61)$$

$$\theta_{4'} = (\pi - (\theta_{3'} - \theta_3)). \quad (4.62)$$

Thus, for mapping of the frames $f_{4''}$ and $f_{4'''}$ to frame f_0 the joint vector $q' = [\theta_1, \theta_2, \theta_3$ and $\theta_{3'}]$ can be used instead of $q' = [\theta_1,\ \theta_2,\ \theta_3,\ \theta_{3''}$ and $\theta_{4''}]$.

4.10.2 Inclusion of Parallelogram Linkage in the Kinematic Model of MMA

In this section an attempt is made to derive the kinematic model of MMA, using the analysis made in Section 4.10.1.

$$^{0}_{4'}\boldsymbol{A} = {}^{0}_{3}\boldsymbol{A}\ {}^{3}_{4'}\boldsymbol{A} \quad (4.63)$$

where

$$ {}^{3}_{4'}\boldsymbol{A} = {}^{3}_{3''}\boldsymbol{A}\,{}^{3''}_{4'}\boldsymbol{A} $$

From Eqns. (4.40) and (4.41),

$$ {}^{3}_{4'}\boldsymbol{A} = \left[\begin{array}{ccc|c} c_{3''4'} & -s_{3''4'} & 0 & a_3 + c_{3''}a_{3''} \\ s_{3''4'} & c_{3''4'} & 0 & s_{3''}a_{3''} \\ 0 & 0 & 1 & 0 \\ \hline 0 & 0 & 0 & 1 \end{array}\right] \tag{4.64} $$

Substituting Eqns. (4.43) and (4.64) in Eqn. (4.63)

$$ {}^{0}_{4'}\boldsymbol{A} = \left[\begin{array}{ccc|c} \tilde{e}_{11} & \tilde{e}_{12} & \tilde{e}_{13} & \tilde{e}_{14} \\ \tilde{e}_{21} & \tilde{e}_{22} & \tilde{e}_{23} & \tilde{e}_{24} \\ \tilde{e}_{31} & \tilde{e}_{32} & \tilde{e}_{33} & \tilde{e}_{34} \\ \hline 0 & 0 & 0 & 1 \end{array}\right] \tag{4.65} $$

where

$$ \begin{aligned} \tilde{e}_{11} &= c_1 c_{233''4'} \\ \tilde{e}_{12} &= -c_1 s_{233''4'} \\ \tilde{e}_{13} &= -s_1 \\ \tilde{e}_{14} &= c_1(c_2 a_2 + c_{23} a_3 + c_{233''} a_{3''}) \\ \tilde{e}_{21} &= s_1 c_{233''4'} \\ \tilde{e}_{22} &= -s_1 s_{233''4'} \\ \tilde{e}_{23} &= c_1 \\ \tilde{e}_{24} &= s_1(c_2 a_2 + c_{23} a_3 + c_{233''} a_{3''}) \\ \tilde{e}_{31} &= -s_{233''4'} \\ \tilde{e}_{32} &= -c_{233''4'} \\ \tilde{e}_{33} &= 0 \\ \tilde{e}_{34} &= (d_1 - s_2 a_2 - s_{23} a_3 - s_{233''} a_{3''} - s_{233''4'}) \end{aligned} $$

Eliminating $\theta_{3''}$ and $\theta_{4'}$ using Eqns. (4.61) and (4.62), Eqn. (4.65) can be simplified as

$$
{}^{0}_{4'}\boldsymbol{A} = \begin{bmatrix} \tilde{f}_{11} & \tilde{f}_{12} & \tilde{f}_{13} & | & \tilde{f}_{14} \\ \tilde{f}_{21} & \tilde{f}_{22} & \tilde{f}_{23} & | & \tilde{f}_{24} \\ \tilde{f}_{31} & \tilde{f}_{32} & \tilde{f}_{33} & | & \tilde{f}_{34} \\ - & - & - & | & - \\ 0 & 0 & 0 & | & 1 \end{bmatrix} \tag{4.66}
$$

where

$$
\begin{aligned}
\tilde{f}_{11} &= -c_1 c_{23} \\
\tilde{f}_{12} &= c_1 s_{23} \\
\tilde{f}_{13} &= -s_1 \\
\tilde{f}_{14} &= c_1(c_2 a_2 + c_{23} a_3 + c_{23'} a_{3''}) \\
\tilde{f}_{21} &= -s_1 c_{23} \\
\tilde{f}_{22} &= s_1 s_{23} \\
\tilde{f}_{23} &= c_1 \\
\tilde{f}_{24} &= s_1(c_2 a_2 + c_{23} a_3 + c_{23'} a_{3''}) \\
\tilde{f}_{31} &= s_{23} \\
\tilde{f}_{32} &= c_{23} \\
\tilde{f}_{33} &= 0 \\
\tilde{f}_{34} &= (d_1 - s_2 a_2 - s_{23} a_3 - s_{23'} a_{3''})
\end{aligned}
$$

From Eqn. (4.66), it can be observed that it contains joint variables as θ_1, θ_2, θ_3 and $\theta_{3'}$ only. Whereas Eqn. (4.65), in addition to these variables also contains $\theta_{3''}$ and $\theta_{4'}$. At this point, parallelogram linkage condition of 2-DOFs system gets embedded into the kinematic analysis of MMA.

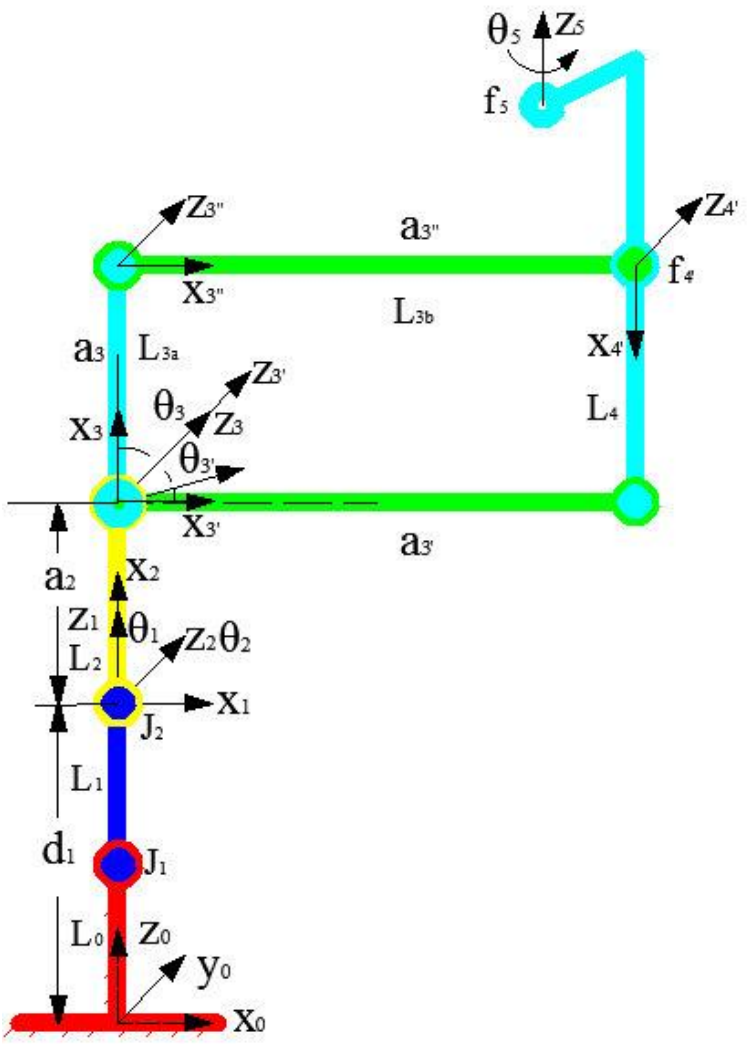

Fig. 4.11: Development of kinematic model using D-H parameter method taking parallelogram linkage in account.

Now, it is desired to define the frame (f_5), attached to distal end of link L_4, with respect to frame $f_{4'}$ (refer Fig. 4.11). However, at this point, an inconsistency in orientation of $x-axis$ ($x_{4'}$) and $z-axis$ (z_5), can be observed. In other words, orientations of $x_{4'}$ and z_5 are completely inconsistent in accordance of D-H parameter method, where according to this method, both x_{i-1} and x_i should be in a plane which is perpendicular to joint axis z_i. Since, the orientation of $x_{4'}$ is fixed according to the parallelogram linkage kinematic analysis made in Section 4.10.1. Also, orientation of joint axis z_5 is fixed as required by the medical/surgical robot's motion. Neither $x_{4'}$ nor z_5 can be altered.

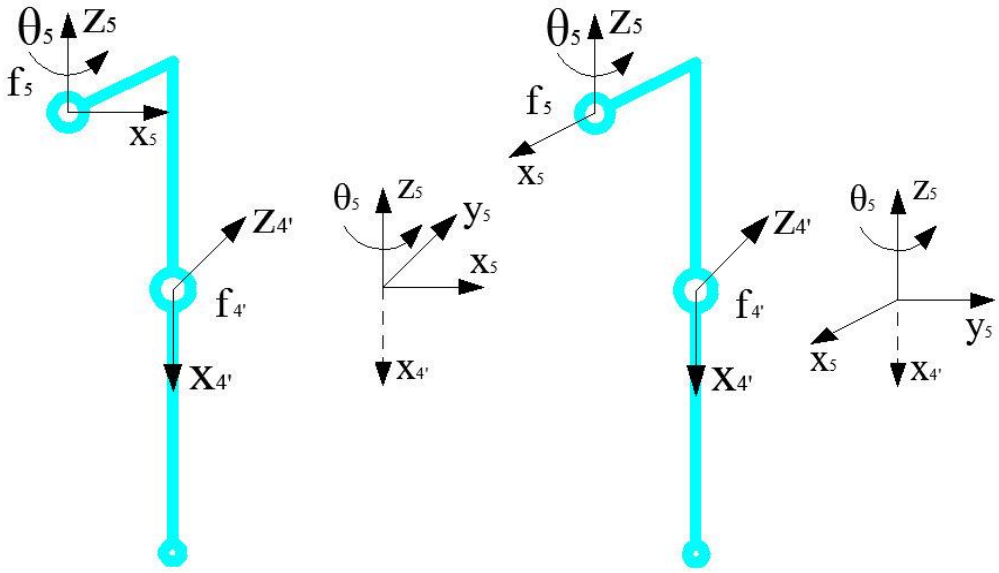

Figs. 4.12-(a) and 4.12-(b): Demonstration of the orientation inconsistency.

With reference to Fig. (4.11), $x - axis$ can be assigned to the distal end of link L_4 in two possible ways. Both are shown in Figs. 4.12-(a) and 4.12-(b). From these figures it can be observed that rotation is not possible from $x_{4'}$ to x_5, about z_5. Thus, there is a problem of orientation inconsistency because of which derivation of kinematic model gets stucked at this point.

Now, from above discussion it can be concluded that D-H parameter method of kinematic modeling cannot be applied for the case of MMA, which is a spatial hybrid manipulator. However, this problem is successfully solved by incorporating the concept of concept of dummy frames (described in Section 4.5.2) to D-H parameter method. The detail of the solution to this problem is presented in Section 4.10.3.

4.10.3 Solution Proposed to Resolve the Orientation Inconsistency

In this section, an effort is made to extend the utility of conventional D-H parameter method to spatial hybrid manipulators. The problem reported in Section 4.10.2 is solved successfully by using the newly introduced concept in the present work, which is the concept of dummy frames. In Fig. 4.13, for the assignment of dummy frame, Fig. 4.12-(b) is considered. The frame shown in red color is a dummy frame whose z-axis can be defined in appropriate direction. In other words, there is no fixed rule to define its z-axis. It can be

taken arbitrarily as required. Thereafter, x-axis is defined in the same way as defined by D-H parameter method. Finally, right hand thumb rule is applied to assign y-axis which completes the frame definition.

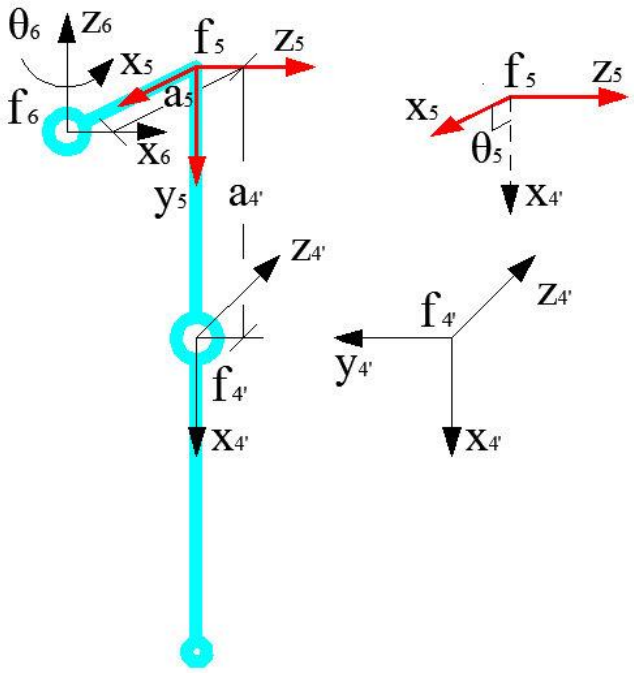

Fig. 4.13: Proposed solution (dummy frame) to achieve orientation consistency.

Now, it can be seen in Fig. 4.13 that orientations of axis $x_{4'}$ and z_5 are consistent satisfying the condition of application of D-H parameter method, as the axes $x_{4'}$ and x_5 form a plane which is perpendicular to z_5. Thus, rotation from $x_{4'}$ to x_5 about z_5 is possible. Similarly, the rotation from x_5 to x_6 about z_6 is also feasible. Hence, it can be concluded that the mapping of frame f_5 to f_4, which was not possible due to orientational inconsistency of axis $x_{4'}$ and z_5 (refer Fig. 4.12), is possible now. It can be clearly seen in Fig. 4.13 that the frame f_6 (originally f_5) is successfully mapped to f_4, with the use of dummy frame f_5. Here, it is important to bring in notice that dummy frame does not corresponds to any joint motion. The joint parameter corresponding to it remains constant as given by D-H parameter method. In the next section D-H parameter method with augmented dummy frames is applied to develop the MMA.

4.10.4 Development of the Kinematic Model using Dummy frames

In this section, the extended D-H parameter method is demonstrated for the case of manipulator for medical applications.

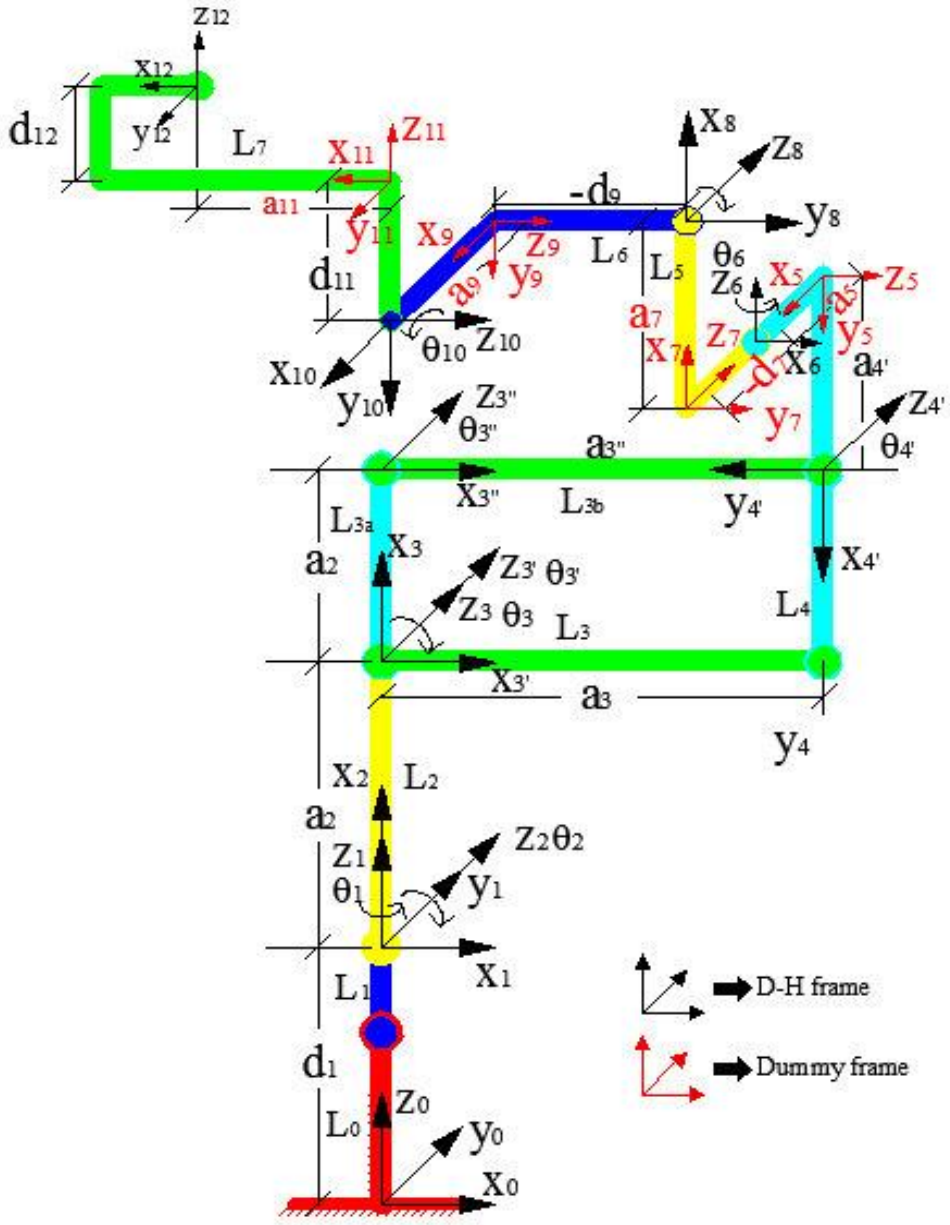

Fig. 4.14: D-H parameters augmented with dummy frames and taking parallelogram linkage in account.

Figure 4.14 shows the line diagram of MMA with augmented dummy frames in addition to D-H frames. Also, the corresponding D-H parameters are marked and are given in Table 4.10. In this kinematic analysis, four dummy frames (shown in red color) are used, leads to four constant joint angle variables.

Table 4.10: D-H parameters of MMA augmented with dummy frames taking parallelogram linkage in account.

S.No.	Link length (a_{i-1})	Link twist (α_{i-1})	Joint offset (d_i)	Joint angle (θ_i)	Home position
1.	$a_0 = 0$	$\alpha_0 = 0$	d_1	θ_1	0
2.	$a_1 = 0$	$\alpha_1 = -90$	$d_2 = 0$	θ_2	-90
3.	a_2	$\alpha_2 = 0$	$d_3 = 0$	θ_3	0
$3''$.	a_3	$\alpha_3 = 0$	$d_{3''} = 0$	$\theta_{3''}$	90
$4'$.	$a_{3''}$	$\alpha_{3''} = 0$	$d_{4'} = 0$	$\theta_{4'}$	90
5.	$-a_{4'}$	$\alpha_{4'} = 90$	$d_5 = 0$	$\theta_5 = \mathrm{C}$	-90
6.	a_5	$\alpha_5 = 90$	$d_6 = 0$	θ_6	90
7.	$a_6 = 0$	$\alpha_6 = -90$	$-d_7$	$\theta_7 = \mathrm{C}$	-90
8.	a_7	$\alpha_7 = 0$	$d_8 = 0$	θ_8	0
9.	$a_8 = 0$	$\alpha_8 = -90$	$-d_9$	$\theta_9 = \mathrm{C}$	90
10.	a_9	$\alpha_9 = 0$	$d_{10} = 0$	θ_{10}	0
11.	$a_{10} = 0$	$\alpha_{10} = 90$	d_{11}	$\theta_{11} = \mathrm{C}$	-90
12.	a_{11}	$\alpha_{11} = 0$	d_{12}	$-$	0
$3'$.	a_2	$\alpha_2 = 0$	$d_{3'} = 0$	$\theta_{3'}$	90
$4''$.	$a_{3'}$	$\alpha_{3'} = 0$	$d_{4''} = 0$	$-$	90

Now, the complete forward kinematic model of MMA taking parallelogram linkage in account, can be derived as

$$ {}^{0}_{12}\boldsymbol{A} = {}^{0}_{1}\boldsymbol{A}\,{}^{1}_{2}\boldsymbol{A}\,{}^{2}_{3}\boldsymbol{A}\,{}^{3}_{3''}\boldsymbol{A}\,{}^{3''}_{4'}\boldsymbol{A}\,{}^{4'}_{5}\boldsymbol{A}\,{}^{5}_{6}\boldsymbol{A}\,{}^{6}_{7}\boldsymbol{A}\,{}^{7}_{8}\boldsymbol{A}\,{}^{8}_{9}\boldsymbol{A}\,{}^{9}_{10}\boldsymbol{A}\,{}^{10}_{11}\boldsymbol{A}\,{}^{11}_{12}\boldsymbol{A} $$

or $\quad = \quad {}^{0}_{4'}\boldsymbol{A}\ {}^{4'}_{8}\boldsymbol{A}\ {}^{8}_{12}\boldsymbol{A}$ (4.67)

${}^{0}_{12}\boldsymbol{A}$

where

$$ {}^{4'}_{8}\boldsymbol{A} = {}^{4'}_{5}\boldsymbol{A}\ {}^{5}_{6}\boldsymbol{A}\ {}^{6}_{7}\boldsymbol{A}\ {}^{7}_{8}\boldsymbol{A} \tag{4.68} $$

$$ {}^{8}_{12}\boldsymbol{A} = {}^{8}_{9}\boldsymbol{A}\ {}^{9}_{10}\boldsymbol{A}\ {}^{10}_{11}\boldsymbol{A}\ {}^{11}_{12}\boldsymbol{A} \tag{4.69} $$

$$ {}^{4'}_{5}\boldsymbol{A} = \left[\begin{array}{ccc|c} c_5 & -s_5 & 0 & a_{4'} \\ 0 & 0 & -1 & 0 \\ s_5 & c_5 & 0 & 0 \\ \hline 0 & 0 & 0 & 1 \end{array}\right] \tag{4.70} $$

$$ = \left[\begin{array}{ccc|c} 0 & 1 & 0 & a_{4'} \\ 0 & 0 & -1 & 0 \\ -1 & 0 & 0 & 0 \\ \hline 0 & 0 & 0 & 1 \end{array}\right] $$

$$ {}^{5}_{6}\boldsymbol{A} = \left[\begin{array}{ccc|c} c_6 & -s_6 & 0 & a_5 \\ 0 & 0 & -1 & 0 \\ s_6 & c_6 & 0 & 0 \\ \hline 0 & 0 & 0 & 1 \end{array}\right] \tag{4.71} $$

$$ {}^{6}_{7}\boldsymbol{A} = \left[\begin{array}{ccc|c} c_7 & -s_7 & 0 & 0 \\ 0 & 0 & 1 & -d_7 \\ -s_7 & -c_7 & 0 & 0 \\ \hline 0 & 0 & 0 & 1 \end{array}\right] \tag{4.72} $$

$$ {}^{7}_{8}\boldsymbol{A} = \left[\begin{array}{ccc|c} c_8 & -s_8 & 0 & a_7 \\ s_8 & c_8 & 0 & 0 \\ 0 & 0 & 1 & 0 \\ \hline 0 & 0 & 0 & 1 \end{array}\right] \tag{4.73} $$

$$ {}^{8}_{9}\boldsymbol{A} = \left[\begin{array}{ccc|c} c_9 & -s_9 & 0 & 0 \\ 0 & 0 & 1 & -d_9 \\ -s_9 & -c_9 & 0 & 0 \\ \hline 0 & 0 & 0 & 1 \end{array}\right] \tag{4.74} $$

$$ \left[\begin{array}{ccc|c} 0 & -1 & 0 & 0 \\ 0 & 0 & 1 & -d_9 \\ -1 & 0 & 0 & 0 \\ \hline 0 & 0 & 0 & 1 \end{array}\right] $$

$$
{}^{9}_{10}\boldsymbol{A} = \left[\begin{array}{ccc|c} c_{10} & -s_{10} & 0 & a_9 \\ s_{10} & c_{10} & 0 & 0 \\ 0 & 0 & 1 & 0 \\ \hline 0 & 0 & 0 & 1 \end{array}\right] \tag{4.75}
$$

$$
{}^{10}_{11}\boldsymbol{A} = \left[\begin{array}{ccc|c} c_{11} & -s_{11} & 0 & 0 \\ 0 & 0 & -1 & -d_{11} \\ s_{11} & c_{11} & 0 & 0 \\ \hline 0 & 0 & 0 & 1 \end{array}\right] \tag{4.76}
$$

$$
{}^{11}_{12}\boldsymbol{A} = \left[\begin{array}{ccc|c} c_{12} & -s_{12} & 0 & a_{11} \\ s_{12} & c_{12} & 0 & 0 \\ 0 & 0 & 1 & d_{12} \\ \hline 0 & 0 & 0 & 1 \end{array}\right] \tag{4.77}
$$

$$
\left[\begin{array}{ccc|c} 1 & 0 & 0 & a_{11} \\ 0 & 1 & 0 & 0 \\ 0 & 0 & 1 & d_{12} \\ \hline 0 & 0 & 0 & 1 \end{array}\right] \tag{4.78}
$$

Substituting appropriate matrices in Eqns. (4.68) and (4.69)

$$
{}^{4'}_{8}\boldsymbol{A} = \left[\begin{array}{ccc|c} -c_8 & s_8 & 0 & (-a_{4'}-a_7) \\ -s_6 s_8 & -s_6 c_8 & -c_6 & c_6 d_7 \\ -c_6 s_8 & -c_6 c_8 & s_6 & (-a_5 - s_6 d_7) \\ \hline 0 & 0 & 0 & 1 \end{array}\right] \tag{4.79}
$$

$$
{}^{8}_{12}\boldsymbol{A} = \left[\begin{array}{ccc|c} 0 & -s_{10} & c_{10} & c_{10}(d_{11}+d_{12}) \\ -1 & 0 & 0 & -d_9 - a_{11} \\ 0 & -c_{10} & -s_{10} & -a_9 - s_{10}(d_{11}+d_{12}) \\ \hline 0 & 0 & 0 & 1 \end{array}\right] \tag{4.80}
$$

Therefore, upon substitution for Eqns. (4.66), (4.79) and (4.80) in Eqn. (4.67)

$$
{}^{0}_{12}\boldsymbol{A} = \left[\begin{array}{ccc|c} \tilde{g}_{11} & \tilde{g}_{12} & \tilde{g}_{13} & \tilde{g}_{14} \\ \tilde{g}_{21} & \tilde{g}_{22} & \tilde{g}_{23} & \tilde{g}_{24} \\ \tilde{g}_{31} & \tilde{g}_{32} & \tilde{g}_{33} & \tilde{g}_{34} \\ \hline 0 & 0 & 0 & 1 \end{array}\right] \tag{4.81}
$$

where

$$
\tilde{g}_{11} = c_1 c_{23} s_8 - c_8 (s_1 c_6 - c_1 s_{23} s_6)
$$

$$
\begin{aligned}
\tilde{g}_{12} &= c_{10}(s_1 s_6 + c_1 s_{23} c_6) + s_{10}\{-c_1 c_{23} c_8 - s_8(s_1 c_6 - c_1 s_{23} s_6)\} \\
\tilde{g}_{13} &= s_{10}(s_1 s_6 + c_1 s_{23} c_6) - c_{10}\{-c_1 c_{23} c_8 - s_8(s_1 c_6 - c_1 s_{23} s_6)\} \\
\tilde{g}_{14} &= c_1(c_2 a_2 + c_{23} a_3 + c_{23'} a_{3''} + c_{23} a_{4'} + c_{23} a_7) + s_1 a_5 + \\
&\quad d_7(s_1 s_6 + c_1 s_{23} c_6) - d_9\{-c_1 c_{23} s_8 + c_8(s_1 c_6 - c_1 s_{23} s_6)\} + \\
&\quad a_9(s_1 s_6 + c_1 s_{23} c_6) - d_{11}\{-s_{10}(s_1 s_6 + c_1 s_{23} c_6) + c_{10}\{-c_1 \\
&\quad c_{23} c_8 - s_8(s_1 c_6 - c_1 s_{23} s_6)\}\} + a_{11}\{c_1 c_{23} s_8 - c_8(s_1 c_6 - \\
&\quad c_1 s_{23} s_6)\} + d_{12}[s_{10}(s_1 s_6 + c_1 s_{23} c_6) - c_{10}\{-c_1 c_{23} c_8 - \\
&\quad s_8(s_1 c_6 - c_1 s_{23} s_6)\}] \\
\tilde{g}_{21} &= s_1 c_{23} s_8 + c_8(c_1 c_6 + s_1 s_{23} s_6) \\
\tilde{g}_{22} &= c_{10}(-c_1 s_6 + s_1 s_{23} c_6) - s_{10}\{s_1 c_{23} c_8 + s_8(c_1 c_6 + s_1 s_{23} s_6)\} \\
\tilde{g}_{23} &= s_{10}(-c_1 s_6 + s_1 s_{23} c_6) - c_{10}\{-s_1 c_{23} c_8 + s_8(c_1 c_6 + s_1 s_{23} s_6)\} \\
\tilde{g}_{24} &= s_1(c_2 a_2 + c_{23} a_{23} + c_{23'} a_{3''} + c_{23} a_{4'} + c_{23} a_7) - c_1 a_5 - \\
&\quad d_7(c_1 s_6 - s_1 s_{23} c_6) - d_9\{-s_1 c_{23} s_8 + c_8(c_1 c_6 - s_1 s_{23} s_6)\} + \\
&\quad a_9(-c_1 s_6 + s_1 s_{23} c_6) - d_{11}\{-s_{10}(-c_1 s_6 + s_1 s_{23} c_6) + c_{10} \\
&\quad \{-s_1 c_{23} c_8 + s_8(c_1 c_6 + s_1 s_{23} s_6)\}\} + a_{11}\{s_1 c_{23} s_8 + c_8 \\
&\quad (c_1 c_6 + s_1 s_{23} s_6)\} + d_{12}[s_{10}(-c_1 s_6 + s_1 s_{23} c_6) - c_{10} \\
&\quad \{-s_1 c_{23} c_8 + s_8(c_1 c_6 + s_1 s_{23} s_6)\}] \\
\tilde{g}_{31} &= -s_{23} s_8 + c_{23} s_6 c_8 \\
\tilde{g}_{32} &= c_{10} c_{23} c_6 + s_{10}(s_{23} c_8 + c_{23} s_6 s_8) \\
\tilde{g}_{33} &= s_{10} c_{23} c_6 - c_{10}(s_{23} c_8 + c_{23} s_6 s_8) \\
\tilde{g}_{34} &= d_1 - s_2 a_2 - s_{23} a_3 - s_{23'} a_{3''} - s_{23} a_{4'} + c_{23} c_6 d_7 - a_7 s_{23} \\
&\quad -d_9(s_{23} s_8 - c_8 c_{23} s_6) + c_{23} c_6 a_9 - d_{11}\{-s_{10} c_{23} c_6 + c_{10} \\
&\quad (s_{23} c_8 + c_{23} s_6 s_8)\} + a_{11}(c_{23} s_6 c_8 - s_{23} s_8) + d_{12}[\, s_{10} c_{23} c_6 - \\
&\quad c_{10}(s_{23} c_8 + c_{23} s_6 s_8)]
\end{aligned}
$$

Thus, the Eqn. (4.81), provides the complete kinematic model of a spatial hybrid manipulator.

4.11 Geometrical validation of kinematic Model

In this section, the model developed in Section 4.10.4, is validated geometrically by substituting D-H parameters (refer Table 4.8), corresponding to assumed home position as shown in Fig. 4.14, in Eqn. (4.81). The validation result is given by

$$ {}^{0}_{12}\boldsymbol{A} = \left[\begin{array}{ccc|c} -1 & 0 & 0 & (a_{3''} - d_9 - a_{11}) \\ 0 & -1 & 0 & -(a_5 + d_7 + a_9) \\ 0 & 0 & 1 & (d_1 + a_2 + a_3 + a_{4'} + a_7 + d_{11} + d_{12}) \\ - & - & - & - \\ 0 & 0 & 0 & 1 \end{array}\right] \tag{4.82} $$

Eqn. (4.82). At this point a comparison of this equation with Fig. (4.14), can be made and it can be observed that position and orientation given by the developed kinematic model is consistent as given by this figure. Also, from Figs. 4.8-(b) and 4.14, it can be observed that $d_5 = (a_3 + a_{4'})$.

4.12 Summary

This chapter deals with kinematic study of spatial hybrid manipulators. First, the general introduction of a spatial hybrid manipulator has been presented. Thereafter, an attempt has been made to apply D-H parameter method to MMA, which is a spatial hybrid manipulator. However, this application leads to two kinds of inconsistencies – *positional inconsistency* and *orientational inconsistency*, as reported in Sections 4.6 and 4.10, respectively. This is due to the reason that D-H parameter method is applicable to serial manipulators only, as reported in Chapter 2. Also, an ambiguity in it is observed by Seth and Uicker [9] in the case of closed-loop robots. The main focus of this work is to extend the utility of D-H parameter method to spatial hybrid manipulators by proposing the concept of *dummy frames*. To the best of authors knowledge, the proposed concept of dummy frames has not been used before in the literature. The inconsistencies observed during the development of kinematic model of MMA have been completely removed by using the concept of dummy frames. The efficacy of the proposed concept has been demonstrated successfully in the field of surgical robots, using a MMA prototype, to obtain geometrical as well as physical consistency of the kinematic model. To file the patent, the details of MMA prototype has been kept confidential by **CSIR-CSIO** Chandigarh, India.

Chapter 5

Gravity Balancing of Robotic Manipulators

5.1 Introduction

Gravity Balancing is an important aspect for robotic manipulators, especially for serial manipulators. Because, in serial manipulators as the number of links keeps on increasing, the gravitational effect due to the weight of succeeding links and joints keeps on increasing on preceding joints [64]. This leads to degradation of performance in terms of load carrying capacity of manipulator, power requirement to operate manipulator etc. So, in order to improve their performance, gravity compensation is provided. Now, question is when the manipulator is considered to be gravity balanced? The answer to this question is given in Section 5.2. In this chapter, first, fundamental concept of gravity balancing along with its broad classifications is described. Thereafter, two different methods of gravity balancing are presented and finally, analytic formulation for gravity balancing of MMA hybrid manipulator is developed.

5.2 Gravity Balancing

A robotic manipulator is referred to as gravity balanced, if joint actuator inputs are not required to keep the system in static equilibrium at its any configuration. Also, a manipulator is said to be statically balanced, if there is no effect of gravity on it and it remains in static equilibrium at its any possible configuration. The following mathematical conditions can be given to a gravity balanced system [65]:

1) During motion, centre of mass does not change inertially.
2) There is no change in potential energy of system as there is a change in its configuration.
3) The system remains gravity balanced for every configuration because of the presence of counterweights.

The above mathematical conditions can be achieved by:

a) Attaching the counterweights to each link of the manipulator, used to fix the centre of mass of the manipulator.

b) Using springs at appropriate places in the manipulator, because the potential energy of system and the spring remains invariant with configuration of the manipulator.
c) Locating the centre of mass using auxiliary parallelograms.

5.3 Literature Review

The gravity balancing can be broadly classified into two categories as:

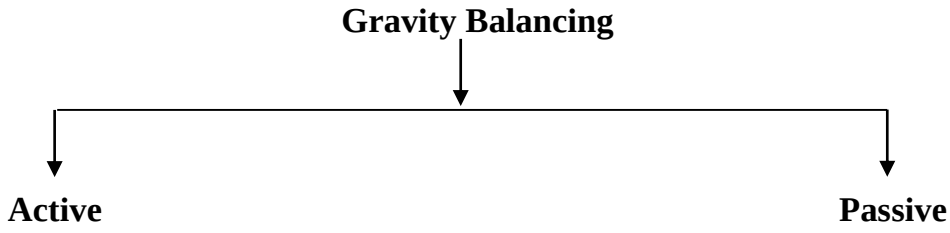

In active gravity balancing, actuator power is continuously applied to keep the system in static equilibrium. To accomplish this, either additional actuators are used, which results in increasing the size, mass and complexity of manipulator, or primary actuators are used, which degrades the dynamic performance of the manipulator [64]. This method of gravity balancing demand large power requirements, because more than half of the available actuator power is used in gravity compensation.

However, the problem of large power requirement in the case of active gravity compensation can be successfully solved by using counter weights or springs [66, 67], which is termed as *passive* gravity compensation. In passive gravity compensation, counter weights are added to make the perpendicular distance between centre of mass and joint axis to be zero. As compared active gravity balancing, the power requirement in this case reduces considerably, which leads to significant improvement in the dynamic performance of the manipulator. However, addition of weights leads to an increase of inertia, complexity and volume of manipulator [67]. So, it is preferable to use the spring elements with or without auxiliary links.

5.3.1 Passive Gravity Compensation Methods:

i. With Springs and Auxiliary Links

A passive mechanical method for gravity balancing of variety of manipulators has been proposed by Nathan and Kumar [64]. The proposed method is based on energy approach and according to this method, gravitational potential energy of manipulator is equalized to strain energy of springs, by using spring elements, cables and cam shaped pullies. The proposed method is illustrated for a single joint. With reference to Fig. 5.1, weight mg is acting at the end point of link having length L. A pulley is employed at the end point, where joint between link and fixed link is formed.

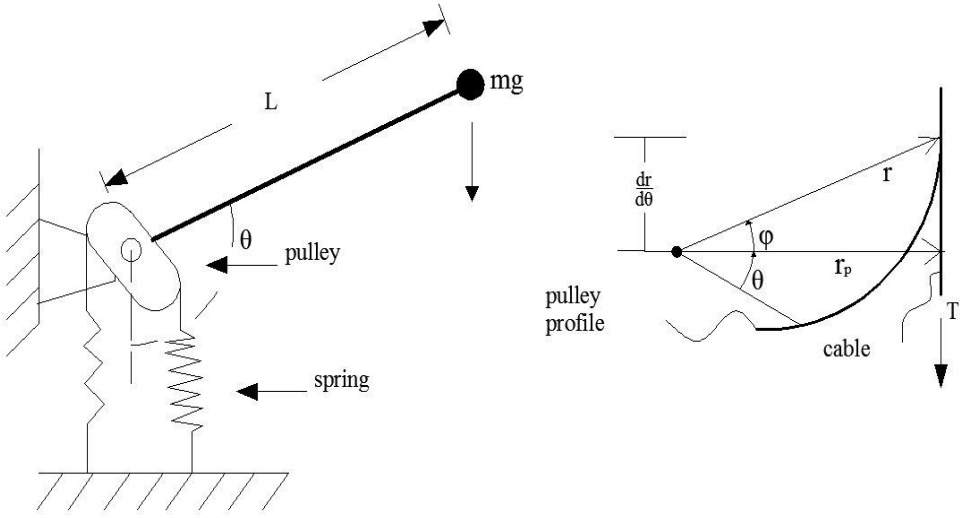

Fig. 5.1: Spring-pulley gravity compensation method for a single joint.

In order to balance the torque induced at joint because of gravity and resisting torque provided by spring-pulley arrangement, the both needs to be equated as,

$$\tau_{comp} = mlg \sin\theta \tag{5.1}$$

If T is the effective spring force, in that case exact gravity balancing requires:

$$mlg \sin\theta = Tr = -kxr \tag{5.2}$$

where

r = effective radius of pulley,

k = effective spring constant,

x = linear displacement of cable.

Differentiating Eqn. (5.2) w.r.t θ

$$mlg\ cos\ \theta = \frac{dT}{d\theta} r + T \frac{dr}{d\theta} \tag{5.3}$$

According to the principle of virtual work and geometry of the system:

$$rd\theta = dx \tag{5.4}$$

For spring to behave linearly, following condition should be satisfied:

$$dT = -rdx \tag{5.5}$$

Combing Eqns. (5.4) and (5.5),

$$\frac{dT}{d\theta} = -kr \tag{5.6}$$

Substituting Eqn. (5.6) into Eqn. (5.3)

$$kr^3 - mgl\ sin\ \theta \frac{dr}{d\theta} + mgrl\ cos\ \theta = 0 \tag{5.7}$$

The above equation leads to the following solution:

$$r(\theta) = \sqrt{\frac{mgl}{k}}\ sin\frac{\theta}{2} \tag{5.8}$$

The Eqn. (5.8) gives the effective radius of the pulley for each angular displacement θ. However, it does not tell about the actual shape of pulley. The actual shape of pulley can be find out by a radius $r_p(\theta)$ at an angular displacement $\varphi(\theta)$:

$$r_p(\theta) = \sqrt{\frac{mgL}{k}}\left[\frac{1}{4}cos^2\frac{\theta}{2} + sin^2\frac{\theta}{2}\right] \quad (5.9)$$

$$\varphi(\theta) = tan^{-1}\left[\frac{1}{2}cot\frac{\theta}{2}\right] \quad (5.10)$$

The proposed method has advantages, over gravity balancing with counter weights, like it is mechanically simple, lower system inertia, lesser energy input. Moreover, primary actuators are not required as in the case of active gravity compensation. Due to this reason, the above method is economical to implement and easy to adapt for different types of arm designs.

Another method of gravity balancing has been proposed by Agrawal and Fatteh [65]. The proposed method is a two-step approach, which is known as the *hybrid strategy*. These steps are:

1. First, locate the centre of mass using auxiliary parallelograms, which is based on knowledge of geometry and inertia property. For this purpose consider an $n - link$ serial manipulator with revolute joints only, as shown in Fig. 5.2. The location of centre of mass (G) from the reference point (O) is given as,

$$\boldsymbol{r}_{OC} = \frac{1}{M}\sum_{i=1}^{n} m_i \boldsymbol{r}_{OC_i} \quad (5.11)$$

where

$$M = \sum_{i=1}^{n} m_i = \text{total mass of the manipulator,} \quad (5.12)$$

m_i = mass of i^{th} link,

$\boldsymbol{r}_{OC_i}$ = location of centre of mass (G_i) of i^{th} link from origin O_i.

Further, $\boldsymbol{r}_{OC_i}$ can be written as:

$$\boldsymbol{r}_{OC_i} = \boldsymbol{r}_{OO_i} + \boldsymbol{r}_{O_iC_i} \quad (5.13)$$

Where O_i is the origin of frame attached to link i. With reference to Fig. 5.2,

$$\boldsymbol{r}_{OO_i} = \sum_{j=1}^{i} (d_j \boldsymbol{z}_{j-1} + a_j \boldsymbol{x}_j) \tag{5.14}$$

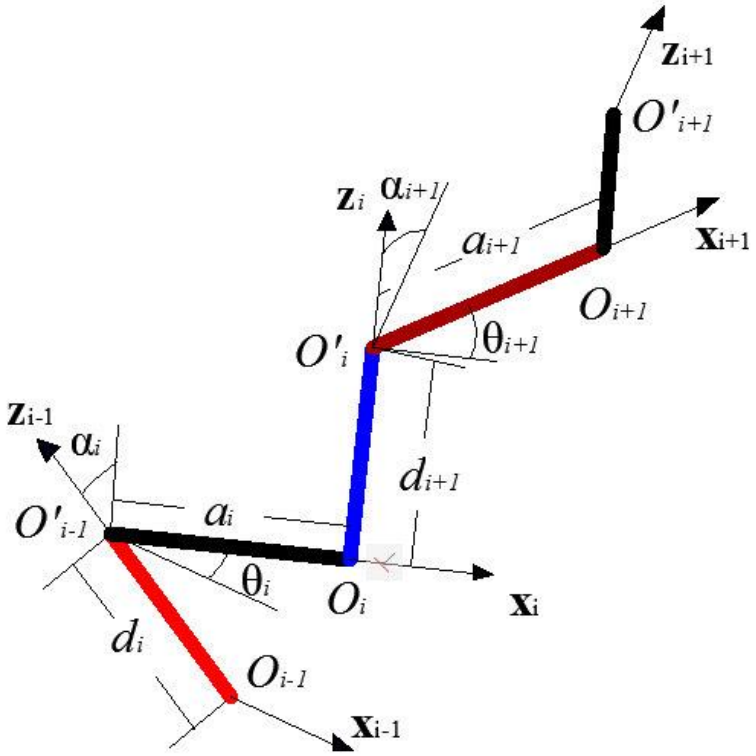

Fig. 5.2: A spatial robotic manipulator with marked D-H parameter.

The location of centre of mass of link $'i'$ w.r.t O_i in its local frame can be written as:

$$\boldsymbol{r}_{O_i C_i} = \beta_{ix} \boldsymbol{x}_i + \beta_{iy} \boldsymbol{y}_i + \beta_{iz} \boldsymbol{z}_i \tag{5.15}$$

Substituting Eqns. (5.14) and (5.15) in Eqn. (5.13),

$$\boldsymbol{r}_{OC} = \frac{1}{M} \sum_{i=1}^{n} m_i \left[\sum_{j=1}^{i} (d_j \boldsymbol{z}_{j-1} + a_j \boldsymbol{x}_j) + \beta_{ix} \boldsymbol{x}_i + \beta_{iy} \boldsymbol{y}_i + \beta_{iz} \boldsymbol{z}_i \right] \tag{5.16}$$

Assuming $d_1 = 0$

$$\boldsymbol{r}_{OC} = \sum_{i=1}^{n} [\gamma_{ix}\boldsymbol{x}_i + \gamma_{iy}\boldsymbol{y}_i + \gamma_{iz}\boldsymbol{z}_i] \tag{5.17}$$

Here, $\gamma_{ix}, \gamma_{iy}\ and\ \gamma_{iz}$ are the factors of geometry and mass distribution of links. Knowing the values of these factors, location of system centre of mass (G) can be obtained, by adding the appropriate auxiliary links to the system.

2. Thereafter, springs are used to make the potential energy invariant with configuration of the system. The total potential energy can be obtained as,

$$V = V_e + V_g \tag{5.18}$$

where,

V_e = elastic potential energy,

$$= \frac{1}{2}k(\xi_1^2 + \xi_2^2 + \xi_3^2)d^2 + \frac{1}{2}k(\delta_1^2 + \delta_2^2 + \delta_3^2) - kd(\delta_1\xi_1 + \delta_2\xi_2 + \delta_3\xi_3),$$

V_g = gravitational potential energy,

$$= Mg(\delta_1\xi_1 + \delta_2\xi_2 + \delta_3\xi_3).$$

The combined potential energy can be given as,

$$V = (Mg - kd)\delta_1\xi_1 + (Mg - kd)\delta_2\xi_2 + (Mg - kd)\delta_3\xi_3 + \frac{1}{2}k(\xi_1^2 + \xi_2^2 + \xi_3^2)d^2 + \frac{1}{2}k(\delta_1^2 + \delta_2^2 + \delta_3^2) \tag{5.19}$$

Now, for potential energy of the system to be constant, the coefficients of configuration variable terms should remain zero. Thus, stiffness of spring is obtained as, $, i = 1, 2, 3$ to zero.

$$\delta_i \xi_i \quad = \quad 0 \qquad \text{for} \quad i = 1, 2, 3.$$

which leads to,

$$k \quad = \quad \frac{Mg}{d} \tag{5.20}$$

This method make it possible to locate the centre of mass of the manipulator in real-time and join this point to inertially fixed frame by means of springs. The importance of this method lies in the fact that there is no effect of the gravitational forces even base of the manipulator is rotated. Whereas, the methods proposed for gravity balancing before the introduction of this method, are meant for a fixed direction of gravity vector. Thereafter, Agrawal and Fatteh has used this method in their work of gravity balancing of class of industrial robots with anthropomorphic designs [66].

ii. With Springs of Zero-Free-Length

Agrawal and Fatteh [65], Dorsser et al. [68], Nathan [69], Pracht [70], Streit, B.J. Gilmore [71], Streit and Shin [72], used the spring of *zero-free-length* and *auxiliary* links, for gravity balancing of robotic manipulators. A zero-free-length spring [73] can be described as a linear spring whose length is zero, when no external load is applied on it. In other words, in these springs, spring force [68] is proportional to total length of spring rather than elongation. A spring of zero free length can be obtained with suitable combination of normal springs.

However, gravity balancing can also be done by means of springs of zero-free-length only without the use of auxiliary links. The same has been done by Deepak and Ananthasuresh, to statically balance a general tree structured linkage loaded with linear springs or constant forces [73], static balancing of four bar linkage [74] and for perfect static balancing of linkages [75]. Lin et al. [76] also uses the zero free length springs to design a gravity balanced general spatial serial type manipulator.

iii. With Normal Springs

The perfect gravity balancing can be achieved by using springs of zero-free-length. Now, the springs of positive and negative-free-length can be assembled, to produce a spring of zero-free-length. However, this arrangement as well as the use of auxiliary links requires considerable space to get accommodate. This is not desirable in some of the practical applications of mechanisms, as it increases the complexity of mechanism and limits the range of motion of links. With reference to this context, Herder [77] described several gravity equilibrators providing the perfect static balancing, by making use of normal springs instead of springs of zero-free-length.

5.4 Gravity Balancing of MMA

In Section 5.3, different techniques of gravity balancing available in the literature, have been reviewed. These techniques include the gravity balancing by means of springs of zero-free-length with or without auxiliary links and normal springs.

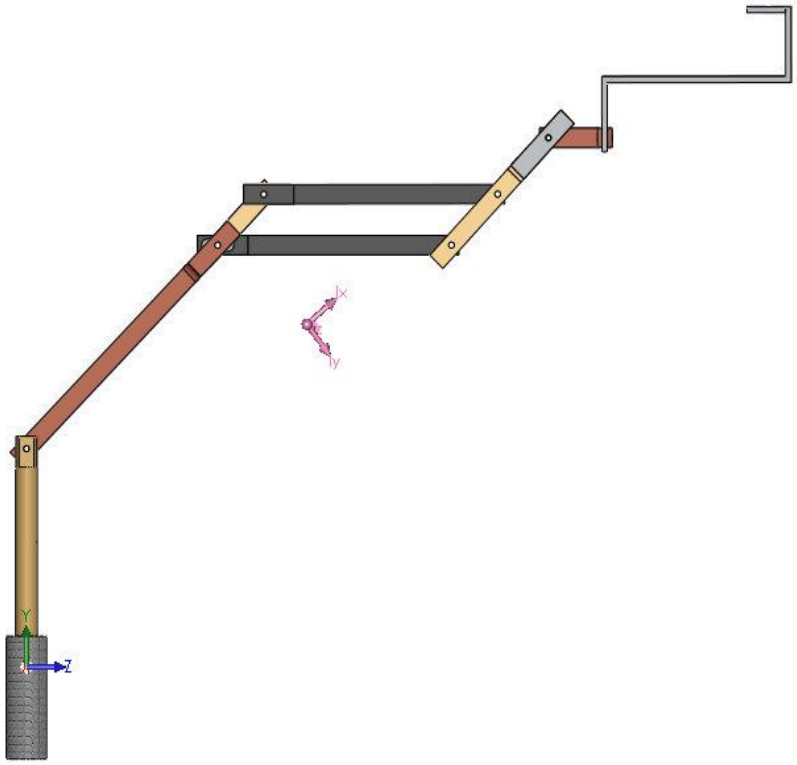

Fig. 5.3: Assumed pose of MMA for gravity balancing.

However, some of the practical applications restricts the use of auxiliary links and zero-free-length springs. This is because, the use of auxiliary links as well as the arrangement of non-zero-free-length of springs, create two problems– i) an increase in complexity of mechanism; ii) limits the range of motion of links, which is undesirable in applications requiring precise movements.

In present work, an effort has been made to statically balance the manipulator for medical applications (MMA). However, the same problem has been observed when auxiliary links are used. In MMA, the use of external links is highly undesirable because, it restricts the motion of surgeon's hand during a surgical task. So, a constraint, of not to use auxiliary links, has been imposed over the gravity balancing of MMA. Now, to do the gravity balancing of same, normal springs are used. The approach used here is, joint torques are equalized to the resisting-torques provided by the attached springs. It is desirable to attach a spring between two consecutive links of MMA. In next Section 5.4.1, the design of the normal spring for static balancing of MMA is developed.

For gravity balancing, the MMA is assumed in an appropriate pose, as shown in Fig. 5.3. In this figure, the second link (refer Fig. 4.8-(a)) is inclined at an angle of 45^0 to horizontal. The idea behind this pose is that the surgeon can easily reach horizontal as well as vertical positions. However, the moments are calculated for a worst configuration i.e where the effect of the gravity is most pronounced. One of the worst configurations is shown in Fig. 5.4.

5.4.1 Spring Design for Gravity Balancing

A spring for each pair of links is designed in two steps. In first step, torque induced at a joint under consideration is calculated. Thereafter, second step involves the calculation of resisting torque provided by the springs.

1. **Calculation of joint torques: -** Figure 5.4, shows the MMA in a pose at which joint torque is maximum at the joint between links L_1 and L_2 (refer Fig. 4.8-(a)). The distance between the joint and point of attachment of spring is fixed, which means that the free length of spring is fixed. In order to compute the centre of mass (C.G), MMA is modeled in SolidWorks environment. Thereafter, aluminium alloy (Alloy 1060) as its material,

has been assigned to it. The mass density of assigned material is taken as 2700 kg/m^3. Thereafter, from the mass-property analysis in the SolidWorks, the centre of gravity of MMA is calculated and it is shown by coordinate system in light-pink color.

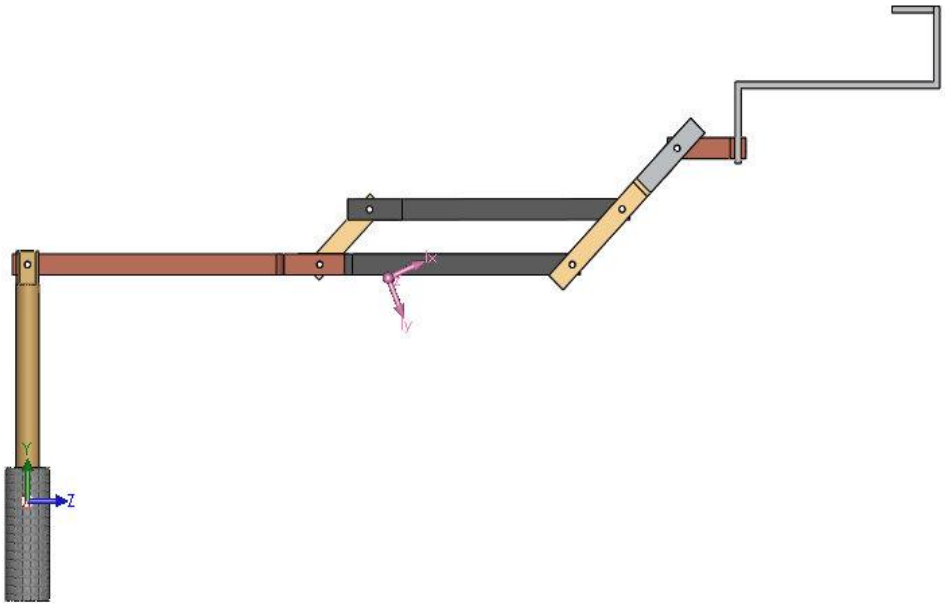

Fig. 5.4: Worst configuration of MMA for 2nd joint (between links L_1 and L_2).

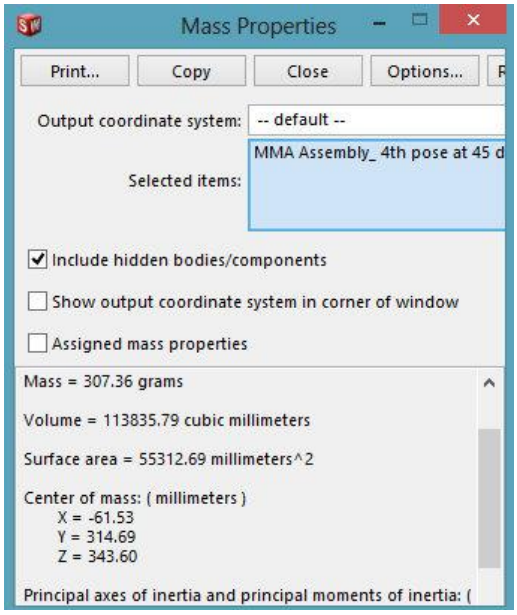

Fig. 5.5: Mass properties of MMA in the pose shown in Fig. 5.3.

The torque induced at joint between links L_1 and L_2 can be calculated by using the mass properties (refer Fig. 5.6), for the worst configuration of MMA. It is assumed that the weight of all links (except of L_0 and L_1, as it does not contribute any gravity load) acts through centre of mass, shown in light-pink color in Fig. 5.4. The parameters of MMA are given in Table 5.1. So, the torque (τ) at the same joint as reported earlier can be calculated as,

$$\tau = \sum_{i=2}^{n} w_i \times r_i = w_{eq} \times r_{eq}, \tag{5.21}$$

where,

w_i = weight of i^{th} link, in Fig. 5.3,

r_i = moment arm of i^{th} link w.r.t the joint axis of L_2 in Fig. 5.3,

w_{eq} = equivalent weight of all links shown in Fig. 5.4 (refer Fig. 5.7),

r_{eq} = equivalent moment arm of MMA shown in Fig.5.4 (refer Fig. 5.7).

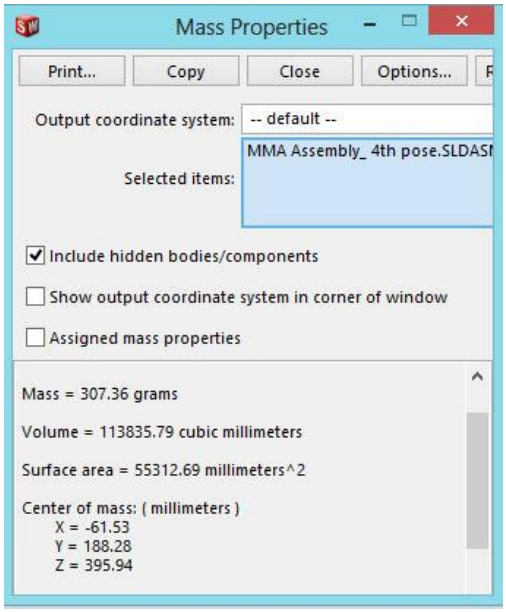

Fig. 5.6: Mass properties at worst configuration (Fig. 5.4).

Using the above methodology, the joint torques are calculated on the first configuration, as shown in Fig. 5.3, is given as,

$$\begin{aligned} w_{eq} &= 307.36 \text{ gms.} \\ r_{eq} &= 343.60\times 10^{-3} \text{ m.} \\ \tau_{Pose_1} &= 307.36 \times 10^{-3} \times 9.8 \times 343.60\times 10^{-3} \\ \tau_{Pose_1} &= 1.0349 \text{ Nm.} \end{aligned} \tag{5.22}$$

Similarly, the joint torque at the second assumed configuration, as shown in Fig. 5.4, is given as,

$$\begin{aligned} \tau_{Pose_2} &= 307.36 \times 10^{-3} \times 9.8 \times 395.94 \times 10^{-3} \\ \tau_{Pose_2} &= 1.1926 \text{ Nm.} \end{aligned} \tag{5.23}$$

Eqn. (5.24) gives the torque acting at the same joint when MMA has a pose as shown in Fig. 5.3.

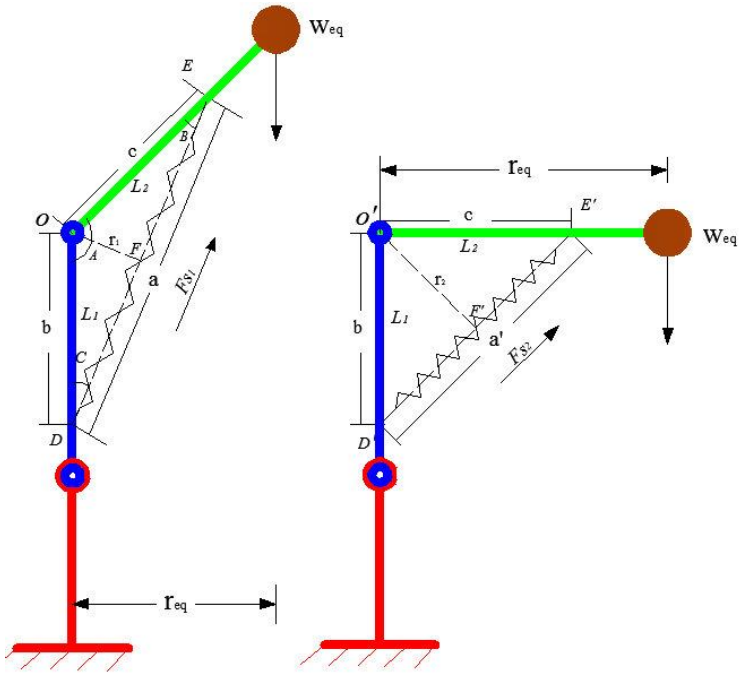

Fig. 5.7-(a): Spring of free-length $L_f = a$, attached at a distance b on link L_1 and c on link L_2, from pivot point O. Fig. 5.7-(b): The pose of MMA at which joint torque is maximum at point O'.

Table 5.1: Masses of different links of MMA.

S.No	Link (L_i)	Mass in gms.
1.	L_2	37.73
2.	L_3	25.87
3.	L_{3a}	7.46
4.	L_{3b}	25.87
5.	L_4	25.57
6.	L_5	16.93
7.	L_6	12.09
8.	L_7	152.59
9.	Packing	3.25
		$\sum m_i = 310.36$

It can be seen from Table 5.1, the mass of the manipulator is found as 310.36 gms, which is found in close agreement with the mass reported by Solidworks 3.5.

2. Now, the torques calculated in previous step must be balanced by the resisting-torque provided by the spring, to be designed. Therefore, following relations can be formulated:

$$\tau_{sp_1} = \boldsymbol{F}_{sp_1} \times r_1 \quad (5.24)$$

$$\tau_{sp_2} = \boldsymbol{F}_{sp_1} \times r_2 \quad (5.25)$$

$$\boldsymbol{F}_{sp_1} = k \times x_1 \quad (5.26)$$

$$\boldsymbol{F}_{sp_2} = k \times x_2 \quad (5.27)$$

Where $\boldsymbol{F}_{sp_1}$ and $\boldsymbol{F}_{sp_1}$ are the spring forces for posture shown in Figs. 5.3 and 5.4 respectively. Also, equivalent Figs., Figs. 5.7−(a) and (b), has been made. r_1 and r_2 are the perpendicular distances between pivot point and an axis of spring, k is the stiffness of spring and x_1, x_2 represents the deformations of spring for prescribed posture. The

deformation $x_1 = 0$, as there is deformation of spring in the pose assumed for gravity balancing.

With reference to Fig. 5.7-(a), the free-length of spring can be calculated by applying the *Sine law* to $\Delta\, ODE$. From geometry of triangle (ODE), it can be derived that:

$$\angle B = \angle C$$
$$\angle A = 135^0$$

$$\Rightarrow \angle B = \angle C = 22.5^0$$

According to Sine law:

$$\frac{a}{sinA} = \frac{b}{\sin B} \tag{5.28}$$
$$a = \frac{b \times \sin A}{\sin B}$$
$$a = 28 \times \frac{sin135^0}{\sin 22.5^0}$$
$$a = 51.7372 \text{ mm.} \tag{5.29}$$

From $\Delta\, ODF$:

$$r_1 = OD \times \sin C$$
$$r_1 = 28 \times \sin 22.5^0$$
$$r_1 = 10.7151 \text{ mm} \tag{5.30}$$

Also, deformation (x_2) of spring, when rotating link L_2 from assumed home position (Fig. 5.7-(a)) to a position as shown in Fig. 5.7-(b), can be calculated as:

$$x_2 = (a - a')$$

Applying Pythagoras theorem to, $\Delta\, O'D'E'$ for a' and $\Delta\, O'D'F'$ for r_2:

$$a' = 39.5979 \text{ mm.}$$

$$\Rightarrow \quad x_2 = 12.1392 \text{ mm.}$$

$$r_2 = 19.7989 \text{ mm.}$$

The equations of resisting torque can be formulated as:

$$\tau_{sp_1} = \boldsymbol{F}_{sp_1} \times r_1$$

$$\tau_{sp_1} = k \times x_1 \times r_1 \tag{5.31}$$

$$\tau_{sp_2} = \boldsymbol{F}_{sp_2} \times r_2$$

$$\tau_{sp_2} = k \times x_2 \times r_2 \tag{5.32}$$

Subtracting Eq. (5.31) from Eq. (5.32) and substituting values of all quantities,

$$\tau_{sp_2} - \tau_{sp_1} = k \times x_2 \times r_2 - k \times x_1 \times r_1$$

For static balancing

$$\tau_{Pose_1} = \tau_{sp_1}$$

$$\tau_{Pose_2} = \tau_{sp_2}$$

$$0.1577 = k(12.1392 \times 19.7989 - 0 \times 10.5171) \times 10^{-6}$$

$$k = 656.146 \text{ N/m.} \tag{5.33}$$

Assuming factor of safety as, $F_s = 1.15.$

Thus required stiffness of spring is:

$$k_s = k \times F_s$$

$$k_s = 656.146 \times 1.15$$

$$k_s = 754.57 \text{ N/m} \tag{5.34}$$

Specifications of the designed spring:

1) **Fixed Parameters: -**
   - Free-length (L_f) = 51.73 mm.
   - Mean coil diameter (D) = 14 mm.
   - Wire diameter (d) = 1.5 mm.
2) **Designed Parameters: -** By using the fixed parameters the other design parameters of spring are calculated which are given in Table 5.2.

Table 5.2: Spring design parameters.

S.No	Spring Parameter (s)	Empirical Relation	Designed Value
1.	Number of turns (N)	$\frac{Gd^4}{8D^3k_s}$	13
2.	Slenderness ratio	$\frac{L_f}{D}$	3.69
3.	Solid length (L_S)	$(n \times d)$	19.50 mm
4.	Spring index (C)	$\frac{D}{d}$	9.33
6.	Pitch (p)	$\frac{L_f}{N-1}$	4.31 mm

5.5 Summary

This chapter deals with gravity balancing of robotic manipulators. It starts with general introduction to gravity balancing followed by literature review in which its broad classifications has been presented. Thereafter, based on these classifications, two different methods of gravity compensation has been discussed and finally, analytic formulation of spring design for gravity balancing of MMA has been developed. This is achieved by modeling the MMA in SolidWorks environment. Also, this formulation corresponds to the worst configuration of prescribed manipulator as the joint torque at this configuration is maximum.

Chapter 6

Conclusions and Future Directions

6.1 Conclusions

From the current work, the following conclusions can be drawn:

- From the thorough literature review, it can be concluded that the most widely used method for manipulator kinematics is the, distal variant of D-H parameter method. However, it is applicable to open-loop serial manipulators only. Moreover, there are couple of ambiguities in it as reported by different researchers.
- It is also concluded from literature review, that S-U method is most general, applicable to any rigid link mechanism. However, due to non-minimal parameter representation, this method is limited to closed-loop robots only.
- From first two observations, it can be concluded that there is no general method which can develop the kinematic model of both open- and closed-loop chains. In this work, the complete kinematic model of a hybrid manipulator, which is a combination of open- and closed-loop chains containing planar and spatial links, has been developed successfully.
- From the work reported in kinematics of general serial manipulators, it can be concluded that, for kinematic description of a chain, D-H parameter method requires only one frame per link, whereas two frames per link are required in S-U method.
- An improvement in classical D-H parameter method has been made by introducing a new concept, coined as concept of *dummy frames.* The introduced concept removes the two kinds of inconsistencies in D-H parameter method, observed during the kinematic study of MMA. Both analytical and physical validations ensure the efficacy of proposed concept. This improvement leads to an *extension* of D-H parameter method to spatial hybrid manipulators.
- Finally, from gravity balancing of robotic manipulator it can be concluded that a number of methods has been developed for gravity compensation. However, these

methods are limited by the application requirements. In the present work, the analytical formulation for the design of spring for the gravity balancing of MMA.

6.2 Future Directions

The work completed in the present thesis, as shown in the Fig. 6.1, can be extended in some directions as

- The work present in this thesis is limited to the kinematic study only, which can be extended for the dynamic study of hybrid manipulators.
- The work is also limited to analytic formulation of spring design for gravity balancing of MMA. The work can be extended to design the spring for actual prototype.

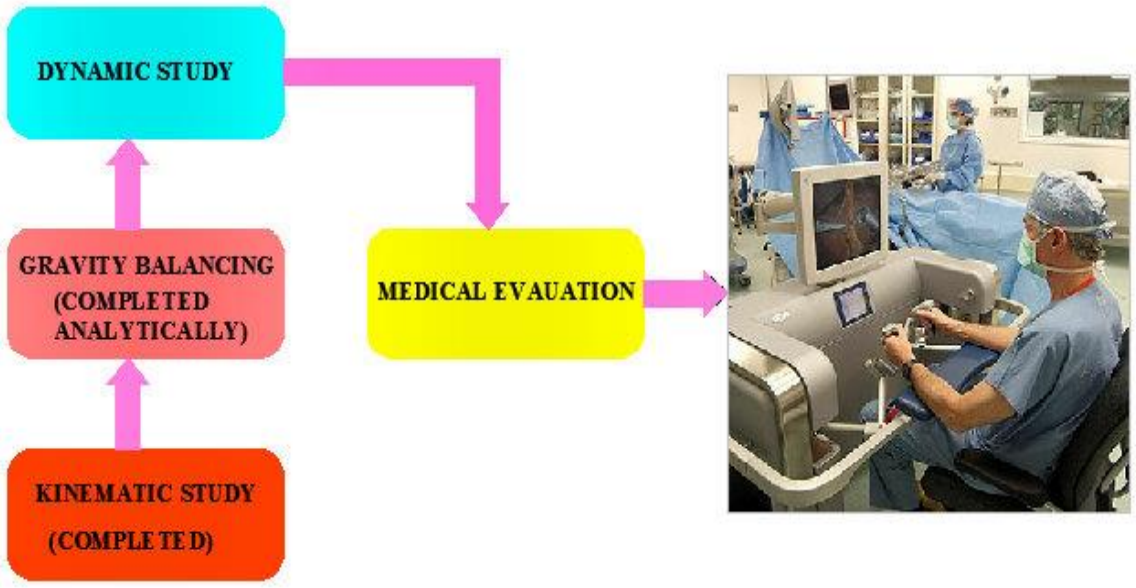

Fig. 6.1: The proposed general Layout of MMA.

- The reported work deals with the MMA, which is a surgeon side manipulator. The work can be extended for a set of coordinated robots, where both the surgeon- and patient-side manipulators works together.

APPENDIX A

Details of *proximal* variant of D-H notation is given in this appendix which is as follows:

1. Draw line diagram of an open kinematic chain, identify and draw all the motion axis with lines of infinite length.
2. Mark these motion axis as z-axis.
3. Next step is to assign x-axis, which is normal at the point of intersection of z_i and z_{i+1}. In case, if they don't intersect then x-axis will be drawn such that it is common normal to z_i and z_{i+1}.
4. Finally, assign y-axis as given by *right hand thumb* rule.
5. Thereafter, calculate D-H parameters which are as follows:
   - Link twist angle (α_i): Angle from z_i to z_{i+1} about x_i.
   - Link length (a_i): Distance from z_i to z_{i+1} along x_i.
   - Joint distance (d_i): Distance from x_{i-1} to x_i along z_i.
   - Joint variable (θ_i): Angle from x_{i-1} to x_i about z_i.

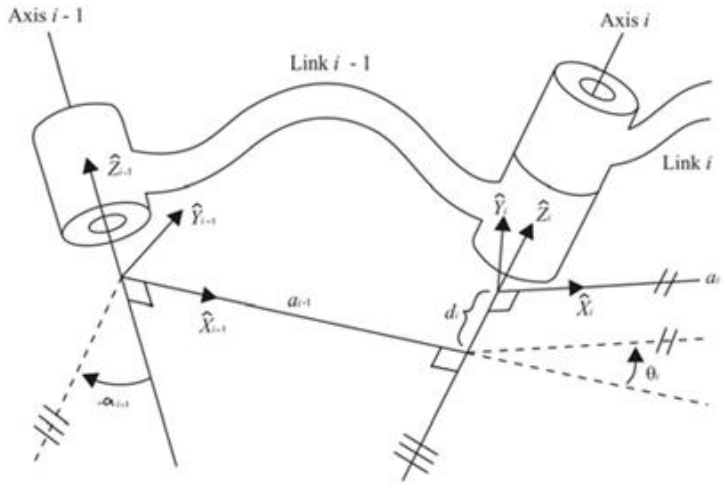

Fig. A1: Geometric Description of D-H parameters [2].

The general homogeneous link coordinate transformation matrix [2] comes directly from D-H parameters:

$$ {}^{i}_{i-1}T = \left[\begin{array}{ccc|c} \cos\theta_i & \sin\theta_i & 0 & a_{i-1} \\ \sin\theta_i \cos\alpha_{i-1} & \cos\theta_i \cos\alpha_{i-1} & -\sin\alpha_{i-1} & -\sin\alpha_{i-1}\, d_i \\ \sin\theta_i \sin\alpha_{i-1} & \cos\theta_i \sin\alpha_{i-1} & \cos\alpha_{i-1} & \cos\alpha_{i-1}\, d_i \\ 0 & 0 & 0 & 1 \end{array}\right] \quad \text{(A1)} $$

REFERENCES

[1] Denavit, J. and Hartenberg, R. S., *"A kinematic notation for lower pair mechanisms based on matrices"*, ASME Journal of Applied Mechanics, vol. 6, pp. 215–221, (1955).

[2] John. J. Craig, *"Introduction to Robotics: Mechanics and Control"*, Reading, MA: Addison-Wesley, (1986).

[3] Harvey Lipkin, *"A note on Denavit–Hartenberg notation in robotics"*, Proceedings of ASME International Design Engineering Technical Conferences & Computers and Information in Engineering Conference (IDETC/CIE), pp. 921–926, Long Beach, California USA (2005).

[4] Kahn, M. E. and Roth, B., *"The near minimum-time control of open-loop articulated kinematic chains"*, ASME Journal of Dynamic Systems, Measurement, and Control, vol. 6, pp. 215–221, (1971).

[5] Featherstone, R., *"A program for simulating robot dynamics*", Working Paper 155, Department of Artificial Intelligence, University of Edinburgh, (1982).

[6] C. R. Rocha, C. P. Tonetto, A. Dias, *"A comparison between the Denavit–Hartenberg and the screw-based methods used in kinematic modeling of robot manipulators"*, Journal of Robotics and Computer-Integrated Manufacturing vol. 27, pp. 723–728, (2011).

[7] R.P, Paul, *"Robot Manipulators Mathematics, Programming and Control"*, MIT Press, Cambridge, MA 1981.

[8] Robert J. Shilling, *"Fundamentals of Robotics Analysis and Control"*, Prentice Hall, Third Impression (2008).

[9] G. R. Pennock and A. T Yang, *"Application of dual-number matrices to the inverse kinematics problem of robot manipulators",* ASME Journal of Mechanisms, Transmissions and Automation, in Design, vol. 107, pp. 201–208, (1985).

[10] M. Bergamasco, B. Allotta, L. Bosio, L. Ferretti, G. Parrini, G.M Prisco, F. Salsedo, G.Sartini, *"An arm exoskeleton system for teleoperation and virtual environments applications"*, Proceedings of IEEE, International Conference on Robotics and Automation, pp. 1449–1454, (1994).

[11] Loredana Zollo, Bruno Siciliano, Cecilia Laschi, Giancarlo Teti and Paolo. Dario, *"An experimental study on compliance control for a redundant personal robot*

arm", Journal of Robotics and Autonomous Systems, vol. 44, pp. 101–129, (2003).

[12] Andrea Maria Zanchettin, Paolo Rocco, Bascetta, Ioannis Symeonidis and Steffen Peldschus, "*Kinematic analysis and synthesis of human arm during a manipulation task*", Proceedings of IEEE, International Conference of Robotics and Automation, pp.2692–2697, (2011).

[13] Nicolas A. Aspragathos and John K. Dimitros, *"A comparative study on three methods for robot kinematics",* IEEE Transaction on Man and Cybernetics Systems, vol. 28, pp. 135–145, (1998).

[14] Kevin Cleary and Thurston Brooks, *"Kinematic analysis of a novel 6-DOF parallel manipulator",* Proceedings of IEEE, International Conference on Robotics and Automation, pp.708–713, (1993).

[15] Bruno Siciliano, Lorenzo Sciavicco, Luigi Villani, Giuseppe Oriolo, *"Robotics, Modelling, Planning and Control",* Advanced Textbook in Control and Signal Processing 2009.

[16] U. Thomas, I. Maciuszek, F.M Wahl, *"A Unified Notation for Serial, parallel and hybrid kinematic structures",* Proceedings of IEEE, International Conference on Robotics and Automation, pp. 2868–2873, (2002).

[17] S. Sahu, B. B. Biswal, Bidyadhar Subudhi, *"A novel method for representing robot kinematics using quaternion theory"*, Proceedings of IEEE, International Conference on Computational Intelligence, Control And Computer Vision In Robotics and Automation, pp.76–82, (2008).

[18] P. N. Sheth, J. J. Uicker, *"A generalized symbolic notation for mechanisms"*, Journal of Engineering for Industry Transactions of the ASME, vo1.93, pp. 102–112, (1971).

[19] Robert H. Vandervaart and Raymond J. Cipra, *"The kinematics of open-loop manipulators using IMP (Integrated Mechanisms Program)"*, Proceedings of IEEE, In American Control Conference, pp.1870–1875, (1984).

[20] Patrick F. Muir and Charles P. Neuman, *"Kinematic modelling of wheeled mobile robots"*, Journal of Robotic Systems, vol. 4, pp. 281–340, (1987).

[21] Bertold Bongardt, *"CAD-2-SIM- Kinematic modelling of mechanisms based on the Sheth-Uicker convention",* International Conference on Intelligent Robotics and Applications, vol. 7101, pp. 465–477, (2011).

[22] P. S. Dutta, Tin-Lup Wong, *"Inverse kinematic analysis of moving base robot with redundant degree of freedom",* CAD/CAM Robotics and Factories of the Future, Robotics and Plant Automation, vol. 3, pp. 139–143, (1989).

[23] Ambarish Goswami, Arthur Quaid, Michael Peshkin, *"Identifying robot parameters using partial pose information",* Proceedings of IEEE, Journal of Control Systems, vol. 13, pp. 6–14, (1993).

[24] Zhumadil Zh. Baigunchekov, Myrzabay B. Izmambetov, B. Nurakhmetov, K. Sartaev and N. Baigunchekov, *"The new parallel manipulator with 6-degree-of-freedom",* Proceedings of 12th IFToMM, World Congress in Mechanism and Machine Science, vol. 5, pp. 641–646, (2007).

[25] Said. M. Megahed, *"Human hand modelling by homogeneous transformation",* Proceedings of IEEE, International Conference on Medicine and Biology Society, vol. 12, pp. 2122–2123, (1990).

[26] Said. M. Megahed, *"Efficient robot arm modeling for computer control",* Journal of Robotic Systems, vol. 10, pp. 1095–1109, (1993).

[27] G. M. Acaccia, L. Bruzzone, R.C. Michelini, R.M. Molfino and M. Calligari, *"Mobile Robots: Kinematics of non-holonomic path-planning ",* Proceeding of the IASTED, International Conference on Modelling, Identification and Control, pp. 714–717, (2001).

[28] Said. M. Megahed and M. Renaud, "Dynamic modelling of robot manipulators containing closed kinematic chains", Advanced Software in Robotics, Liege, Belgium, (1983).

[29] B. Roth, "Overview on Advanced Robotics: Manipulation", Proceedings of IEEE, International Conference on Robotics and Automation (ICRA-1985), pp. 559–570, Tokyo, Japan, (1985).

[30] Tomislav Reichenbach and Zdenko Kovacic, *"Collision free path planning in robot cells using virtual 3D sensors",* Cutting Edge Robotics, Vedran Kordic, Aleksander Lazinica and Munir Meran (Ed.), Pub: Pro Literatur Verlag, Germany, (2005).

[31] W. Khalil, J. F. Kleinfinger, *"A new geometric notation for open and closed-loop robots,"* Proceedings of IEEE International Conference on Robotics and Automation, vol. 3, pp. 1174–1179, (1986).

[32] Lorenzo Fluckinger, Charles Baur, Raymond Clavel, *"CINEGEN: A rapid prototyping tool for robot manipulators",* Fourth International Conference on Motion and Vibration Control, vol. 1, pp. 129–134, Zurich, (1998).

[33] Lorenzo Fluckinger, *"A robot kinematics using virtual reality and automatic kinematics generator",* Proceedings of 29^{th} International Symposium on Robotics, pp.123–126, Birmingham (UK), (1998).

[34] W. Khalil and C. Chevallereau, *"An efficient algorithm for the dynamic control of robots in Cartesian space",* Proceedings of IEEE, 28^{th} Conference on Decision and Control, pp. 582–588, (1987).

[35] M. Gautier and W. Khalil, *"A direct determination of minimum inertial parameters of robots",* Proceedings of IEEE, International Conference on Robotics and Automation, pp. 1682–1687, (1988).

[36] Wisama Khalil and Sylvain GUEGAN, *"Inverse and direct dynamic modelling of Gough-Stewart robots",* IEEE Transaction on Robotics and Automation, pp. 754–762, (2004).

[37] W. Khalil and Ouarda Ibrahim, *"General solution for dynamic modelling of parallel robots"* Journal of Intelligent and Robotic Systems, vol. 49, pp. 19–37, (2007).

[38] O. Ibrahim and W. Khalil, *"Kinematic and dynamic modelling of 3-RPS parallel manipulator",* Proceedings of 12th IFToMM World Congress, (2007).

[39] Sylvain GUEGAN, W. Khalil and Philippe LEMOINE, *"Identification of dynamic parameters of the orthoglide"*, Proceedings of IEEE, International Conference on Robotics and Automation, vol. 3, pp. 3272–3277, (2003).

[40] M. Gautier, *"Numerical Calculation of the base inertial parameters of robots",* Proceedings of IEEE, International Conference on Robotics and Automation, pp. 1020–1025, (1990).

[41] W. Khalil, S. Besnard and P. Lemoine, *"Comparison study of the parametric calibration methods",* vol. 15, pp. 56–67, (2000).

[42] F. Bennis and W. Khalil, *"Minimum inertial parameters of robots with parallelogram closed loops",* Transactions of IEEE on System, Man Cybernetics, vol. 21, pp. 318–326, (1991).

[43] W. Khalil, G. Garcia and J. F. Delagrade, *"Calibration of geometric parameters of robots without external sensors",* Proceedings of IEEE, International Conference on Robotics and Automation, vol. 3, pp. 3039–3044, (1995).

[44] B. Perrin, Chevallerau and C. Verdier, *"Calculation of direct dynamic model of walking robots: comparison between two methods",* Proceedings of IEEE, International Conference on Robotics and Automation, vol. 2, pp. 1088–1093, (1997).

[45] W. Khalil, Ph. Lemoine and M. Gautier, *"Autonomous calibration of robots using planar points",* World Automation Congress, Robotic and Manufacturing Systems, vol. 3, (1996).

[46] W. Khalil, *"Dynamic modelling of robots using recursive Newton-Euler techniques",* International Conference on Informatics in Control, Automation and Robotics, (2010).

[47] W. Khalil, Pedro Pablo Restrepo, *"An efficient algorithm for calculation of filtered dynamic models of robots",* Proceedings of IEEE, International Conference on Robotics and Automation, vol. 1, pp. 323–328, (1996).

[48] Liang Ma, Wei Zhang, Damien Chablat, Fouad Bennis and Francois Guillaume, *"Multi-objective optimization method for posture prediction and analysis with consideration of fatigue effect and its application case",* Journal of Computer and Industrial Engineering, vol. 57, pp. 1235–1246, (2009).

[49] W. Khalil and Frederic Boyer, *"An efficient calculation of computed torque control of flexible manipulators",* Proceedings of IEEE, International Conference on Robotics and Automation, vol. 1, pp. 609–614, (1995).

[50] Gentiane Venture, Wisama Khalil, Maxime Guatier and Philippe Bodson, *"Dynamic modelling and identification of a car",* Proceedings of the World Congress of International Federation of Automatic Control, (2002).

[51] W. Khalil and J. F. Kleinfinger, *"Minimum operations and minimum parameters of the dynamic models of tree structure robots",* IEEE Journal of Robotics and Automation, vol. RA-3, pp. 517–526, (1987).

[52] W. Khalil, Maxime Guatier and Philippe Lemoine, *"Identification of the payload inertial parameters of industrial manipulators",* Proceedings of IEEE, International Conference on Robotics and Automation, pp. 4943–4948, (2007).

[53] Guy Bessonnet and Philippe Sardain, *"Optimal dynamics of actuated kinematic chains. Part-1: Dynamic modelling and differentiations",* European Journal of Mechanics A/Solids, vol. 24, pp. 452–471, (2005).

[54] Ph. Poignet, M. Guatier, W. Khalil and M. T. Pham, *"Modelling simulation and control of high speed machine tools using robotics formalism",* Journal of Mechatronics, vol. 12, pp. 461–487, (2002).

[55] M. T. Pham, M. Guatier and P. Poignet, *"Identification of joint stiffness with bandpass filtering",* Proceedings of IEEE, International Conference on Robotics and Automation, vol. 3, pp. 2867–2872, (2001).

[56] N. Pio Belifiore and Augusto Di Benedetto, *"Connectivity and redundancy in spatial robots",* The International journal of robotic Research, vol. 12, pp. 1245–1261, (2000).

[57] Peter I. Corke, *"A simple and systematic approach to assigning D-H parameters"*, IEEE Transactions on Robotics, vol. 23, pp. 590–594, (2007).

[58] Minas V. Liarokapis, Panagiotis K. Artemiadis and Kostas J. Kyriakopoulos, *"Quantifying anthromorphism of robot hands",* Proceedings of IEEE, International Conference on Robotics and Automation, pp. 2041–2046, (2013).

[59] S. Sahu, B. B. Biswal and Bidyadhar Subudhi, *"A novel method representing robot kinematics using quaternion theory",* Proceedings of IEEE sponsored Conference on Computational Intelligence, Control and Computer Vision In Robotics & Automation, pp. 76–82, (2008).

[60] You-Liang Gu and J. Y. S. Luh, *"Dual-number transformation and its application to robotics"*, IEEE Journal of Robotics and Automation, vol. RA–6, pp. 615–623, (1987).

[61] J. Ronney, *"A comparison of representation of general spatial screw displacement"*, Environ. Planning (England), Series- B, vol. 5, pp. 89–99, (1978).

[62] Janez Funda, Russell H. Taylor and Richard P. Paul, *"On homogeneous transformations, quaternion and computational efficiency"*, Transactions of IEEE, on Robotics and Automation, vol. 6, pp. 382–388, (1990).

[63] S. S. Rattan, *"Theory of Machines"*, Tata McGraw Hills Education Private Limited, (2009).

[64] Nathan Ulrich and Vijay Kumar, *"Passive gravity compensation for robot manipulators"*, Proceedings of IEEE, on Robotics and Automation, pp. 1536–1541, (1991).

[65] Sunil K. Agrawal and Abbas Fattah, *"Gravity balancing of spatial robotic manipulators"*, Journal of Mechanism and Machine Theory, vol. 39, pp. 1331–1344, (2004).

[66] Sunil K. Agrawal and Abbas Fattah, *"Gravity-balancing of classes of industrial robots"*, Proceedings of IEEE, on Robotics and Automation, pp. 2872–2877, (2006).

[67] I. Simionescu, L. Ciupitu, Luciana Ionita, I. Ion and M. Ene, *"Elastic systems for static balancing of robot arms"*, 13th World Congress of Machine and Mechanism Science, (2011).

[68] Wouter D. van Dorsser, Rogier Barents, Boudewijn M. Wisse and Just L. Herder, *"Gravity balanced arm support with energy-free adjustment"*, Journal of Medical Devices, vol. 1, pp.151–158, (2007).

[69] R. M. Nathan, *"A constant force generation mechanism"*, Journal of Mechanical Design, vol. 107, pp. 508–512, (1985).

[70] P. Pracht, P. Minotti, M. Dahan, *"Synthesis and balancing of cam-modulated linkage"*, Proceedings of ASME Design Technology Conferences-The Design Automation Conferences, vol. 10, (1987).

[71] D. A. Streit, B. J. Gilmore, *"Perfect spring equilibrators for rotatable bodies"*, Journal of Mechanical Design, vol. 115, pp. 604–611, (1993).

[72] D. A. Streit, B. J. Gilmore, *"Perfect spring equilibrators for rotatable bodies"*, ASME Journal of Mechanisms, Transmissions, and Automation in Design, vol. 111, pp. 451–458, (1989).

[73] S. R. Deepak and G. K. Ananthasuresh, *"Static balancing of spring-loaded planar revolute-joint linkages without auxiliary links"*, 14th National Conference on Machines and Mechanisms, pp. 37-44, NIT Durgapur, India (2009).

[74] S. R. Deepak, and G. K. Ananthasuresh, *"Static balancing of a four-bar linkage and its cognates"*, Mechanism and Machine Theory, vol. 48, pp. 62–80 (2012).

[75] S. R. Deepak and G. K. Ananthasuresh, *"Perfect static balance of linkages by addition of spring but not auxiliary bodies"*, ASME Journal of Mechanisms and Robotics, vol. 4, pp. 021104-1–12, (2012).

[76] P. Y. Lin, W. B. Shieh, and D. Z. Chen, *"Design of a gravity- balanced general spatial serial-type manipulator"*, ASME Journal of Mechanisms and Robotics, vol. 2, pp. 031003, (2010).

[77] Freek L. S. te Riele and Just L. Herder, *"Perfect static balancing with normal springs"*, Proceedings of ASME Design Engineering Technical Conferences and Computers and Information in Engineering Conference, pp. 1–8, (2001).

ONLINE REFERENCES

[G1] http://www.gametechinternational.com/gti_index/l5ace-kt-750.jpg

[G2] http://www.superdroidrobots.com/images/customPages/HD2-Gen5-5Axis.jpg

[G3] http://robot.gmc.ulaval.ca/images/tmp/KukaRobot.png

[G4] http://www.strongarmindustries.com/images/strongarm/electric1.jpg

[G5] http://www.3mech.titech.ac.jp/ms_sugimoto/ms_sugimoto_images/hybrid_parallel.JPG

[G6] http://bloximages.newyork1.vip.townnews.com/hickoryrecord.com/content/tncms/assets/v3/editorial/7/7b/77b38ed4-81ed-11e2-ab07-0019bb30f31a/512fd248bed7e.preview-2700.jpg

[G7] http://www.robocatz.com/images/News-Da-Vinci-Surgical-Robot-4.jpg